Title

Potential Urban Heat Island Countermeasures and Building Energy Efficiency Improvements in Los Angeles County

Authors

Robinson, Alastair
Fernandes, Samuel
Hong, Tianzhen
et al.

Publication Date

2024-06-01

Peer reviewed

Building Technologies Department
Building Technologies and Urban Systems Division
Lawrence Berkeley National Laboratory

Potential Urban Heat Island Countermeasures and Building Energy Efficiency Improvements in Los Angeles County

Alastair Robinson, Samuel Fernandes, Tianzhen Hong, Sang Hoon Lee, Ronnen Levinson, and Mary Ann Piette

June 2024

doi:10.20357/B7M30K

Disclaimer

Copyright Notice

Acknowledgments

The work described in this study was conducted at Lawrence Berkeley National Laboratory (LBNL) and funded through the American Recovery and Reinvestment Act of 2009 (ARRA), Pub. L. 111-5, and is dependent on a Federal agreement (DE-EE0000905) authorized by the Energy Efficiency Block Grant (EECBG), CFDA Number 81.128. It was also supported by the Regents of the University of California for the U.S. Department of Energy under Contract No. DE-AC02-05CH11231.

The authors would like to thank David Fork (Google) for facilitating access to panoptic land cover classification rasters and albedo rasters used with permission from Google, and for reviewing outputs from Task 1. We thank Minh Le (LAC ISD) for facilitating and supporting access to the east LA building campus at which UAW flights and data gathering took place. We also thank Minh Le, Steve Steinberg, Lujuana Medina, and An Dang (LAC ISD) for supporting and guiding this project. We thank Yujie Xu (LBNL) for helping curate the weather data used in the EnergyPlus simulations. We thank Jiachen Zhang (University of Southern California) and Arash Mohegh (California Air Resources Board) for their insights about albedo cooling effectiveness (urban heat island effect mitigation via reflective surfaces).

The authors thank the following experts for reviewing this report (affiliations do not imply that those organizations support or endorse this work):

- David Fork, Google
- Lucy Hutyra, Google
- Nora Hart, LBNL

Email addresses of authors

Alastair Robinson*: ACRobinson@LBL.gov
Samuel Fernandes: SGFernandes@LBL.gov
Tianzhen Hong: THong@LBL.gov
Sang Hoon Lee: SangHLee@LBL.gov
Ronnen Levinson: RMLevinson@LBL.gov
Mary Ann Piette: MAPiette@LBL.gov

* Corresponding author

Suggested citation

Robinson, A., Fernandes, S., Hong, T., Lee, S.H., Levinson, R., and Piette, M. (2024). *Potential Urban Heat Island Countermeasures and Building Energy Efficiency Improvements in Los Angeles County*. Lawrence Berkeley National Laboratory. https://doi.org/10.20357/B7M30K

Abstract

Los Angeles County has been experiencing increasing numbers of very hot days and heatwaves later into the summer. Scientists predict a significant increase in days with temperatures over 95 °F [35 °C] over the next 15-20 years. As the climate warms, deploying energy efficiency technologies at scale can be an effective method to address the associated increase in urban temperatures, particularly during periodic heatwaves.

Utilizing existing information and data, the research project provided the Los Angeles County Internal Services Department with supplementary datasets and tools that support the identification and prioritization of neighborhoods/districts, building clusters, and specific buildings for retrofits, according to criteria identified and developed during the analysis process. There was a focus on the County's multi-family residential building stock, to enable low-cost energy retrofits that also support improvement of thermal resilience and occupant health and comfort.

Urban fabric analysis indicated that there are substantial opportunities to reduce unwanted solar heating of buildings and pavements and cool the urban environment with reflective roofs, walls, and pavements. On average, albedo (solar reflectance) values for roofs (0.19) and pavements (0.15) are currently quite low. The potential increases in roof and pavement albedos are 0.33, and 0.25 respectively, indicating substantial opportunities for brightening.

Building stock analysis determined that there are over 43,000 multi-family residential buildings, holding over 150,000 housing units in Los Angeles County, that represent priority opportunities for large-scale energy efficiency policies and activities to alleviate the impacts of the urban heat island effect.

Building energy simulations were conducted for 13 multifamily residential buildings, to evaluate a low-cost energy efficiency retrofit package. Implementation of these measures in the baseline housing units is expected to reduce annual electricity use by 17%, lower peak electricity demand by 19%, and provide net annual energy cost savings of $183 per housing unit. Importantly, annual hours of heat stress for building occupants are expected to be dramatically reduced by implementation of the energy efficiency retrofit—and for buildings with existing air-conditioning, eliminated.

Unmanned Aerial Vehicle (UAV) flights were conducted as a remote-sensing proof-of-concept for building energy performance evaluation. This approach represents an opportunity for inspection and analysis of existing building stocks, where energy performance can be documented using infrared imaging and 3D photogrammetry. Machine-learning algorithms developed by Berkeley Lab researchers were employed to detect thermal anomalies on building facades and to indicate issues potentially related to moisture, infiltration, and/or exfiltration. The potential benefits can be seen via the implementation of this method at the building test site, which highlighted areas around windows and facade surface corners as locations for further inspection.

Table of Contents

Table of Figures

List of Tables

Abbreviations

AC	Air Conditioning
BTUS	Building Technology & Urban Systems
CAD	Computer-Aided Design
CST	Cooling Setpoint Temperature
DOE	Department of Energy
DX	Direct Exchange
EAEI	Energy Analysis and Environmental Impacts
ECM	Energy Conservation Measure
ESDR	Energy Storage and Distributed Resources
ETA	Energy Technologies Area
EUI	Energy Use Intensity
GIS	Geographic Information System
HPI	Healthy Places Index
LAC	Los Angeles County
LAC ISD	Los Angeles County Internal Services Department
LARIAC	Los Angeles Region Imagery Acquisition Consortium
LBNL	Lawrence Berkeley National Laboratory
LCC	Land Cover Class
MF	Multi Family
MFR	Multi-Family Residential
RGB	Red-Green-Blue
RTU	Rooftop Unit
SET	Standard Effective Temperature
TIFF	Tag Image File Format
UAV	Unmanned Aerial Vehicle
UHI	Urban Heat Island
UHIE	Urban Heat Island Effect
UHII	Urban Heat Island Intensity
USD	United States Dollar

Background

The Los Angeles County Internal Services Department (LAC ISD) provides a range of support services to other County departments in the areas of energy and environmental programs management, among other purchasing, contracting, facilities, information technology, parking, and mail services. Los Angeles County (LAC) is the most populous county in the United States with an area of more than 4,000 square miles [10,400 km²], nearly ten million inhabitants, 88 incorporated cities, and a nominal gross domestic product of approximately 790 billion USD [1].

LAC has been experiencing increasing numbers of very hot days and heatwaves later into the summer. Scientists predict that some coastal areas and central Los Angeles will experience three times more days of temperatures over 95 °F [35 °C] by the year 2041, rising to 15-20 days annually from several days per year during the period from 1981 to 2000. Greater impacts will be felt in the San Fernando and San Gabriel Valleys, which historically have had over 60 days above 95 °F each year, and are forecast to experience over 100 such days annually by the year 2041 [2].

LAC ISD engaged Lawrence Berkeley National Laboratory (LBNL, a.k.a. "Berkeley Lab") to conduct an applied research study focused on techniques and technologies that help mitigate the urban heat island (UHI) impacts of a hotter climate. Berkeley Lab's analysis supports LAC ISD's goals of prioritizing neighborhoods, building clusters, and individual buildings for improvements; and modeling the energy and carbon savings and thermal resilience impacts of the selected energy efficiency measures. The research team also developed a proof-of-concept approach to recommending building envelope energy efficiency measures based on airborne drone-based infrared thermal imaging.

1 Introduction and overview

As the climate warms, deploying energy efficiency technologies at scale can be an effective method to address the associated increase in urban temperatures, particularly during periodic heatwaves.

These heatwaves are becoming increasingly common in Southern California [3–5]. Local authorities in Los Angeles County are increasingly focused on addressing the social and economic impacts of the challenges associated with an increase in average summer temperatures generally, and extreme weather events specifically.

The research project aimed to provide LAC ISD with processes and methods that support assessment of the County's building stock, and enable initiatives that support improving energy performance, thermal resilience, and occupant health and comfort. This work focused on the evaluation of low-cost retrofit opportunities in the multi-family residential (MFR) sector. MFR buildings house a significant portion of the population across LAC. Targeting MFR buildings offers LAC an opportunity to effect change in energy efficiency, urban heat island impacts, occupant economic security, and health at scale, in that many dwellings (apartment units) benefit from a single building retrofit.

Utilizing existing information and data, the Berkeley Lab team developed supplementary datasets and tools that support the identification and prioritization of neighborhoods/districts, building clusters, and specific

buildings for retrofits, according to criteria identified and developed during the analysis process. The new datasets and map layers are intended for use in identifying and prioritizing buildings from the LAC stock that would most benefit from energy efficiency and urban heat island retrofit measures.

A stated intention of LAC ISD is that the newly created datasets and map layers be integrated into an existing LAC ISD software platform and used to develop programs and incentives targeted at the deployment of specific technologies in target communities or buildings. Pairing these resources with LAC's property ownership database will help LAC ISD engage with local landlords and facilitate the desired energy efficiency retrofits. For example, LAC's Equity Explorer [6], a data tool that uses a series of filters to identify areas of need would be further enriched by a map layer that identifies MFR buildings that are in relatively poor condition, and therefore priority candidates for improvement.

The project team used Berkeley Lab's CityBES building stock modeling tool to evaluate energy retrofits for the selected buildings, which were prioritized based on the project team's datasets. Low-cost building envelope technologies can be effective methods for reducing cooling energy use and boosting building energy efficiency by limiting the impact of hot weather on thermal conditions within living spaces. Ceiling fans are a low-cost method of expanding the thermal comfort temperature range by the cooling effect of air movement. The benefits for building occupants are both social (comfort and health) and economic (lower energy costs).

We implemented a proof-of-concept for detecting energy transfer anomalies in the building envelope utilizing unmanned aerial vehicle (UAV)-mounted infrared imaging. This drone-based approach is a promising tool for conducting rapid site envelope energy efficiency assessments and could be deployed as an energy efficiency prioritization tool, following the completion of a building stock analysis process outlined in Figure 1.

This project comprised the following activities:

- Characterize the urban fabric of LAC from high-resolution land-cover rasters and albedo (solar reflectance) rasters, with attention to the albedos and tree covers of roofs, property parcels, and census tracts
- Identify opportunities for reduction of the urban heat island impacts in existing MFR buildings, via the deployment of shading and surface treatment technologies
- Identify tax parcels (units of private land) and buildings for which energy efficiency and urban heat island retrofit measures would be of most benefit from these activities
- Evaluate energy and carbon savings, and thermal resilience impacts of retrofit measures of prioritized buildings in areas with high heat vulnerability
- Demonstrate a method of building efficiency assessment that relies on drone-based thermal imaging and machine learning algorithm-based data processing to complement data-driven approaches for these retrofits

Figure 1 below outlines the conceptual approach in our analysis. It indicates the down-selection process inherent in our method and reflects the scale at which research and analysis are conducted for each task.

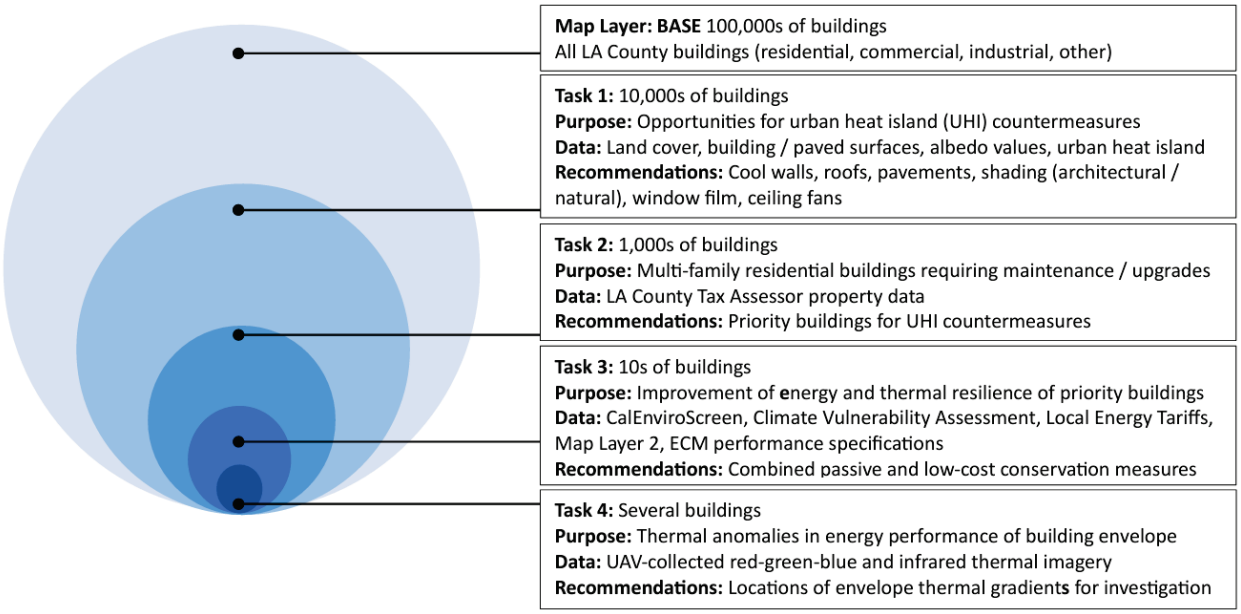

Figure 1. Prioritization methodology for urban heat island countermeasures retrofit modeling and remote building performance assessment.

The method developed is a possible template for future research, relying on data that is available publicly and via project collaborators.

2 Sources of data and information

Table 1 identifies and describes the input data that provided the basis for analysis.

Table 1. Data input and type, source, and description by project task.

Project Task	Data / Information Name and Format	Origin / Source	Description
Task 1	DPW_COUNTY_BOUNDARY, shapefile	LAC ISD	Shapefile outlining boundary of LAC
	LACounty_Parcels, shapefile	LAC ISD	Feature class detailing the outlines and characteristics of approximately 2.4 million property parcels in LAC
	cb_2018_us_county_500, shapefile	United States Geological Survey (USGS)	Shapefile outlining boundaries of U.S. census tracts as of 2018, including 2,651 tracts in LAC
	LARIAC6_2021_Spring, map layer	LAC ISD	Online ArcGIS map layer containing color aerial images of LAC at 2” (5 cm) resolution taken in spring 2021 for the Los Angeles Region Imagery Acquisition Consortium (LARIAC)
	LARIAC6_Buildings_2020, feature class	LAC ISD	LARIAC feature class detailing the horizontal outlines (perimeters) and heights of about 3.3 million buildings in LAC as of 2020
	LANDCOVER_2016, tag image file format (TIFF)	LAC ISD	Raster detailing eight classes of land cover—tree canopy, grass/shrubs, bare soil, water, buildings, roads/railroads, other paved, tall shrubs—at 9” (23 cm) resolution
	Panoptic land cover rasters, TIFF	Google (proprietary)	Raster set detailing 10 classes of land cover in LAC— building, tree, natural ground, water, driveway, parking lot, paved road, unpaved road, sidewalk, or other human-made feature—at 40-cm resolution
	Albedo rasters, TIFF	Google (proprietary)	Raster set that covers most of the populated areas of LAC (including 87.9% of LARIAC6 buildings), except for the Lancaster and Palmdale regions in the northeast. Raster pixels are 64-bit floating point values ranging from 0 (no reflectance) to 1 (complete reflectance).
	Roof segment slopes, shapefile	Google (proprietary)	Shapefile covering most of LAC (including 84.9% of LARIAC6 buildings) that reports the slope of roof segments (planar roof elements). Each shape is a point whose attributes include slope angle (degrees from horizontal) and

Project Task	Data / Information Name and Format	Origin / Source	Description
			azimuth angle (degrees clockwise from north).
	Urban Heat Island Index (UHII), shapefiles	Altostratus, Inc.	Set of four shapefiles giving tract-specific values of UHII in four regions: Lancaster, San Fernando, Santa Clarita, and South Coast Air Basin West (SOCABWEST). These four regions do not fully cover LAC and include only 72.6% of LARIAC6 buildings. No additional shapefiles within LAC are available.
Task 2	Tax parcel dataset, shapefile	LAC ISD	Shapefile representing all land parcels in LAC
	Property Use and Building Type Classifications, published document	LA County (Office of the Assessor)	Summary translations for the system of codes denoting building types and characteristics for tax parcels
	Construction Quality Classification, screenshots of published documents	LA County (Office of the Assessor)	Summary translations for the system of codes denoting property construction quality. Code benchmark denoted to support evaluation.
Task 3	Building footprint from LARIAC6	LAC ISD	Shapefiles with building footprint polygons for buildings in LA County
	Property Use and Building Type	LA County (Office of the Assessor)	Summary translations for the system of codes denoting building types and characteristics for tax parcels
	MF building list from Task 2	Task 2	MF building list with poor construction
Task 4	Building GeoJSON	RGB images acquired during Unmanned Aerial Vehicle (UAV) flight	GeoJSON files of the buildings with UAV flights in LA county. (GeoJSON is a format for encoding a variety of geographic data structures.)
	3D photogrammetry (lidar point cloud)	Pix4d cloud software	LAS files of the buildings with UAV flights in LA County. (The LAS format is a file format designed for the interchange and archiving of lidar point cloud data.)

3 Task 1—Identification of opportunities to mitigate the urban heat island effect

3.1 Task overview

Solar-reflective ("cool") roofs and walls can save energy in an air-conditioned building or improve thermal comfort in an unconditioned ("free-running") building by reducing the building's solar heat gain. Trees and artificial canopies (e.g., shade sails) that shade the building can do the same. Solar heating of dark, dry urban surfaces, including roofs, walls, and pavements, also aggravates the urban heat island effect (UHIE), or the extent to which the near-ground outside air temperature in a city exceeds that in surrounding rural areas. Heat-island countermeasures such as cool roofs, cool walls, cool pavements, and urban vegetation (including but not limited to trees) mitigate the UHIE, further lowering demand for air conditioning and boosting thermal comfort.

In this task, we analyzed a wide variety of geospatial datasets with geographic information system (GIS) software to assess the potential to implement urban heat island (UHI) countermeasures in LAC. We focused on the albedos (solar reflectances) and potential increases to the albedos of roofs, pavements, property parcels, and census tracts; the extent to which buildings are likely to be shaded by trees; and the potential for planting more trees near buildings.

Trees and other vegetation can also reduce the UHIE through evapotranspiration—a phenomenon that has been widely studied in Los Angeles [7–13].

3.2 Task data sources

LBNL acquired from LAC ISD and other sources, including the United States Geological Survey (USGS), Google, and Altostratus, Inc.

Datasets from LAC ISD and Google were received under a two-year LBNL-LAC ISD-Google mutual non-disclosure agreement (NDA) executed 2022-03-22.

Sample images of each of the following datasets are shown in Section 1 of Appendix A.

LAC, U.S. census tract, and property parcel boundaries. LAC ISD provided DPW_COUNTY_BOUNDARY, a file geodatabase feature class outlining the boundary of LAC, and LACounty_Parcels, a feature class detailing the outlines and characteristics of approximately 2.4 million property parcels in LAC. We downloaded from USGS cb_2018_us_county_500, a shapefile outlining boundaries of U.S. census tracts as of 2018, including 2,651 tracts in LAC.

Aerial image rasters. LAC ISD provided server access to LARIAC6_2021_Spring, an online Esri ArcGIS map layer containing color aerial images of LAC at 2" (5 cm) resolution taken in spring 2021 for the Los Angeles Region Imagery Acquisition Consortium (LARIAC) (Figure 2a).

Building shapefiles. LAC ISD provided LARIAC6_Buildings_2020, a LARIAC feature class detailing the horizontal outlines (perimeters) and heights of about 3.3 million buildings in LAC as of 2020.

Land cover rasters. LAC ISD supplied LANDCOVER_2016, a tag image file format (TIFF) raster detailing eight classes of land cover—tree canopy, grass/shrubs, bare soil, water, buildings, roads/railroads, other paved, tall shrubs—at 23 cm (9") resolution (Figure 2b). Google provided proprietary "panoptic" rasters detailing 10 classes of land cover in LAC: building, tree, natural ground, water, driveway, parking lot, paved road, unpaved road, sidewalk, or other human-made feature—at 40-cm resolution. We received for each land-cover class (LCC) a set of 28 tag image file format (TIFF) rasters (land-cover "tiles") that collectively cover all of LAC. Raster pixels are 4-bit integers equal to 1 if the class applies, or 0 otherwise.

Both the 23-cm LANDCOVER_2016 raster from LAC ISD and the 40-cm panoptic rasters from Google offer excellent information about land cover in LAC. We elected to use Google's panoptic rasters because (a) they distinguish four classes of paved surface—paved road, sidewalk, parking lot, and driveway—while the LANDCOVER_2016 raster has only two classes for paved surfaces—roads/railroads and other paved— and (b) pixels classified as roads/railroads in LANDCOVER_2016 may or may not be paved roads.

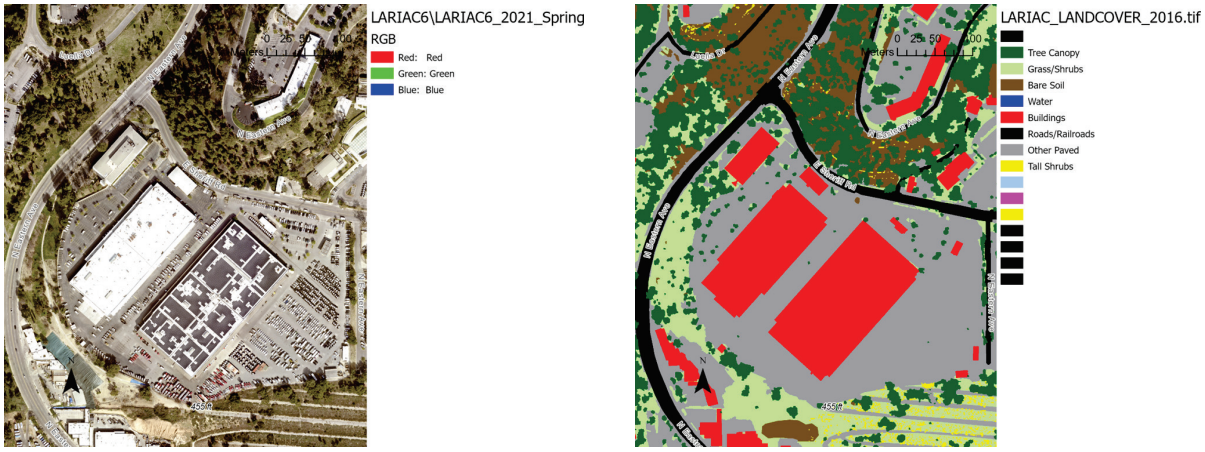

(a) (b)

Figure 2. Excerpts from (a) LAC ISD color aerial image layer LARIAC6_2021_Spring and (b) LAC ISD land-cover raster LARIAC_LANDCOVER_2016 containing the LAC ISD building site (building at upper left of parking lot).

Albedo rasters. Google provided 177 proprietary albedo rasters (albedo "tiles") that collectively cover most of the populated areas of LAC (including 87.9% of LARIAC6 buildings), except for the Lancaster and Palmdale regions in the northeast. Raster pixels are 64-bit floating point values ranging from 0 (no reflectance) to 1 (complete reflectance).

Roof segment slope shapefiles. Google provided a shapefile covering most of LAC (including 84.9% of LARIAC6 buildings) that reports the slope of roof segments (planar roof elements). Each shape is a point whose attributes include slope angle (degrees from horizontal) and azimuth angle (degrees clockwise from north).

Urban heat island index shapefiles. The urban heat island *effect* (UHIE) is the urban minus nonurban air temperature difference [K]. The urban heat island *index* (UHII) [°C·h], computed as the time integral of the UHIE over a 6-month period spanning summers 2006 and 2013 (June, July, and August of each year), quantifies the extent and severity of urban heat islands. It was assessed across California by Altostratus, Inc. for the California Environmental Protection Agency (CalEPA). Altostratus provided four shapefiles giving tract-specific values of UHII in four regions: Lancaster, San Fernando, Santa Clarita, and South Coast Air Basin West (SOCABWEST). These four regions do not fully cover LAC and include only 72.6% of LARIAC6 buildings. No additional shapefiles within LAC are available from the CalEPA project.

3.3 Task methods

We evaluated the source geospatial datasets to identify opportunities to apply UHI countermeasures, such as reflective roofs, reflective walls, reflective pavements, and shade trees, within LAC. We also developed a highly simplified approach to estimate the potential reductions in outside air temperature that could be achieved by increasing the solar reflectance of roofs, walls, or pavements in LAC.

Using the GIS tool ArcGIS Pro 3, we

- Merged the land-cover tiles provided by Google to create 10 land-cover rasters (one per LCC) covering all of LAC
- Merged the albedo tiles provided by Google to create an albedo raster covering most of LAC
- Merged the UHII shapefiles provided by Altostratus
- Cross-referenced buildings, parcels, and tracts
- Calculated LCC distributions of each parcel and tract
- Calculated the albedo of each parcel and tract, and the albedo of each land-cover class within each parcel and tract
- Calculated the median roof-segment slope for each building, using this value to classify building roofs as low-slope or high-slope
- Calculated the gross roof area, gross wall area, and low-slope gross roof area of each LARIAC6 building, as well as the corresponding areas contained within each parcel and tract
- Calculated the fractions of land area within 10 m of each building that is occupied by trees, natural ground, or other buildings, then computed mean values of these “proximity fractions” by parcel and tract
- Estimated the extent to which roof, wall, and pavement albedos could be increased within each parcel and tract
- Estimated potential reductions in summer-afternoon outside air temperature that could be achieved in each tract by raising roof, wall, and/or pavement albedos

The process is detailed and illustrated in Section 2 of Appendix A.

3.4 Task outcomes

Summary statistics for all Task 1 outputs are reported in Table A-3 (Appendix A). Maps and histograms of each outcome are provided in Section 3 of Appendix A.

Land cover class fractions by tract. While roofs and pavements cover only 7% and 9% of LAC, the median values of roof, pavement, tree, and natural ground fractions of individual tracts are 27%, 31%, 13%, and 17%, respectively. This indicates that there are substantial roof and pavement areas available to modify, and substantial natural ground areas available to plant trees, where people live.

Albedos and potential albedo increase by tract. Median values of tract, roof, and pavement albedos are 0.16, 0.19, and 0.15, respectively, suggesting that on average they are currently quite dark.

The median value of the low-slope fraction of gross roof area is 38%, indicating that in a typical tract, more than a third of the gross roof area could be surfaced with high-albedo (typically white) roofing products.

Median values of potential increases to tract, roof, and pavement mean albedos are 0.17, 0.33, and 0.25, respectively, indicating substantial opportunities for brightening. (Potential increases to tract albedo will always be lower than potential increases to roof or pavement albedo because tracts contain other features, such as trees and natural ground, that will not be brightened.)

Figure 3 illustrates the potential increases in mean roof albedo by tract.

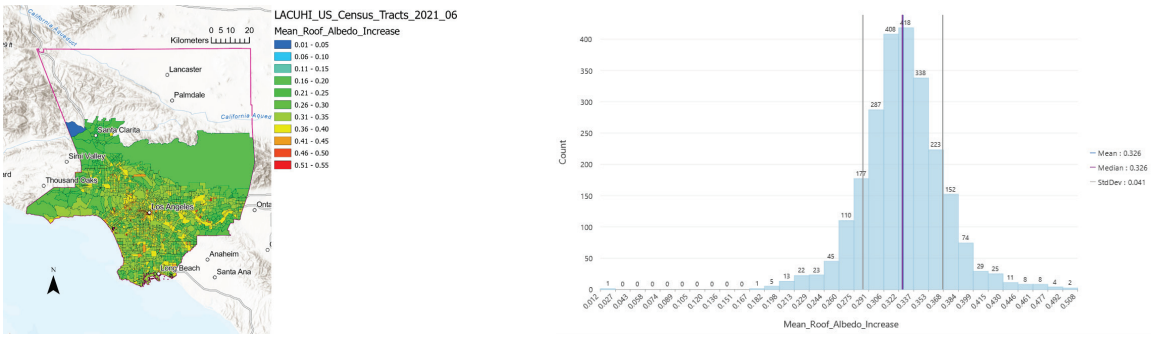

(a) (b)

Figure 3. Map (a) and histogram (b) of potential increase in mean roof albedo (scale 0 – 1) by tract.

Tree, natural-ground, and building proximities by tract. Median values of tree, natural-ground, and LARIAC buildings proximities are 16%, 18%, and 23%, respectively, suggesting that (a) many buildings are not closely treed, (b) there is a modest amount of natural ground near buildings available to plant trees, and (c) the 10-m wide buffer around a building is more likely to contain neighboring buildings than trees or natural ground.

Summer afternoon air temperature reduction[1]**.** The median values of roof, wall, and pavement density are 25%, 42%, and 31%, respectively, indicating that a typical tract has substantially more gross wall area than gross roof area. Median values of potential cool-roof, cool wall, cool pavement, and cool roof + cool wall + cool pavement UHIE reduction are 0.75, 0.72, 0.48, and 1.11 K, respectively. Walls yield smaller median UHIE reductions than roofs even though median wall density exceeds median roof density because the "albedo cooling effectiveness" (UHIE-reduction factor) for walls is only 28% that for roofs. However, we can see that based on

[1] Summer afternoon air temperature reductions are extrapolated from the results of prior studies and should be considered indicative rather than definitive.

the rough extrapolation method used here, a cool-surface campaign targeting roofs, walls, and pavements could yield a median 1.1 K reduction in summer-afternoon air temperature.

3.5 Task conclusions and recommendations

There are substantial opportunities to reduce unwanted solar heating of buildings and pavements in LAC and mitigate the UHIE with cool roofs, walls, and pavements. There is also sufficient natural ground near buildings to potentially double the number of shade trees near buildings.

We propose using GIS software to further analyze the geospatial data in the building, parcel, and tract feature classes and/or relate them to external data. Here are a few examples.

- Using UHI countermeasures to reduce excess heat exposure. What tracts in LAC have a high pollution burden per CalEnviroScreen [14] and high potential UHIE reduction?
- Identifying cities or districts that could benefit from UHI countermeasures. Which cities or districts contain the tracts with the top-decile or top-quartile values of roof/wall/pavement surface density, potential albedo increase, or potential UHIE reduction?
- Identifying opportunities for accelerated replacement of roofs or pavements. What is the roof/pavement age (years since last permitted installation or replacement) vs. potential increase in roof/pavement albedo, by parcel or tract?

We also recommend using the albedo and tree-cover datasets generated by our analysis as inputs to building energy simulations and urban climate simulations to predict the energy savings, comfort improvements, heat danger reduction, and UHIE mitigation attainable from heat island countermeasures across LAC.

4 Task 2—Identification of priority tax parcels and buildings

4.1 Task overview

The objective for this task was to identify and prioritize multi-family residential buildings that offered opportunities for significant energy and demand savings, for inclusion in the energy efficiency retrofit analysis in Task 3. Separately, a final dataset was also shared with LAC ISD, for their direct use and separate prioritization process for identifying building clusters and prioritizing specific parcels and buildings for energy efficiency upgrades.

LAC ISD prioritized MFR because energy efficiency upgrades to this building type offer a scale-economy opportunity by benefiting numerous dwellings at a single site. This scale benefit is seen at every step of the project lifecycle and so has a multiplier effect on the cost-effectiveness of the approach. The initial engagement and scheduling of work, preparation and construction staging, coordination and work execution, and commissioning and completion of retrofit work can all be done in contract with a single owner at a single location, which hugely reduces the per-dwelling transaction and implementation costs. To further enhance these benefits, MFR parcels containing a high number of homes were prioritized.

Renters in MFR properties are generally less economically secure than renters in single-family residential properties, and renters are unlikely to invest in energy-efficient technologies for their accommodation. Landlords

are not typically the direct beneficiaries of energy efficiency investments that they make and so are not incentivized to make these investments themselves. This well-understood "split incentive" can result in a gradual decline of a building's overall condition. An objective for LAC ISD was to explore mechanisms by which these dual disincentives could be addressed, while simultaneously tackling other socio-economic and environmental policy priorities.

Tackling buildings in poor overall condition is an LAC ISD priority. Poor building condition tends to indicate poor energy efficiency performance; improving insulation, reducing solar gain, and supporting passive cooling strategies offer an opportunity for significant reductions in energy consumption and peak electricity demand, and savings in energy costs and carbon emissions.

Implementing energy efficiency upgrades in poorly performing buildings also tends to benefit underserved and disadvantaged communities, as the building stock tends to be in worse condition in these areas. By addressing this market, the economic benefits of energy efficiency are felt in local communities as a whole, as resources otherwise spent on energy will instead be used to procure other goods and services.

4.2 Method and data sources

Analysis for Task 2 was based on the interrogation of a single LAC ISD dataset–the LAC Tax Assessor Parcel data [15]. The parcel database represents total taxable land assets in the county and contains over 2.4 million individual records (one per land parcel). Each record contains numerous data fields that detail the land parcel and its permanent structures. The data fields of interest include (1) building type, denoted by current use of the primary structure; (2) number of permanent structures present (maximum of five per parcel); (3) number of residential units within each structure; and (4) current construction quality of each structure. Item 4 is a numerical score that can be compared to a minimum standard for new construction in most municipalities.

Utilizing geographic information system software (Esri ArcGIS Pro 3), we queried the parcel database according to building type and construction quality to identify multi-family residential buildings deemed by the Tax Assessor to be in relatively poor condition, and to determine the number of residential units contained within each of those buildings.

An important benefit of employing database analysis tools with graphical outputs is the essential support for and insight into multi-characteristic analysis. Data records can be viewed both in the context of the research and more generally: it is possible to check, verify, and—if need be—amend an analysis framework to incorporate desired records, and implement corrective action based on observations of the data (i.e., where there are records present that look erroneous given the search criteria). This process can be invaluable when interrogating such a large dataset.

The Tax Assessor database contains information and data for each land parcel (data row) in many tens of fields (data columns). Several of the data fields are of particular interest for the Task 2 analysis:

- Use Code (Property type and number of structures per parcel)
- Unit Numbers (Building)
- Quality Classification (Building)

Use Code: a field containing an alphanumeric code for each tax parcel, indicating the current primary use of the building(s) on the parcel. The submitted code represents the predominant or majority use in cases where there is more than one use. There is a single Use Code assigned to each tax parcel.

Unit Numbers: fields each containing an integer, indicating how many residential units are present within each building on the tax parcel. There are up to five submissions for numbers of Units (Units1, Units2, …Units5) that correspond to a maximum of five buildings per tax parcel. Prioritization of parcels and buildings with high unit numbers reflects the scale-economy benefits of retrofitting multiple units at a single location.

Quality Classification: each field in this field group contains an alphanumeric code, and includes an integer that represents the overall construction quality and condition rating for each building, per the Tax Assessor inspection. Up to five ratings are submitted for each parcel (QualityClass1 through QualityClass5) according to the number of buildings present. Values for each building range from 1 to 14, with higher scores being better, with a score of 5.5 being equivalent to the minimum standard for new construction in most local municipalities. Prioritization of parcels and buildings for energy efficiency retrofits is based on the construction quality rating applied to each building. This single score for each building reflects a multi-category property assessment, the outline for which is provided in the California State Board of Equalization Residential Building Costs Handbook [16].

4.3 Task outcomes

There are two main outputs from this task: (1) a dataset of buildings for use in Task 3 analysis, and (2) a larger dataset of buildings of interest to LAC ISD.

Dataset 1: Buildings to prioritize for building energy efficiency measures. We queried the parcel database for MFR priorities based on (a) the Property Use classification “05” (Five or More Apartments or Units or Cooperative or Own-your own projects not separately parceled), and (b) the Building Design Type classification “05” (Five or More Apartments or Multi-story Apartment – (Five Stories and Over)). This Property Use class was prioritized because each building contains many units. This process excluded Building Design Type classification “03” and “04” which also have an MFR designation. These excluded classes largely have fewer units per parcel and therefore are a lower priority. LAC ISD also requested that buildings outside the City of Los Angeles be prioritized since the Los Angeles Department of Water and Power (LADWP) has primary responsibility for those in the city.

The resulting parcel dataset can be characterized as having the following properties:

- MFR building categorized as “05” Property Use type
- MFR buildings with many units (≥5, ranging up to a maximum of 241)
- MFR buildings with low Quality Class scores (2-5)
- LAC ISD MFR building located outside the City of Los Angeles

Dataset 2: A larger set of buildings of interest to LAC ISD. We produced a separate dataset for use by LAC ISD that adopts broader qualifying criteria for MFR parcels/buildings. This translated to a significantly larger sample size and included buildings with low numbers of units therein. This dataset is shown in Figure 4 has the following properties:

- Includes Property Use classifications “03”, “04”, and “05” [2]
- Includes MFR buildings within the City of Los Angeles, presumably for sharing with LADWP.

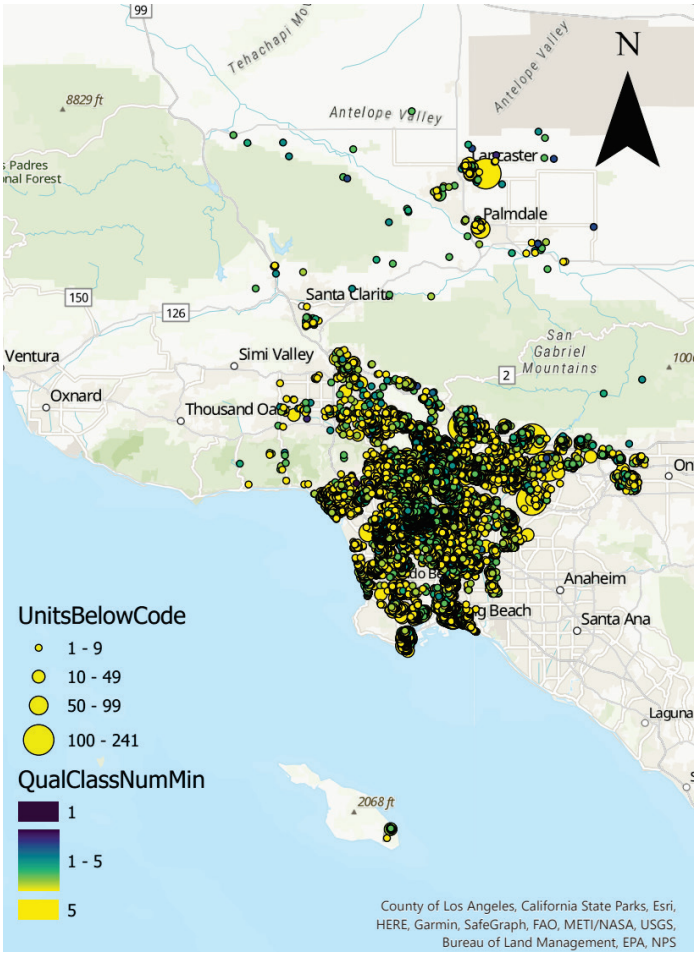

Figure 4. Filled circles locate all tax parcels designated as multi-family residential and assessed as below code equivalent; each circle’s size indicates the total number of units below code and its color corresponds to the minimum assessment rating for units on that parcel. A rating of 5.5 is considered code equivalent; the map contains units assessed with ratings of ≤5.

4.4 Task conclusions and recommendations

There is a vast stock of MFR buildings (>43K buildings, holding over 150K individual homes) in Los Angeles County that are reportedly below the code-equivalent threshold, representing a significant opportunity for building upgrades to reduce the UHI effect. The far larger number of buildings assessed as being in a good state of repair may also present good opportunities for scale energy efficiency policies generally, and activities to ameliorate the impacts of the urban heat island effect on residents specifically, as any energy system upgrades

[2] Property Use Classification 03 represents parcels with a “total of three residential units (any combination)”, while Property Use Classification 04 represents parcels with a “total of four residential units (any combination)”. The term “any combination” means the parcel can contain any mix of single-unit dwellings and/or multi-unit dwellings.

are likely to have left opportunities to raise building envelope albedos. As such, the output dataset from Task 2 may prove to be a valuable resource for LAC ISD.

The method utilized for this task is a reminder that insightful data is being routinely collected, although data owners may not always be aware of what utility it has beyond its original intended purpose. It is worth describing data libraries in such a way that the full range of characteristics they represent can be fully understood, and consequently that these data are more widely utilized. Information on construction quality, construction materials and type, and the presence of amenities such as air-conditioning are examples of data specific to individual properties that are of value beyond the realm of the intended primary user (the tax assessor).

We recommend that the construction quality rating system be augmented to support a more detailed understanding of individual aspects of the building's character, construction quality, and condition. This would require tax assessors to observe, collect, and record a little more information, but the resulting data for specific priority characteristics would add further value and utility to the Tax Assessor dataset. In the context of this project, such activity would result in better targeting of buildings for energy efficiency retrofits than is currently possible.

5 Task 3—Building modeling and simulation

5.1 Task overview

With climate change, there is an increasing occurrence of extreme weather events such as heatwaves and wildfires. Meanwhile, power outages are increasing in the U.S. The compound impact of heatwaves and power outages poses a serious health risk for residents due to indoor heat exposure, especially for those living in disadvantaged communities where housing lacks adequate cooling (aging cooling equipment or no air-conditioning [AC]) and is poorly constructed or maintained, with a leaky and less-insulated envelope.

This task used building modeling techniques to simulate the thermal performance of vulnerable multi-family buildings in LAC. We then evaluated mitigation measures to reduce energy use and energy costs, and to improve the thermal safety of residents in those affected buildings under current and future weather conditions.

5.2 Task methods

5.2.1 Data and process to select the vulnerable multi-family buildings

We screened the multi-family buildings in disadvantaged communities based on open data from the state of California and LAC, including various social and environmental metrics at the census tract level. We then ranked the census tracts that were within the county but outside the Los Angeles City limits that needed more attention based on an integrated set of factors. Those factors included the CalEnviroScreen 4.0 score, Healthy Places Index (HPI), Social Vulnerability Index, Equity Explorer Index, HPI Extreme Heat Index, and the construction quality dataset for the MFR units from Task 2. From the ranking, 13 multi-family buildings with a total of 108 housing units were selected from four census tracts in the district of El Monte. Figure 5 shows the location of the four selected disadvantageous communities. Table 2 shows the selected top four census tracts represented in geoid in

El Monte with the multifamily housing units that can benefit from retrofits to address environmental and social issues. These housing units are assumed to use residential electric split direct exchange (DX) coils for cooling and natural gas furnaces for heating. About 20% of the housing units are assumed to have no space cooling for the thermal resilience study during the power outage conditions during heatwaves.

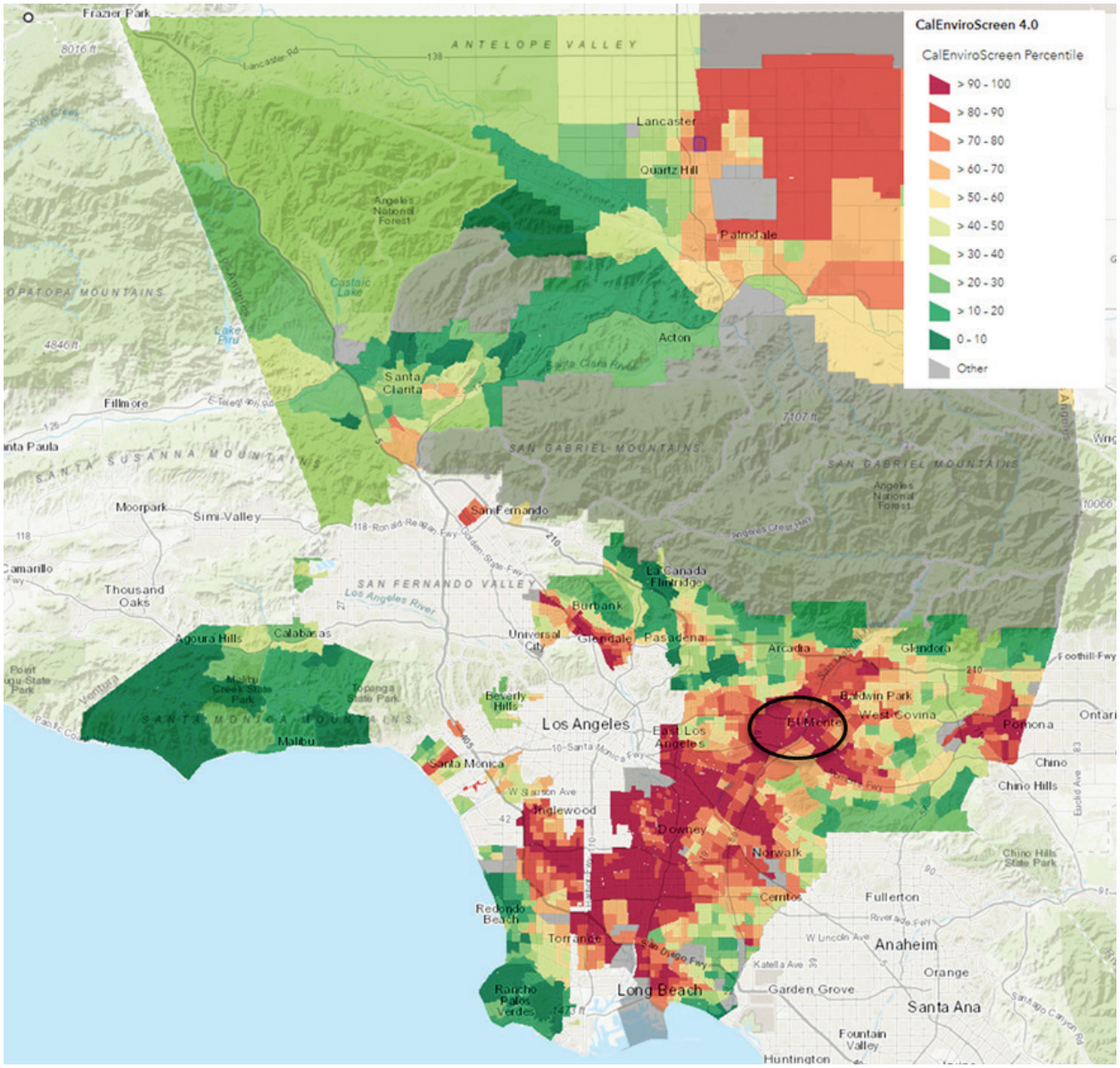

Figure 5. The location of the disadvantaged communities in El Monte from the CalEnviroScreen 4.0 color-coded map of LA County.

Table 2. Four selected census tracts with the multifamily buildings' construction quality and environmental and social index data

Geoid	Number of multi-family buildings	Total multi-family units	Multi-family building gross floor area [m²]	Units below construc-tion code	Construc-tion quality class number	CalEnviro Screen 4.0 score[a]	Healthy Places Index value[b]	Social Sensitivity Index tercile[c]	Equity Explorer Index percentile[d]
6037433403	2	24	1,457	15	4.75	51	-0.81	3	95.9
6037432802	9	65	5,730	65	5.00	64	-0.94	2	97.1
6037433305	1	22	1,648	22	5.00	52	-0.88	3	84.8
6037433402	1	6	335	6	5.00	56	-0.78	2	80.4

[a] A higher CalEnviroScreen 4.0 score signifies increased vulnerability

[b] A lower Healthy Places Index value signifies poorer health

[c] The top tercile of the Social Sensitivity Index (3) is most vulnerable

[d] A higher Equity Explorer Index percentile signifies increased need

5.2.2 Building model creation and simulation

We modeled the 13 multi-family buildings using the CityBES tool [17] to evaluate their energy and thermal resilience performance. The 2019 LARIAC5 GIS data was used for building footprint generation. The assessor's data included in the GIS dataset [18] was used to determine the vintage of the buildings, which assigns the multi-family building's baseline envelope and system efficiency parameter values based on the Title 24 requirements under the specific vintage and the California building climate zone (CZ 06). The exterior roof albedo input used the dataset generated in Task 1. All multi-family buildings were built before 1980, which indicates poor envelope insulation and construction quality. Task 2 dataset shows that the construction quality is lower than or equal to the code requirement. The baseline multi-family building energy models assume 1 air change per hour (ACH) infiltration with natural ventilation and no ceiling fan. The study assumed an AC system with various cooling setpoint temperature controls. Three out of 13 baseline multi-family buildings, comprising 22 units (20.4%), were assumed to have no AC system installed. The remaining 10 multi-family buildings have mechanical cooling systems. Among them, seven buildings with 48 units (44.4%) have a cooling setpoint temperature (CST) of 75 °F (23.9 °C), reflecting normal AC operation, and three buildings with 38 units (35.2%) have an increased CST of 78 °F (25.6 °C), assuming some residents in the disadvantaged community choose to raise their cooling setpoint to reduce their utility bill. For the energy efficiency analysis, we evaluated seven energy conservation measures (ECMs), focusing on low-cost building envelope and low-energy cooling interventions. These include cool roofs, cool walls, solar control window films, air sealing, internal window blinds, natural ventilation, and ceiling fans. Table 3 details the seven ECMs modeled in CityBES. These measures focus on reducing solar heat gain through windows or walls/roofs and decreasing heat transfer from outdoors to indoors through the envelope or air infiltration. The building energy simulations were conducted using the EnergyPlus simulation engine and the 2018 actual microclimate data and the projected 2058 future weather data generated from the Weather Research Forecast (WRF) + Urban Canopy Model (UCM) simulations based on the Intergovernmental Panel on Climate Change (IPCC) Representative Concentration Pathway (RCP) 8.5 climate change scenario.

Table 3. Passive and low-power ECMs applied to the multi-family buildings.

Measure type	Measure name	Measure description
Passive measure	Cool wall coating	Exterior wall - Apply cool wall coating yielding wall solar reflectance of 0.60
	Cool roof coating	Roof - Apply cool roof coating yielding roof solar reflectance of 0.60
	Solar control film for windows	Window - Add solar-control window film with thermal transmittance 0.87 Btu/h·ft²·°F (4.94 W/m²·K) and solar heat gain coefficient 0.45
	Interior shading (blinds)	Window - Use window shades during the summer months (May - September) daytime (10 am – 7 pm)
	Air sealing	Infiltration - Seal leaks to reduce infiltration from 1 air change per hour (ach) to 0.3 ach
	Natural ventilation	Window - Enable natural ventilation for rooms with window(s) with an effective opening fraction of 0.4
Low-power measure	Ceiling fan	Ventilation - Add ceiling fan in residential buildings allowing a higher cooling setpoint temperature (82 °F [28 °C]) in summer without increasing thermal discomfort

5.3 Task outcomes

For energy performance analysis, this task evaluated annual site energy use, annual greenhouse gas emissions, annual utility costs, and peak electricity demand in 2018 and 2058 weather conditions. For thermal resilience analysis, this task used heat index and standard effective temperature (SET) to evaluate the occupants' thermal comfort and heat exposure under the heatwave events for 2018 and 2058.

The baseline multi-family buildings in disadvantaged communities in El Monte under 2018 weather data show a higher annual heating natural gas site energy use intensity (EUI) (median 2.0 kWh/ft² [21.3 kWh/m²]) than the electricity EUI for cooling (median 1.5 kWh/ft² [16.3 kWh/m²]). The climate change reflected in 2058 future weather data shows that the buildings will have a 26% increase in cooling electricity EUI to 1.9 kWh/ft² (20.6 kWh/m²) and a 31% reduction in heating natural gas EUI to 1.4 kWh/ft² (14.8 kWh/m²) compared to the baseline EUI in 2018. This tells us there needs to be more attention given to the increased cooling load from buildings in the future. Climate change increases the total median electricity usage by 7% and reduces the total median natural gas by 8% for multi-family buildings from 2018 to 2058.

Under the 2018 weather conditions, the retrofit ECM package is composed of seven measures—cool roof, cool walls, solar-control window films, blinds, natural ventilation, air sealing, and ceiling fans—which yield an electricity savings of 17%. Also, the package contributes to the 19% peak electricity demand reduction. However, it increases natural gas usage by 53%. Among the measures in the ECM package, the cool roof, cool walls, and solar control window films reduce cooling energy usage during the summer, but they contribute to a penalty in heating load during the winter.

California has higher percentages of renewable and hydropower sources for electricity generation than any other state in the U.S., yielding electricity primary energy and CO_2e emission factors lower than the U.S. average. The CO_2e emission factor is 0.6 lbs/kWh (272 g/kWh) for electricity and 0.5 lbs/kWh (225 g/kWh) for natural gas for California 2021 average. The source energy factor is 2.05 for electricity and 1.09 for natural gas. Due to these factors, and the estimated building energy performance described above, there is a 9% increase in the CO_2e emission intensity and a 3% increase in the source energy for the buildings in the retrofit case.

Heat exposure under the heat danger and caution conditions can be evaluated using the heat index metric. During the five days (120 hours) of heatwave events of July 6 to 10 in 2018 and 2058, if buildings had grid power and were mechanically cooled to either normal CST or the increased CST, building occupants would not face any heat danger or caution conditions. However, if buildings were connected to the power grid but not mechanically cooled (no AC), they would face heat danger conditions all the time during the heatwave period. This is partly caused by the internal heat gains from appliance usage. The retrofit could reduce the heat danger hours by 50% in 2018 and 34% in 2058 for the housing units with power connected but without mechanical AC systems.

If the buildings lose power due to grid power interruption during the heatwave period, about 90% of the housing units would experience about 21 hours of heat danger conditions and 91 hours of heat caution conditions in 2018, and about 50 hours of danger and 64 hours of caution with the 2058 future weather. The retrofit helps to eliminate the heat danger condition, but there are still many hours of heat caution conditions. Among the measures from the ECM package, natural ventilation contributes the most to mitigating the heat-related danger risk during power outages, as the indoor temperature is higher than the outdoor temperature. Ceiling fans increase air movement near human skin, helping occupants maintain thermal comfort under the increased indoor air temperatures [19].

Heat stress can also be evaluated during the heatwave period based on the SET (standard effective temperature) metric. Heat stress hour is defined as an hour when indoor SET is higher than 86 °F (30 °C). If AC systems can be operated normally during the heatwave event, the housing units face about five heat stress hours. If buildings can run AC with the increased cooling setpoint temperature, they may face 18 heat stress hours. As the SET metric includes the indoor air temperature as a key factor, increasing the CST from 75 °F (23.9 °C) to 78 °F (25.6 °C) leads to slightly more heat stress hours (about 10 hours out of the entire 120 hours of the heatwave period) for the baseline MF buildings. Nevertheless, the CST increase serves as an effective demand response strategy to reduce cooling demand during the heatwave period to mitigate grid burden. If the MF units with AC systems are retrofitted, they will not experience heat stress conditions. However, if buildings have power but do not have AC, occupants would be exposed to heat stress hours all the time during the heatwave period. This is partly caused by the internal heat gain from appliance use. The retrofit can reduce 34% of the heat stress hours for these buildings. If buildings are under power outage conditions, all units would face heat stress conditions all the time (120 hours). If retrofitted, the heat stress hours would be reduced to 41 hours (62% reduction) in 2018, and to 61 hours (46% reduction) in 2058.

5.4 Task conclusions and recommendations

We screened all census tracts in LAC and ranked them to select four census tracts in El Monte that need more attention to energy burden and overheating risk. Thirteen multi-family buildings with a total of 108 units were selected in those four census tracts for analysis. We developed a baseline building dataset in CityBES to model the 13 buildings for energy and resilience performance. Next, we developed an ECM package with seven passive

and low-power ECMs for the retrofit scenario, which includes the cool roof, cool walls, solar control window films, air sealing, internal window blinds, natural ventilation, and ceiling fans. We conducted building energy simulations using the 2018 actual microclimate data and the projected 2058 future weather data based on the IPCC RCP 8.5 climate change scenario.

The future weather leads to an increase in annual electricity usage by 7% due to the cooling load increase and a decrease in natural gas usage by 8% from the reduced heating load due to climate warming in 2058 compared to 2018 weather conditions. Under the 2018 weather conditions, the retrofit scenario with the ECM package can save 17% of annual electricity use from the reduced cooling loads but increase 53% of the annual natural gas use due to the heating penalty of the winter season. The ECM package reduces the peak electricity demand by 19% and reduces the annual energy cost by about $183 per housing unit. Under the 2058 projected weather, the ECM package can achieve an 11% annual electricity use savings but with a 47% increase in annual natural gas usage, resulting in an overall 10% increase in the annual total site energy.

We evaluated the heat exposure of residents under the danger and caution conditions using the heat index metric, and under heat stress hours using the SET metric for the five-day (120 hours) heatwave from July 6 to 10. When the buildings have grid power and are mechanically cooled, they would not face any heat danger or caution conditions. This confirms that AC is a life-essential need for residents during a heatwave. For the multi-family buildings without AC systems but still connected to the power grid, they would face heat danger conditions and heat stress hours almost all hours during the heatwave period, both in 2018 and 2058. During a heatwave event, it is strongly recommended to minimize the use of electric appliances to reduce internal heat gains. If the buildings are retrofitted with the ECM package, the danger hours can be reduced by 50% in 2018 and 34% in 2058.

If the current baseline multi-family buildings lose power from the grid during the heatwave event, occupants would face more heat-related danger conditions, from a median of 21 hours in 2018 to a median of 50 hours in 2058 due to climate change. However, if the buildings are retrofitted, they would not face danger conditions based on the heat index metric during the heatwave period coincident with power outages in current and future weather conditions. If using the SET metric, all the baseline multi-family housing units would face the heat stress condition all the time during the five-day heatwave period (120 hours) due to a power outage. If retrofitted, the heat stress hours are reduced to 41 hours in 2018 (a 62% reduction) and 61 hours in 2058 (a 46% reduction).

In summary, the multi-family apartment units in disadvantaged communities in LA County are facing a growing risk of indoor overheating during hot summer days, especially for those without AC. The heat stress risk increases due to climate change. Retrofitting these housing units with passive envelope measures and low-energy active measures (such as a ceiling fan) can reduce utility costs for households and more importantly, can significantly reduce danger-level heat risk during the worst case: combining a heatwave with coincident power outages. During the retrofits (energy efficiency upgrades, decarbonization) of buildings to reduce utility costs and carbon emissions, policymakers and building owners should consider the health benefits and thermal safety of residents from improvement in thermal resilience.

Further modeling and analysis to consider in future studies:

1. Conduct energy efficiency and heat-related impact analysis for each passive or low-power measure. This will enable ECMs to be prioritized by decision-makers of LAC.

2. The energy modeling and simulation task can further explore fuel-switching ECMs as LAC aims to decarbonize the building stock. Fuel switching with all-electric systems for heating, service hot water, and cooking may increase the grid's energy burden and peak load.
3. The energy, carbon, and heat-related impact analysis for more MF buildings (e.g., including MF buildings with more housing units per building) at a broader scale in LAC can provide more comprehensive findings for program development.

6 Task 4—Building asset identification and thermal anomaly detection

6.1 Task overview

This task focused on applications of unmanned aerial vehicle (UAV) imagery to a smaller sample of buildings, as compared to previous tasks. In this capacity, the concept under development and demonstration here may fit into a workflow that supports Task 2 and/or Task 3 by (a) providing additional data for the building down selection process and (b) helping to identify and prioritize specific energy efficiency measures according to what the data acquired and processed from the UAV flights indicate regarding thermal performance of the building envelope. The approach seems suitable for assessing the thermal efficiency of the building envelope in larger structures, provided there is sufficient clearance from vegetation up to a specific height (up to 400 ft or 122m, limited by UAV capabilities). These larger buildings, prioritized by LAC, present significant opportunities for implementing energy efficiency enhancements at a scalable level. UAVs offer access to high-resolution imagery of buildings, and these images can be used to generate high-resolution 3D models with the processed data fed to algorithms to perform the assessment and asset evaluation.

Figure 6 shows how Task 4 interfaces with other tasks in this project. Task 2 leveraged parcel data and identified priority areas for action, including building clusters and local communities. The Task 2 output was a primary dataset firstly for the Task 3 team to prioritize buildings for analysis of energy efficiency measures, and secondly for the Task 1 team that identified UHI countermeasures. The Task 3 group looked through the datasets of underprivileged multi-family communities using open data sourced from the state of California and Los Angeles County (LAC). This involved analyzing diverse social and environmental metrics at the census tract level. The team then prioritized and ranked census tracts located within the county but outside the city limits of Los Angeles that could benefit from a detailed assessment, utilizing a comprehensive set of integrated factors. The Task 4 team then leveraged this preliminary scan and ranking to identify the location for the proof-of-concept UAV building assessment.

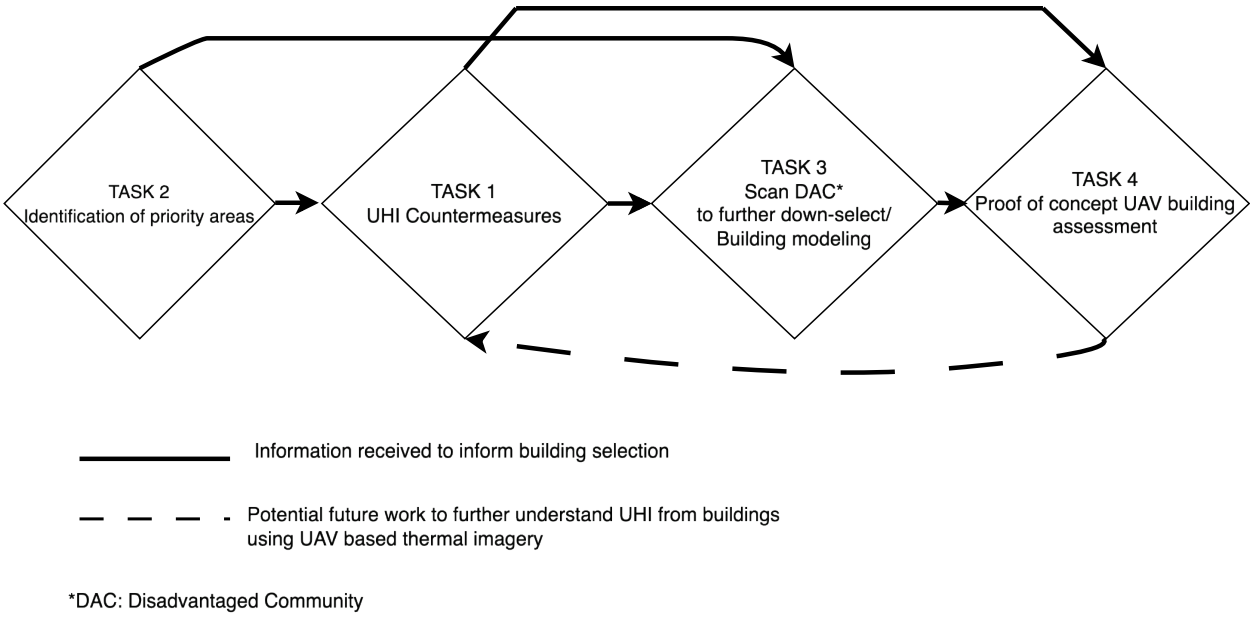

Figure 6. Inter-relationship between tasks or task dependencies.

6.2 Task data sources/data collection

The East LA Civic Center (located at 4801 E. 3rd Street) was identified as the site for Task 4 because retrofit opportunities identified at this site would benefit a low-income neighborhood and because this location had a planned microgrid pilot in the near future, which could potentially benefit from any building energy modeling efforts. The Berkeley Lab Team conducted two flights at the East LA Civic Center location to capture the necessary data needed for post-processing. The East LA Civic Center includes the Civic Center Library, East Los Angeles County Hall, Courthouse, Probation Department, Sheriff's Station, Edward R. Roybal Comprehensive Health Center, and Belvedere Park Lake. Flight 1 took place on September 30, 2022, from 10:30 am to 3:00 pm and flight 2 took place on November 3, 2022, from 9:00 am to 3:00 pm. UAV imagery data were captured using a red-green-blue (RGB) camera and a thermal camera for the six buildings at the site. However, only two of these buildings had a good clearance from vegetation to allow completely unobstructed UAV flights for complete post-processing. These buildings were the East LA Courthouse and the East LA Civic Center Library. The other four target buildings were surrounded by vegetation (trees) which made it very difficult to get the required UAV images to complete a 3D reconstruction for post-processing. The collected UAV images were uploaded into the Pix4D cloud software for post-processing. Figure 7 below are examples of images from the drone flights.

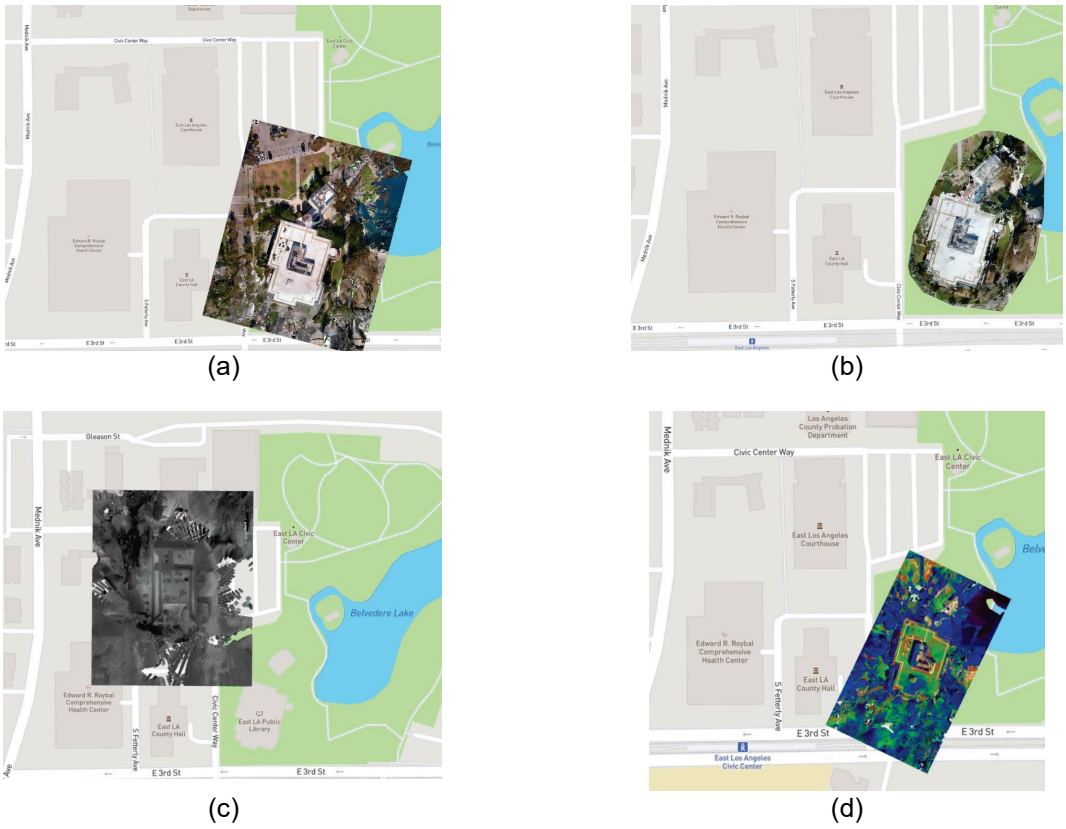

Figure 7. RBG and thermal images captured in drone flights, including (a) top view of UAV RGB images of the East LA Civic Center Library viewed from PIX4D software; (b) top view of the East LA Civic Center Library showing areas closer to the building; (c) thermal image of the East LA Courthouse; and (d) thermal image of the East LA Civic Center Library.

6.3 Task methods

Figure 8 shows the workflow used in the post-processing of the UAV images to create the data layer. We extract the building 3D geometry from drone RGB images, project the 3D points onto 2D space, and finally create a thermally segmented image on which the thermal anomaly detection algorithm is run. A thermal segmented image divides the visual content into distinct segments according to the associated temperature values. The algorithms aim to help automate the extraction of asset information for audits. Information such as the building's footprint or a façade's window-to-wall ratio may be unavailable or challenging to get manually.

One of the unavoidable questions encountered while designing a UAV-based process is the flight path or pattern. Planning a drone flight necessitates an awareness of multiple factors such as distance from target, altitude, speed, overlap, and pattern. Other common drone flight obstacles include battery life, a limited resource, and legal regulations of air space. We overcame these barriers and successfully created a data layer with UAV data and 3D reconstruction using PIX4D cloud. Photos taken during our test drone flight were used in the program Pix4D to generate a 3D point cloud from the 2D images. The program extracts pixels from 2D images by triangulation and locates individual pixels from photos within a 3D point cloud model. During this process, images of inferior quality and images that did not capture the subject were rejected by the program. Using Pix4D modeler, the

program runs a 15-point process that results in a report output noting the efficiency of the photos used in generating the model, image overlap, and location, among other variables. This output notes weaknesses of the image retrieval process and should influence future flights.

UAV images obtained during the flights were processed first using Pix4D for the 3D Reconstruction and then using the Auto Building footprint and Aerial 3D Building Reconstruction from Drone Imagery (A3DBR) library [20]. The thermal images are initially converted to radiometric images for visual inspection. Radiometric images provide temperature data within the image for post-processing, while thermal images only highlight relative temperature differences. These radiometric images can be used to identify hot spots, cold spots, and temperature gradients that may indicate potential issues on the facade and are used as inputs to the thermal analysis pipeline.

The steps involved in the extraction are described in more detail in Figure 8.

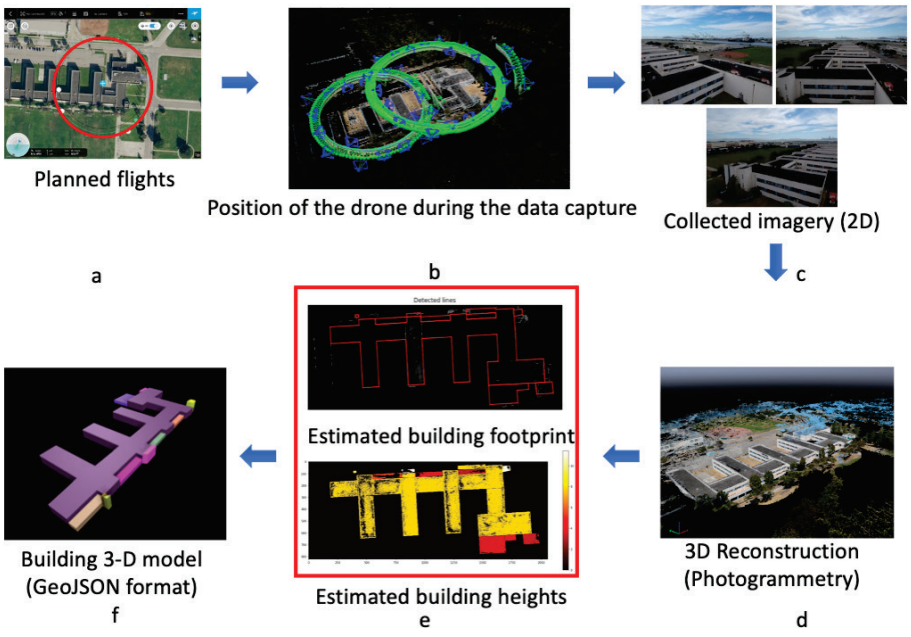

Figure 8. Overview of workflow to generate building asset information from UAV imagery, including (a) planned flights using Pix4D mapper; (b) UAV/drone position during data capture using Pix4D flight planner; (c) images gathered from UAV flight; (d) 3D reconstruction from Pix4D using photogrammetry; (e) machine-learning generated information with estimated building footprint and height using A3DBR; and (f) building 3D model in GeoJSON format from A3DBR. Reproduced with permission from Touzani et al. [21].

Photogrammetry. The set of overlapping 2D RGB images captured by the drone system is processed using the Pix4D photogrammetry software, which generates a set of data points in 3D space. This is achieved by detecting features that are shared across images and using them in conjunction with GPS data to determine 3D points. This set of data points in a 3D space is called a point cloud. Pix4D uses a fully automated process to achieve accurate 3D reconstruction based on the 2D image sets.

Projection of the 3D point clouds into a 2D space. After the point cloud is extracted, the points in the cloud are projected into a 2D grid (top-down view) with a resolution of 0.1 m. This permits a count of the number of

points in a 0.1 m × 0.1 m area. As a result, within this grid, the grid cells corresponding to the building facades will have a very high point density when used for asset extraction and can provide more detailed information.

Thermal segmentation of the building facade image. The Priority-Matrix (P-matrix) file from Pix4D contains information about the internal and external camera parameters from the thermal camera in addition to the RGB camera. We use this information and overlay it with the converted thermal image (temperature-only information) to get thermally segmented building facades, which segment the image based on temperature values.

Potential thermal anomaly detection. The goal of the thermal image anomaly analysis was to use the thermal image information to detect temperature regions in the image that were beyond a particular predefined threshold and would warrant further inspection. A detailed overview of the workflow to identify potential thermal anomalies is shown in Figure 9.

Unusual temperature values on building facades are detected through an image thresholding processing method. In this approach, pixel temperature values that deviate from a pre-established threshold are used as indicators of an anomaly. Specifically, we utilized a threshold value of the outside air temperature (OAT) within a range of ±5 °C degrees to highlight areas in the image that may exhibit potential thermal anomalies.

Finally, a contour was applied to the areas that had a potential thermal anomaly.

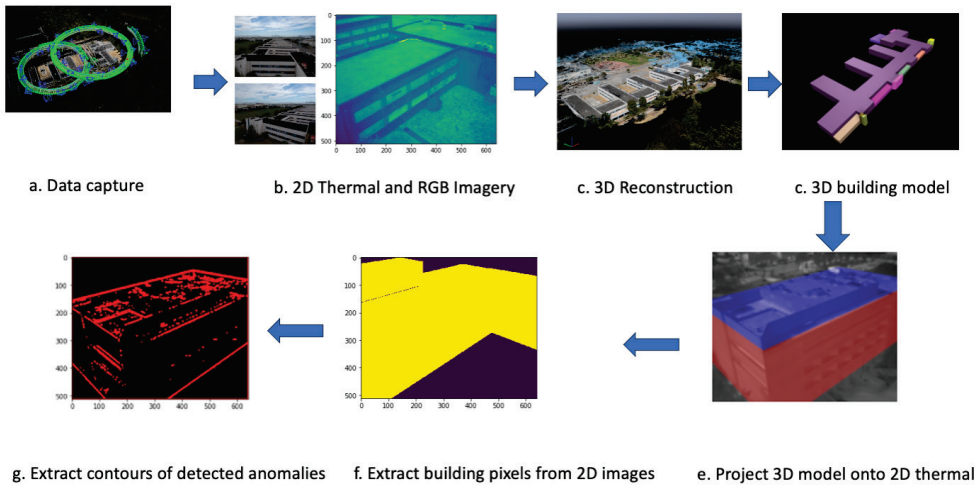

Figure 9. Overview of the workflow to identify potential thermal anomalies, including (a) flight plan for data capture using Pix4D mapper; (b) 2D thermal and RGB images; (c) 3D reconstruction from Pix4D; (d) 3D building model in GeoJSON format; (e) projection of 3D model onto 2D image; (f) extraction of building pixels from 2D image; and (g) detecting anomalies in thermal data and overlaying them onto building facades. Reproduced with permission from Touzani et al. [21].

The RGB images for our dataset were recorded with a Zenmuse XT2 [22] visual camera and a FLIR Tau 2 thermal camera on a DJI Matrice 200 drone [23]; both cameras were factory-calibrated. For the RGB flights, the UAV path was planned and captured using an orbital flight plan in Pix4D capture at normal flight speed (5-7 m/s) and 80% frontal and side overlap. Thermal images were captured by manual flights approximately 5 m

away from each building facade. Due to the high overlap of images, similarities from feature points identified in each image can be extracted to conduct photogrammetry.

Photogrammetry allows the estimation of the three-dimensional coordinates of points on an object in a generated 3D space involving measurements made on images taken with a high overlap rate. Photogrammetry can be used to create a 3D point cloud model of the recorded region.

The data layer, which includes the RGB images, thermal images and 3D point cloud model from LA occupies 200 GB and is only available to the LAC ISD team for research purposes.

Sample thermal images can be found in Figure 10.

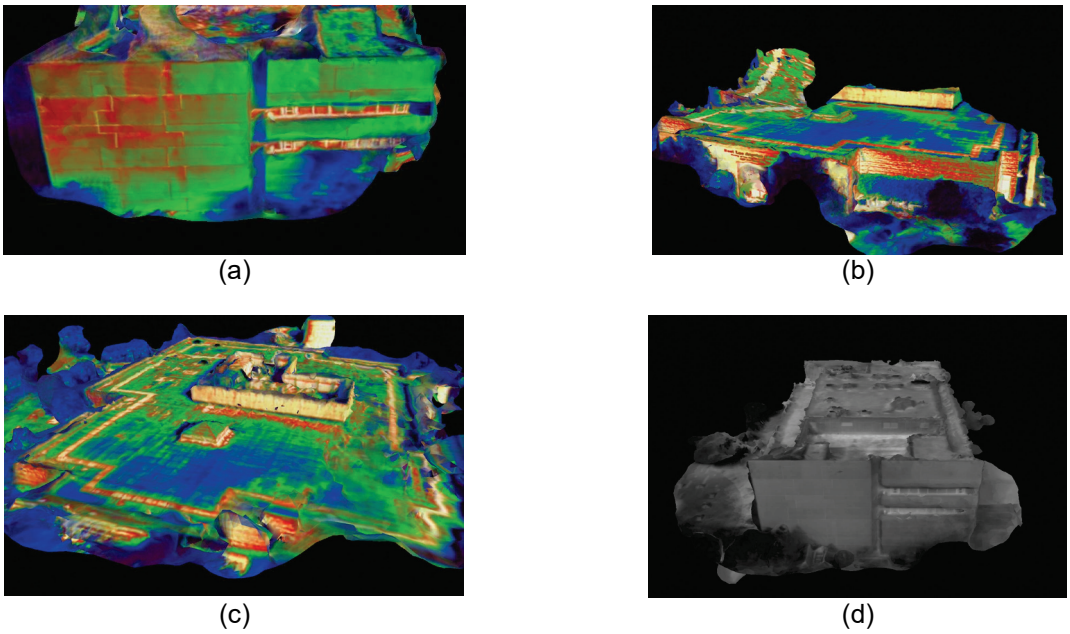

Figure 10. Sample thermal images for the East LA Civic Center Courthouse building, including (a, b, c) courthouse building south, west, and rooftop facades with false-color temperature information; and (d) raw thermal image of courthouse building south façade.

6.4 Task outcomes

The information in Table 4 could be retrieved from the two main buildings at which a complete 360-degree field of view flight was obtained.

Table 4. Building information extracted from UAV data.

Building name	Building GeoJSON	Footprint (m^2)	Number of floors detected	Building height (m)	Number of Roof Top Units (RTUs) detected
East LA Civic Center Library	On Pix4D cloud	1,080	1	8.2	5
East LA Courthouse	On Pix4D cloud	3,080	4	28.2	1

Figure 11 and Figure 12 show examples of the thermal analysis pipeline applied to the east and west-facing facades of the courthouse building. Both images indicate areas around many of the windows have temperature differential outside the predefined threshold, indicating a potential thermal anomaly, that warrants further investigation.

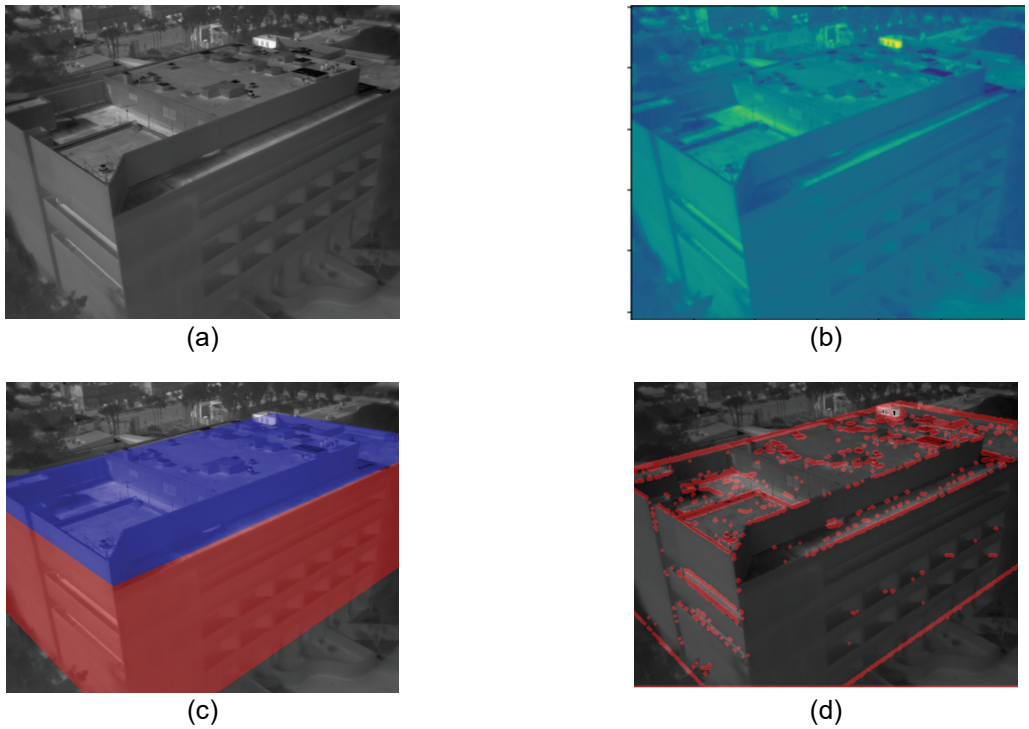

Figure 11. Thermal analysis of the east façade of the courthouse, including (a) thermal image of east façade; (b) radiometric image of east façade; (c) semantic segmentation model of building facades; and (d) potential areas of thermal anomalies.

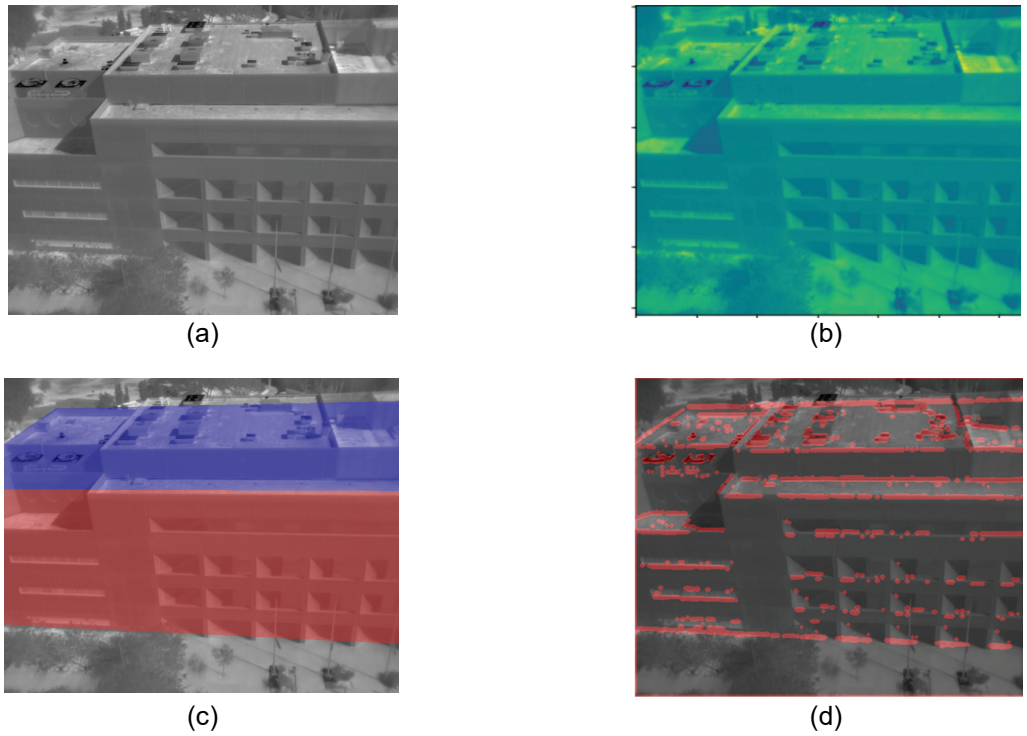

Figure 12. Thermal analysis of the west façade of the courthouse, including (a) thermal image of west façade; (b) radiometric image of west façade; (c) semantic segmentation model of building facades; and (d) potential areas of thermal anomalies.

6.5 Task conclusions and recommendations

UAVs with remote sensing gear present an opportunity for analysis and inspection of existing building stocks, where architects, engineers, building energy auditors as well as owners can document building performance, visualize heat transfer using infrared imaging, and create digital models using 3D photogrammetry. UAVs offer researchers and professionals from various industries a distinct aerial vantage point. This perspective facilitates convenient exploration of remote or hard-to-reach areas while ensuring the safety of the operator. In this task, Berkeley Lab conducted UAV flights to conduct remote building asset identification and thermal anomaly detection. We conducted drone flights at an identified location within a disadvantaged community in East LA to capture UAV data for proof-of-concept of building assessment. The UAV data was processed using Berkeley Lab's multi-step processing analysis algorithms.

First, a 3D point cloud model of the building was developed using photogrammetry. The model is available for use by the LAC team and can be processed in other 3D modeling and CAD software such as Rhino3D. Second, the point cloud model was processed through Berkeley Lab's machine learning algorithms to extract and identify asset information such as building footprint and height, presence and number of RTUs, and potential thermal anomalies on facades that warrant further inspection and could indicate moisture, infiltration, or exfiltration issues.

The next steps involve identifying prospects for integrating this technology into the workflow of the LAC ISD. Additionally, future research avenues include the development of a ranking algorithm to assess buildings for

envelope retrofit possibilities based on facade scores, as well as the exploration of estimating UHI effects from buildings using thermal images captured by UAVs. Furthermore, there's potential for further research to expand on the outlined workflows and establish a standardized methodology for conducting remote building audits.

7 Project summary

7.1 Task 1: Identification of opportunities to mitigate the urban heat island effect

Solar-reflective ("cool") roofs and walls can save energy in an air-conditioned building or improve thermal comfort in an unconditioned ("free-running") building by reducing the building's solar heat gain. Trees and artificial canopies (e.g., shade sails) that shade the building can do the same. Heat-island countermeasures such as cool roofs, cool walls, cool pavements, and urban vegetation (including but not limited to trees) mitigate the UHIE, further lowering demand for air conditioning and boosting thermal comfort.

Task 1 analyzed a wide variety of geospatial datasets with GIS software to assess the potential to implement UHI countermeasures in LAC. We focused on the albedos (solar reflectances) and potential increases to the albedos of roofs, pavements, property parcels, and census tracts; the extent to which buildings are likely to be shaded by trees; and the potential for planting more trees near buildings. We found substantial opportunities to reduce unwanted solar heating of buildings and pavements in LAC and mitigate the UHIE with cool roofs, walls, and pavements. There is also sufficient natural ground near buildings to potentially double the number of shade trees near buildings.

All analysis outputs have been captured in ArcGIS databases shared with LAC ISD. We propose using GIS software to further analyze the geospatial data in the building, parcel, and tract feature classes and/or relate them to external data. We also recommend using the albedo and tree-cover datasets generated by our analysis as inputs to building energy simulations and urban climate simulations to predict the energy savings, comfort improvements, heat danger reduction, and UHIE mitigation attainable from heat island countermeasures across LAC.

7.2 Task 2: Identification of priority tax parcels and buildings

In Task 2, the objective was to identify and prioritize MFR tax parcels and buildings according to their characteristics, and current building structure and fabric condition. We found that there was a vast stock of MFR buildings (>43K buildings, containing over 150K individual homes) in Los Angeles County, appraised by the Tax Assessor and being below the minimum standards acceptable for current new construction. Many more MFR buildings likely offer great opportunities for energy efficiency interventions at scale. We also make recommendations for future Tax Assessor data collection. There appears to be value in increasing the number of data points that capture the construction quality, building conditions, and characteristics of individual structures assessed. At present, a single value for construction quality represents the condition of everything from the structural, through the electrical, to the interior finishing. Disambiguating evaluation of these characteristics will enrich the knowledge and understanding of the existing built environment. This has multiple potential

applications, including support of the kind of programmatic energy efficiency retrofit prioritization activity that LAC ISD is pursuing with this project.

7.3 Task 3: Building modeling and simulation

With the increasing frequency and intensity of extreme weather events, the compound impacts of heatwaves and power outages pose a serious health risk for residents due to indoor heat exposure, especially for those living in disadvantaged communities with limited or no air conditioning. In Task 3, we selected 13 heat-vulnerable multifamily buildings in El Monte (LAC) and employed CityBES to evaluate their energy and thermal resilience performance. A retrofit package with seven passive and low-power active measures—a cool roof, cool walls, solar control window films, air sealing, internal window blinds, natural ventilation, and ceiling fans—was evaluated under 2018 weather conditions and projected 2058 future weather conditions. Our findings:

1. Under the 2018 weather conditions, the retrofit package reduces the peak electricity demand by 19% and reduces the annual energy cost by $183 per housing unit.
2. The future 2058 weather leads to an increase in annual electricity usage by 7% and a decrease in natural gas usage by 8% for the baseline buildings.
3. The baseline housing units without air conditioning would face heat danger conditions almost all the time during the five-day heatwave period, both in 2018 and 2058. The retrofit package could significantly reduce the heat danger hours by 50% in 2018 and 34% in 2058. However, there are still a significant number of heat danger hours, implying AC is a life-essential need for residents during heatwaves.
4. The baseline buildings under power outages lead to heat danger conditions for occupants during the entire heatwave period. With retrofits, the building occupants would experience about 21 hours and 50 hours of heat danger conditions in 2018 and 2058, respectively. This demonstrates that retrofits with these passive measures can significantly reduce the heat danger condition during a power outage.

These results indicate that during the decision-making of energy and climate retrofits for housing in DACs, policymakers, and building owners should consider the co-benefits of reducing indoor heat-related mortality while lowering energy costs.

7.4 Task 4: Building asset identification and thermal anomaly detection

In Task 4, the aim was to demonstrate the use of UAVs to conduct remote building asset identification and thermal anomaly detection. We conducted UAV flights at an identified location in East LA and captured data for proof of concept of a remote building assessment. Two work products were produced from this task. First, a 3D model of the building was developed using photogrammetry. The model is available for use by the LAC ISD team and can be processed in other 3D modeling and CAD software such as Rhino3D. Second, the machine learning algorithms developed by Berkeley Lab were applied to process the 3D point cloud model. This process aimed to extract and recognize asset details, including the building footprint and height, as well as the identification of elements like roof-top units. Additionally, the algorithms were employed to detect potential

thermal anomalies on facades, signaling areas that merit closer inspection and could indicate issues related to moisture, infiltration, or exfiltration.

Future research could build on the presented workflows to develop a standardized approach for remote building audits using UAVs.

References

[1] Los Angeles Almanac, Gross Domestic Product and Comparisons for Los Angeles County, California, (2024). https://www.laalmanac.com/economy/ec001.php (accessed February 5, 2024).

[2] Country of Los Angeles Department of Public Health, Extreme Heat and Climate Change, (2024). http://publichealth.lacounty.gov/eh/climatechange/ExtremeHeatNClimateChange.htm (accessed February 5, 2024).

[3] T. Kurzweil, Heat wave scorches Southern California. When will it end?, KTLA (2023). https://ktla.com/news/local-news/heat-wave-scorches-southern-california-when-will-it-end/ (accessed February 5, 2024).

[4] L. Beckett, 'It's too hot': Los Angeles melts under its worst heatwave of the year, The Guardian (2022). https://www.theguardian.com/us-news/2022/sep/02/los-angeles-extreme-heatwave-emergency (accessed February 5, 2024).

[5] C. Greenspon, Another Weekend, Another Heat Wave For LA, LAist (2021). https://laist.com/news/climate-environment/another-weekend-another-heat-wave-for-la (accessed February 5, 2024).

[6] Los Angeles County, Equity Explorer, (2024). https://experience.arcgis.com/experience/9d7a43397ea84ab98a534be5b5376fba (accessed February 5, 2024).

[7] C.P. Loughner, D.J. Allen, D.-L. Zhang, K.E. Pickering, R.R. Dickerson, L. Landry, Roles of Urban Tree Canopy and Buildings in Urban Heat Island Effects: Parameterization and Preliminary Results, Journal of Applied Meteorology and Climatology 51 (2012) 1775–1793. https://doi.org/10.1175/JAMC-D-11-0228.1.

[8] E. Litvak, K.F. Manago, T.S. Hogue, D.E. Pataki, Evapotranspiration of urban landscapes in Los Angeles, California at the municipal scale, Water Resources Research 53 (2017) 4236–4252. https://doi.org/10.1002/2016WR020254.

[9] E. de Guzman, Evaluating the Impact of Trees on Residential Thermal Conditions in Los Angeles Using Community Science, Cities and the Environment (CATE) 16 (2023). https://doi.org/10.15365/cate.2023.160208.

[10] D.E. Pataki, H.R. McCarthy, E. Litvak, S. Pincetl, Transpiration of urban forests in the Los Angeles metropolitan area, Ecological Applications 21 (2011) 661–677. https://doi.org/10.1890/09-1717.1.

[11] H. Taha, G. Ban-Weiss, S. Chen, H. Gilbert, H. Goudey, J. Ko, A. Mohegh, A. Rodriguez, Jonathan Slack, T. Tang, R. Levinson, Modeling and Observations to Detect Neighborhood-Scale Heat Islands and Inform Effective Countermeasures in Los Angeles, California Energy Commission, Sacramento, CA, 2018. https://www.energy.ca.gov/sites/default/files/2019-11/Energy_CCCA4-CEC-2018-007_ADA.pdf.

[12] A. Mohegh, R. Levinson, H. Taha, H. Gilbert, J. Zhang, Y. Li, T. Tang, G. Ban-Weiss, Observational evidence of neighborhood scale reductions in air temperature associated with increases in roof albedo, Climate 6 (2018) 98. https://doi.org/10.3390/cli6040098.

[13] R. Levinson, G. Ban-Weiss, S. Chen, G. Haley, H. Goudey, J. Ko, Y. Li, A. Mogegh, A. Rodriguez, J. Slack, H. Taha, T. Tang, J. Zhang, Monitoring the Urban Heat Island Effect and the Efficacy of Future

Countermeasures, California Energy Commission, Sacramento, CA, 2019. https://doi.org/10.20357/B7DW2D.

[14] L. August, CalEnviroScreen 4.0, OEHHA (2021). https://oehha.ca.gov/calenviroscreen/report/calenviroscreen-40 (accessed February 5, 2024).

[15] Los Angeles County Assessor, Parcels Dataset, (n.d.). https://egis-lacounty.hub.arcgis.com/documents/4d67b154ae614d219c58535659128e71/about (accessed February 6, 2024).

[16] California State Board of Equalization, Residential Building Costs - Assessors Handbook, (2020). https://www.boe.ca.gov/proptaxes/pdf/ah53120.pdf.

[17] Lawrence Berkeley National Lab, City Buildings, Energy, and Sustainability (CityBES), (2024). https://citybes.lbl.gov/ (accessed February 5, 2024).

[18] Los Angeles County Office of the Assessor, Los Angeles County Assessor Portal, (2024). https://portal.assessor.lacounty.gov/ (accessed February 5, 2024).

[19] M. Luo, H. Zhang, Z. Wang, E. Arens, W. Chen, F.S. Bauman, P. Raftery, Ceiling-fan-integrated air-conditioning: thermal comfort evaluations, 2 (2021) 928–951. https://doi.org/10.5334/bc.137.

[20] Lawrence Berkeley National Laboratory, Aerial 3D reconstruction, (2021). https://github.com/LBNL-ETA/a3dbr (accessed December 15, 2023).

[21] S. Touzani, M. Wudunn, S. Fernandes, A. Zakhor, R. Najibi, J. Granderson, A machine learning approach to estimate windows-to-wall ratio using drone imagery, in: Remote Sensing Technologies and Applications in Urban Environments VI, SPIE, 2021: pp. 62–69. https://doi.org/10.1117/12.2602157 (accessed January 15, 2024).

[22] DJI, Zenmuse XT2, (2019). https://www.dji.com/zenmuse-xt2 (accessed December 17, 2023).

[23] DJI, Matrice 200 Series - DJI, (2019). https://www.dji.com/matrice-200-series (accessed December 17, 2023).

Appendix A: Urban heat island countermeasures (Task 1)

Ronnen Levinson
Energy Technologies Area
Lawrence Berkeley National Laboratory

1 Source datasets

Lawrence Berkeley National Laboratory (LBNL) acquired from the Los Angeles County Internal Services Department (LAC ISD) and other sources, including the United States Geological Survey (USGS), Google, and Altostratus, Inc. a wide variety of geospatial datasets to assess the potential to implement urban heat island (UHI) countermeasures in Los Angeles County (LAC). The most pertinent are

- LAC, U.S. census tract, and property parcel boundary shapefiles
- Building shapefiles
- Aerial image rasters
- Land cover rasters
- Albedo (solar reflectance) rasters
- Roof segment slope shapefiles
- Urban heat island index shapefiles

Datasets from LAC ISD and Google were received under a two-year LBNL-LAC ISD-Google mutual non-disclosure agreement (NDA) executed on 2022-03-22.

1.1 LAC, U.S. census tract, and property parcel boundaries

LAC ISD provided `DPW_COUNTY_BOUNDARY`, a file geodatabase feature class [1] outlining the boundary of LAC, and `LACounty_Parcels`, a feature class detailing the outlines and characteristics of approximately 2.4 million property parcels[1] in LAC (Figure A-1).

[1] LACounty_Parcels includes 2,417,260 parcels, of which 1,869,643 (77.3%) contain at least one building present in the LARIAC6_Buildings_2020 feature class.

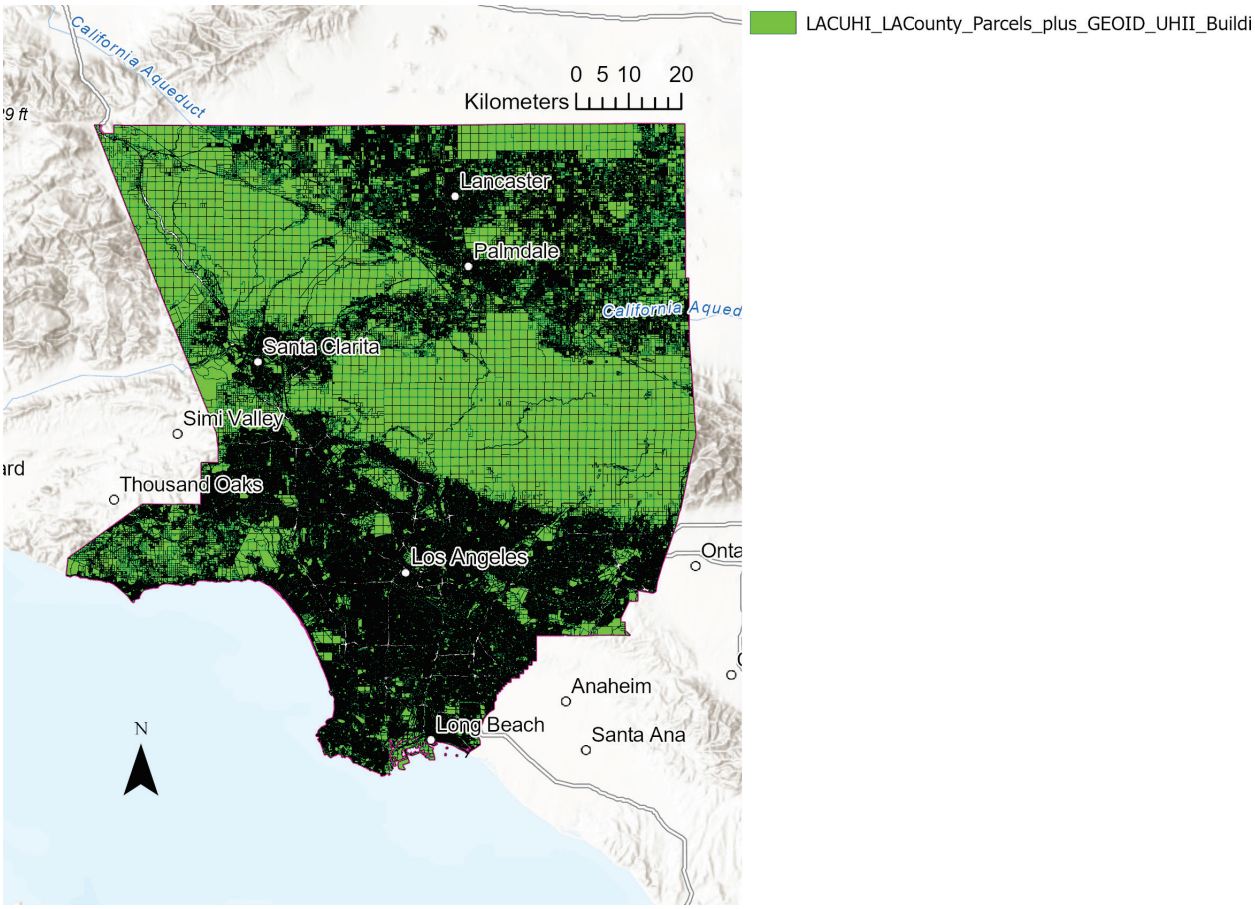

Figure A-1. Property parcels in mainland LAC from LAC ISD feature class `LACounty_Parcels`.

We downloaded from USGS `cb_2018_us_county_500`, a shapefile outlining boundaries of U.S. census tracts as of 2018, including 2,651 tracts in LAC (Figure A-2).

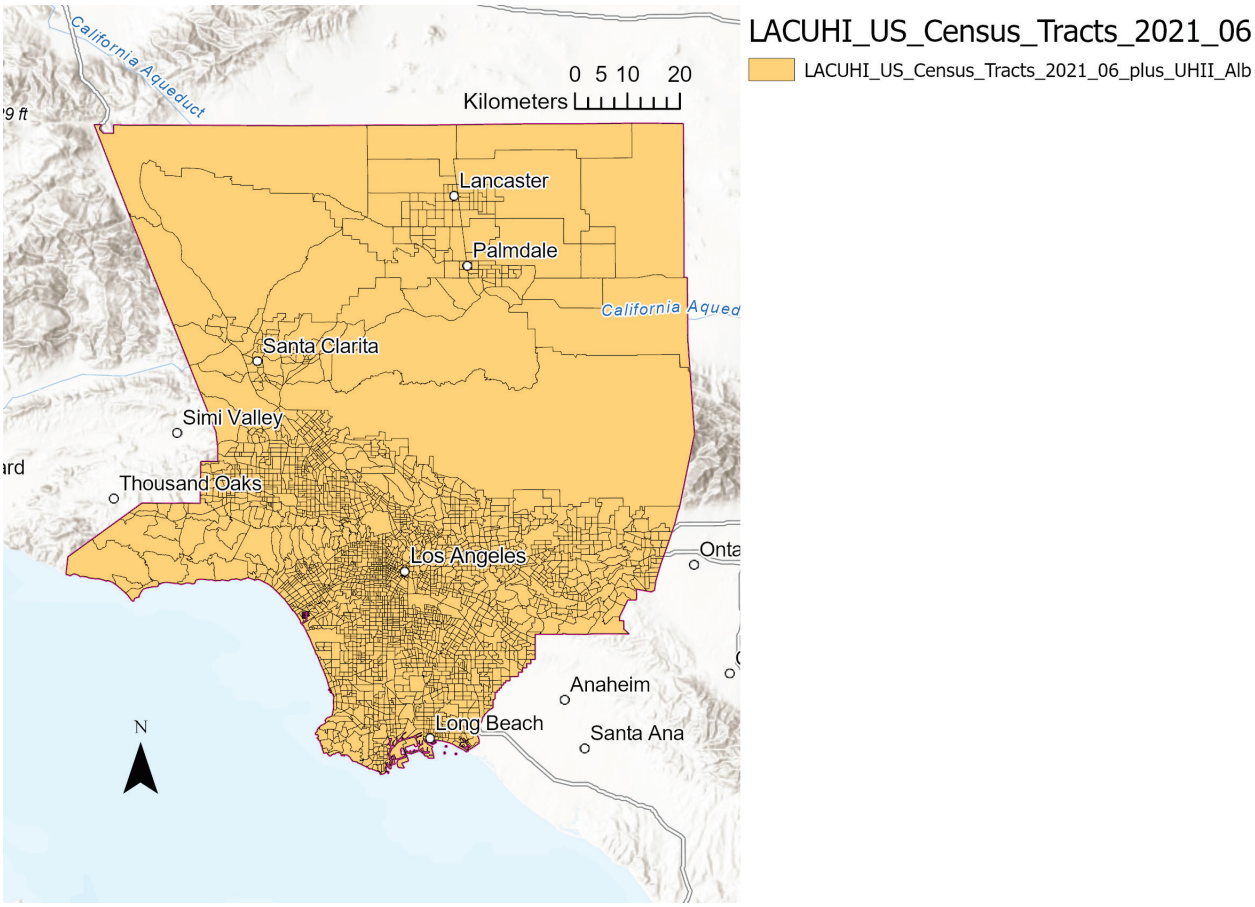

Figure A-2. Census tracts in mainland LAC from USGS shapefile `cb_2018_us_county_500`.

1.2 Aerial image rasters

LAC ISD provided server access to `LARIAC6_2021_Spring`, an online ArcGIS map layer containing color aerial images of LAC at 2” (5 cm) resolution taken in spring 2021 for the Los Angeles Region Imagery Acquisition Consortium (LARIAC) [2].

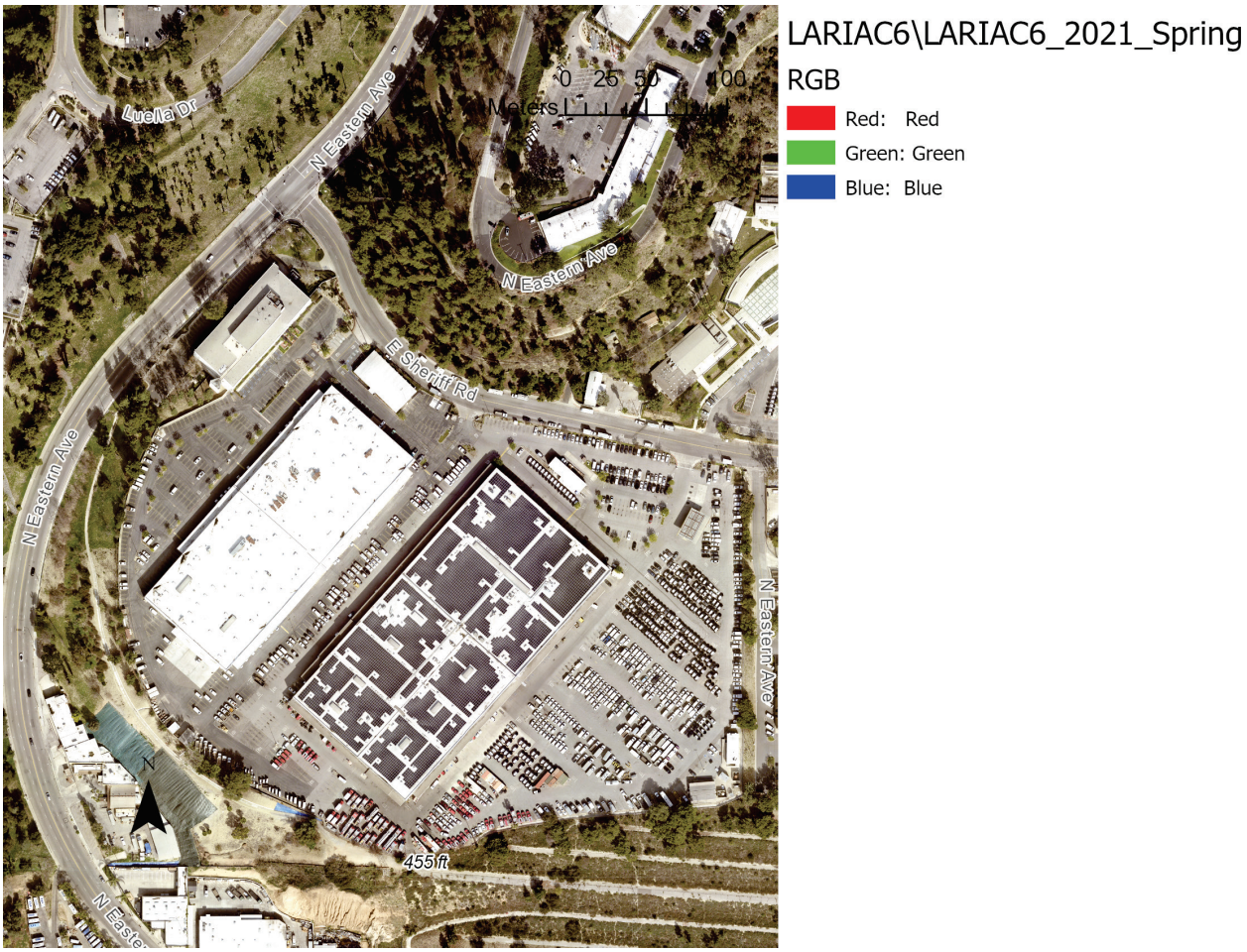

Figure A-3. Excerpt from LAC ISD color aerial image layer `LARIAC6_2021_Spring`.

1.3 Building shapefiles

LAC ISD provided `LARIAC6_Buildings_2020`, a LARIAC feature class detailing the horizontal outlines (perimeters) and heights of about 3.3 million buildings[2] in LAC as of 2020.

1.4 Land-cover rasters

LAC ISD supplied `LANDCOVER_2016`, a tag image file format (TIFF) raster detailing eight classes of land cover—tree canopy, grass/shrubs, bare soil, water, buildings, roads/railroads, other paved, tall shrubs—at 9” (23 cm) resolution (Figure A-4).

[2] LARIAC6_Buildings_2020 includes 3,293,177 entries, of which 3,258,813 (99.0%) are buildings and the rest are courtyards.

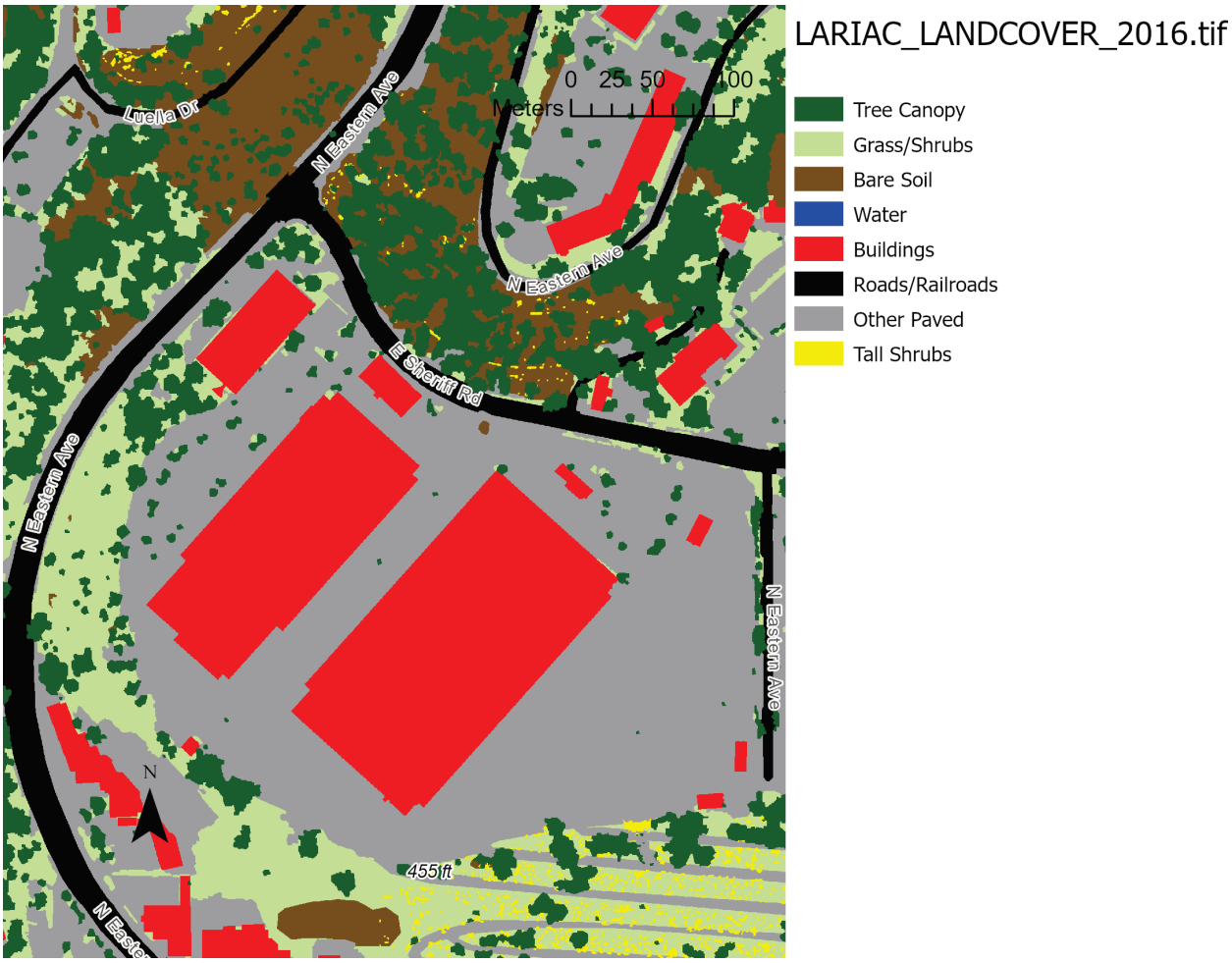

Figure A-4. Excerpt from LAC ISD land-cover raster `LARIAC_LANDCOVER_2016`.

Google provided proprietary year-2021 "panoptic" rasters detailing 10 classes of land cover in LAC—building, tree, natural ground, water, driveway, parking lot, paved road, unpaved road, sidewalk, or other human-made feature—at 40-cm resolution. We received for each land-cover class (LCC) a set of 28 tag image file format (TIFF) rasters (land-cover "tiles") that collectively cover all of LAC. Raster pixels are 4-bit integers equal to 1 if the class applies, or 0 otherwise.

Figure A-5. Excerpt from Google's panoptic parking lot raster, colored blue (pixel value 1) where a parking lot covers the land.

Both the 23-cm `LANDCOVER_2016` raster from LAC ISD and the 40-cm panoptic rasters from Google offer excellent information about land cover in LAC. We elected to use Google's panoptic rasters because (a) they distinguish four classes of paved surface—paved road, sidewalk, parking lot, and driveway—while the LANDCOVER_2016 raster has only two classes for paved surfaces—roads/railroads and other paved—and (b) pixels classified as roads/railroads in `LANDCOVER_2016` may or may not be paved roads.

1.5 Albedo rasters

Google provided 177 proprietary albedo rasters (albedo "tiles") that collectively cover most of the populated areas of LAC (including 87.9% of LARIAC6 buildings), except for the Lancaster and Palmdale regions in the northeast[3] (Figure A-6). Raster pixels are 64-bit floating point values ranging from 0 (no reflectance) to 1 (complete reflectance) (Figure A-7).

[3] Those regions were not included in the imagery from which Google generated its albedo raster.

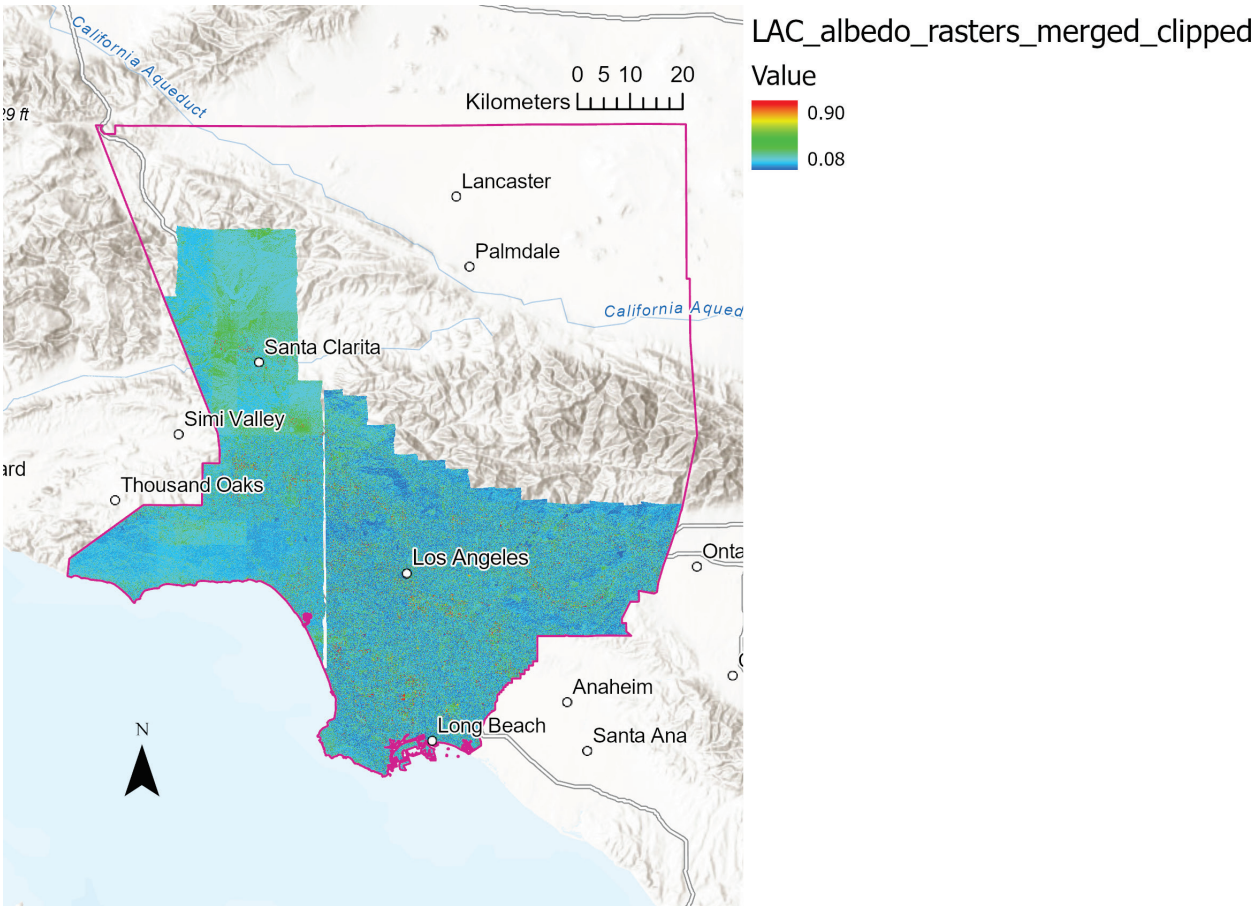

Figure A-6. Extent to which Google's merged albedo tiles (stretch-color raster) fill mainland LAC (magenta border).

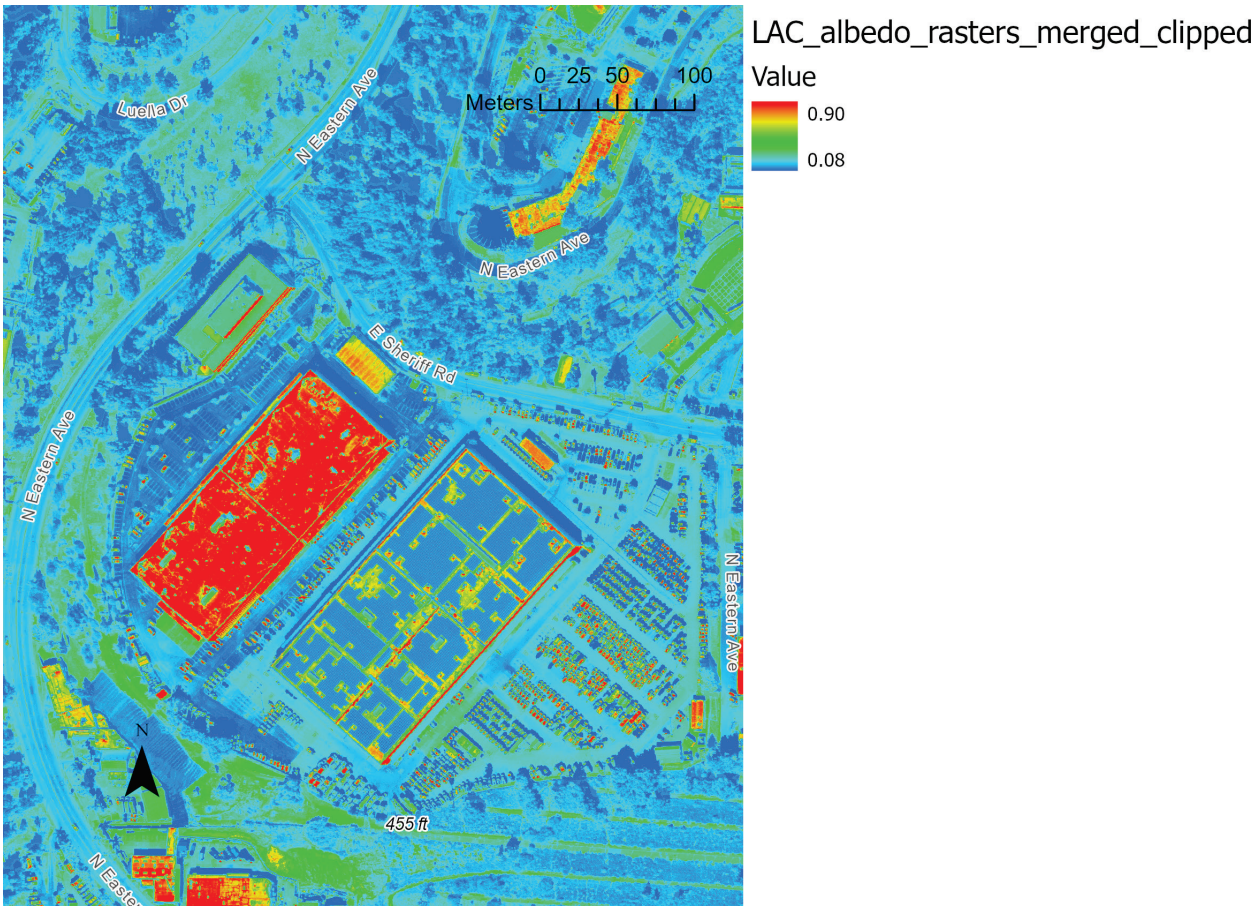

Figure A-7. Excerpt from Google's albedo raster showing albedos (scale 0 – 1) of roofs, pavements, and other features. Note the high albedo of the white roof on the large building at left and the low albedo of the photovoltaic-covered potions of the roof on the large building at right (compare to the aerial image in Figure A-3).

1.6 Roof segment slope shapefiles

Google provided a shapefile covering most of LAC (including 84.9% of LARIAC6 buildings) that reports the slope of roof segments (planar roof elements). Each shape is a point whose attributes include slope angle (degrees from horizontal) and azimuth angle (degrees clockwise from north).

Figure A-8. Extent to which Google's roof segment slope points cover mainland LAC (magenta border).

1.7 Urban heat island index shapefiles

The urban heat island *effect* (UHIE) is the urban-nonurban air temperature difference [K]. The urban heat island *index* (UHII) [°C·h], computed as the time integral of the UHIE over 6 months spanning summers 2006 and 2013 (June, July, and August of each year), quantifies the extent and severity of urban heat islands. This metric was defined and assessed across California by Altostratus, Inc. for the California Environmental Protection Agency (CalEPA) [3,4].

Altostratus provided four shapefiles giving tract-specific values of UHII in four regions: Lancaster, San Fernando, Santa Clarita, and South Coast Air Basin West (SOCABWEST). These four regions do not fully cover LAC and include only 72.6% of LARIAC6 buildings (Figure A-9). No additional shapefiles within LAC are available from the CalEPA project [3].

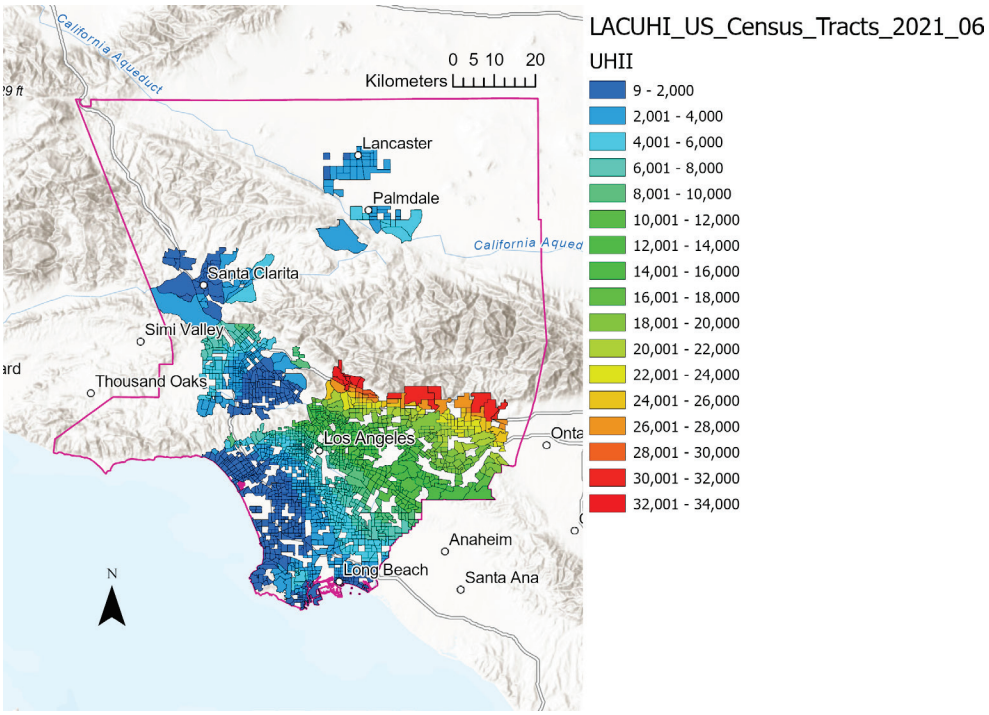

Figure A-9. Extent to which the CalEPA's tract-level UHII shapes cover mainland LAC (magenta border). UHII has units of °C·h.

2 Algorithm to generate urban heat island countermeasure recommendations based on source datasets

2.1 Overview

We evaluated the geospatial datasets identified in Section 1 to identify opportunities to apply UHI countermeasures, such as reflective roofs, reflective walls, reflective pavements, and shade trees, within LAC. We also developed a highly simplified approach to estimate the potential reductions in outside air temperature that could be achieved by increasing the solar reflectance of roofs, walls, or pavements in LAC.

To do so, we

- Merged the land-cover tiles provided by Google to create 10 land-cover rasters (one per LCC) covering all of LAC
- Merged the albedo tiles provided by Google to create an albedo raster covering most of LAC
- Merged the UHII shapefiles provided by Altostratus
- Cross-referenced buildings, parcels, and tracts
- Calculated LCC distributions of each parcel and tract
- Calculated the albedo of each parcel and tract and the albedo of each land-cover class within each parcel and tract
- Calculated the median roof-segment slope for each building, using this value to classify building roofs as low-slope or high-slope
- Calculated the gross roof area, gross wall area, and low-slope gross roof area of each LARIAC6 building, as well as the corresponding areas contained within each parcel and tract
- Calculated the fractions of land area within 10 m of each building that are occupied by trees, natural ground, or other buildings, then computed mean values of these "proximity fractions" by parcel and tract
- Estimated the extents to which roof, wall, and pavement albedos could be increased within each parcel and tract
- Estimated potential reductions in summer-afternoon outside air temperature that could be achieved in each tract by raising roof, wall, and/or pavement albedos

2.2 Computational platform

All geospatial calculations were performed in ESRI ArcGIS Pro version 3.0 [5], including the Spatial Analyst extension, on a desktop PC with a 10-core, 20-processor 2.80 GHz Intel i9-10900 CPU; 64 GB of RAM; and about 3 TB of available space on a pair of internal solid-state drives (SSDs). Note that even with these resources, operations on large (GB+) geospatial datasets such as merging land-cover or albedo tiles or calculating proximity fractions required many hours. We advise storing such datasets only on internal

SSDs since using external SSDs, internal or external hard disk drives, network drives, or cloud drives will increase computational time substantially.

Unless otherwise identified, all functions referenced below are ArcGIS Pro tools.

2.3 Merging land-cover tiles, albedo tiles, and UHII shapefiles

We applied the raster-merging function `MosaicToNewRaster()` to the land-cover tiles provided by Google to create 10 land-cover rasters (one per LCC) covering all of LAC, and to the albedo tiles provided by Google to create an albedo raster covering most of LAC.

Since we expect the LARIAC building outlines to identify building pixels more accurately than the panoptic rasters, we also created an 11th land-cover raster based on the LARIAC building outlines. LARIAC buildings form the 11th LCC.

We used `Merge()` to combine the four UHII shapefiles in a single feature class.

2.4 Cross-referencing buildings, parcels, and tracts

We duplicated the building, parcel, and tract feature classes as starting points for enhanced versions of these datasets.

We used `SpatialJoin()` to add to the building feature class fields identifying the assessor identification number (AIN) of the parcel and the geographic identifier (GEOID) of the tract containing each building, and to add to the parcel feature class a field identifying the GEOID of the tract containing each parcel.

2.5 Calculating land-cover class distributions of each parcel and tract

We used `ZonalStatisticsAsTable()` to compute parcel- and tract-mean values of each of the 11 land-cover rasters. Each new field *X*_FRACTION is the fraction of the parcel or tract covered by land-cover class *X.* We also added the field to the parcel and tract feature classes to make them easier to use.

We added to the parcel and tract feature classes the fields

- roof_FRACTION = LARIAC_buildings_FRACTION
- pavement_FRACTION = road_paved_FRACTION + sidewalk_FRACTION + parking_lot_FRACTION + driveway_FRACTION

2.6 Calculating the albedo of each parcel and tract and albedo by land-cover class within each parcel and tract

We used `ZonalStatisticsAsTable()` to compute parcel- and tract-mean values of the albedo raster.

We created an albedo raster specific to each LCC by duplicating the albedo raster and setting to <Null> all pixels that do not belong to the class. We then used `ZonalStatisticsAsTable()` to compute parcel- and tract-mean values of each LCC-specific albedo raster. Each new field *X*_MEAN_ALBEDO is the mean albedo of LCC *X* within the parcel or tract.

We used `CalculateField()` to add to the parcel and tract feature classes the fields

- roof_MEAN_ALBEDO = LARIAC_buildings_MEAN_ALBEDO
- Mean_Pavement_Albedo = (road_paved_FRACTION × road_paved_MEAN_ALBEDO) + (sidewalk_FRACTION × sidewalk_MEAN_ALBEDO) + (parking_lot_FRACTION × parking_lot_MEAN_ALBEDO) + (driveway_FRACTION × driveway_MEAN_ALBEDO) / pavement_FRACTION

2.7 Calculating the median roof-segment slope for each building, identifying low-slope roofs, and computing low-slope gross roof area

We used `SpatialJoin()` to find the building identifier (BLD_ID) of the building containing each roof-segment slope measurement point, then used `SummaryStatistics()` with case field BLD_ID to calculate the median, mean, minimum, maximum, standard deviation, range, and count of roof-segment slopes for each building. (We could not simply apply `SummarizeWithin()` to the roof-segment points because that function does not calculate medians.)

Low-slope roofing materials [6] are typically installed on roof decks with pitch < 2:12 (slope angle 9.46°), while high-slope roofing materials [7] are typically installed on steeper roof decks. The low-slope limit ranges from 2:12 to 3:12 depending on the defining body; e.g., the International Code Council uses 3:12 [8]. To allow for noise in remote measurement of roof segment slope, we classified the *entire* roof as low-slope[4] if its median slope angle is < 14.04° (pitch 3:12). We added to the building feature class the field Low_Slope_Roof, equal to 1 if low-slope and 0 otherwise.

2.8 Computing gross roof area, gross wall area, and low-slope gross roof area by building, parcel, and tract

We used `CalculateField()` to add three fields to the building feature class:

- Gross_Roof_Area = building outline area (Shape_Area), treating roof as horizontal; set to <Null> if CODE ≠ Building
- Gross_Wall_Area = building perimeter (Shape_Length) × building height (HEIGHT); set to <Null> if CODE ≠ Building

[4] A roof may have both low-slope and high-slope segments, but we did not try to determine the portion of each building's gross roof area that is low-slope because the distribution of slope measurements points on a given roof is irregular.

- Low_Slope_Roof_Gross_Area = Low_Slope_Roof × Gross_Roof_Area

We used `SpatialJoin()` to add corresponding fields to the parcel and tract feature classes—sums of gross roof area, gross wall area, and low-slope gross roof area within each parcel or tract. We then used `CalculateField()` to add to the parcel and tract feature classes the field

- Low_Slope_Fraction_of_Gross_Roof_Area = Low_Slope_Roof_Gross_Area / Gross_Roof_Area

2.9 Calculating the fractions of land area within 10 m of each building that are occupied by trees, natural ground, or other buildings by building, parcel, and tract

Assuming that trees and neighboring buildings within O(10 m) of the target building are likely to shade the walls (and possibly the roof) of the target building during some hours of the year, we used `MultipleRingBuffer()` to create a 10-m wide annular buffer around each building shape in the building feature class[5]. Think of the shape like a 10-m wide inner tube stretched around the building (Figure A-10).

We added to the building feature class the following fields computed with `ZonalStatisticsAsTable()`:

- TREE_PROXIMITY_GOOGLE: Area fraction of a 10-m-wide buffer around the building occupied by trees in Google's panoptic tree raster. The higher this value, the more likely that the building's walls (and perhaps roof) are sometimes shaded by nearby trees.
- NATURAL_GROUND_PROXIMITY_GOOGLE: Area fraction of a 10-m-wide buffer around the building occupied by natural ground in Google's panoptic natural ground raster. The higher this value, the greater the potential to shade a building's walls (and perhaps roof) by planting trees on natural ground near the building.
- BUILDING_PROXIMITY_GOOGLE: Area fraction of a 10-m-wide buffer around the building occupied by neighboring buildings in Google's panoptic buildings_raw raster. The higher this value, the more likely that the building's walls (and perhaps roof) are sometimes shaded by nearby buildings.
- BUILDING_PROXIMITY_LARIAC: Area fraction of a 10-m-wide buffer around the building occupied by neighboring buildings in a rasterization of the LARIAC6 building shapefile. The higher this value, the more likely that the building's walls (and perhaps roof) are sometimes shaded by nearby buildings. BUILDING_PROXIMITY_LARIAC may be slightly more accurate than BUILDING_PROXIMITY_GOOGLE because the borders of neighboring buildings are better captured by the LARIAC building shapes.

[5] A ring O(1 m) wide would miss features that could shade the central buildings, while a ring O(100 m) wide would include features that would rarely if ever shade the central building. We have no plans to optimize this value as life is too short to spend in such an exercise.

Figure A-10. Excerpt from buffer-ring feature class showing 10-m-wide buffer rings drawn around buildings.

We then used `SpatialJoin()` to add to the parcel and tract feature classes mean values of tree, natural ground, building_Google, and building_LARIAC proximities within each parcel or tract.

2.10 Estimating the extents to which roof, wall, and pavement albedos could be increased within each parcel and tract

We used `CalculateField()` to add to the parcel and tract feature classes fields containing our assumptions about the aged albedos of cool low-slope and high-slope roofs, cool pavement, cool walls, and conventional walls:

- Cool_Low_Slope_Roof_Albedo = 0.70
- Cool_High_Slope_Roof_Albedo = 0.40
- Cool_Pavement_Albedo = 0.40
- Cool_Wall_Albedo = 0.60
- Conventional_Wall_Albedo = 0.25

We then calculated for each parcel and tract the mean value of assumed cool roof albedo

- Mean_Cool_Roof_Albedo = Low_Slope_Fraction_of_Gross_Roof_Area × Cool_Low_Slope_Roof_Albedo + (1 - Low_Slope_Fraction_of_Gross_Roof_Area) × Cool_High_Slope_Roof_Albedo

as well as potential mean increases in albedos if surfaces are made cool:

- Mean_Roof_Albedo_Increase = Mean_Cool_Roof_Albedo - roof_MEAN_ALBEDO
- Wall_Albedo_Increase = Cool_Wall_Albedo – Conventional_Wall_Albedo
- Mean_Pavement_Albedo_Increase = Cool_Pavement_Albedo – Mean_Pavement_Albedo
- Mean_Road_Paved_Albedo_Increase = Cool_Pavement_Albedo – road_paved_MEAN_ALBEDO
- Mean_Sidewalk_Albedo_Increase = Cool_Pavement_Albedo – sidewalk_MEAN_ALBEDO
- Mean_Parking_Lot_Albedo_Increase = Cool_Pavement_Albedo – parking_lot_MEAN_ALBEDO
- Mean_Driveway_Albedo_Increase = Cool_Pavement_Albedo – driveway_MEAN_ALBEDO

2.11 Estimating potential reductions in summer-afternoon outside air temperature that could be achieved in each tract by raising roof, wall, and/or pavement albedos

We estimated the potential reductions in summer-afternoon outside air temperature[6] that could be achieved in each tract by raising roof, wall, and/or pavement albedos by using linear relations between albedo rise and air temperature reduction based on past studies of urban heat island in LAC [9,10]. These crude calculations consider only modified surface (roof, wall, or pavement) albedo rise and modified surface density (modified surface area / tract area), neglecting spatial variations in air temperature reduction that may result from wind patterns and other geographic considerations. Mesoscale climate simulations incorporating the existing and potential cool values of surface albedo detailed above would predict outside air temperature reductions more accurately, but such work is outside the scope of the current project.

Krayenhoff et al. [11] define "albedo cooling effectiveness"

$$\mathrm{ACE} = -\frac{\Delta T}{\Delta \rho_{\mathrm{N}}} = -\frac{\Delta T}{\Delta \rho_{\mathrm{S}}\, \lambda_{\mathrm{S}}} \qquad (1)$$

where ΔT is the increase in the UHIE; $\Delta \rho_{\mathrm{N}}$ is the neighborhood scale, plan area-averaged increase in albedo attained by increasing roof, wall, or pavement albedo; $\Delta \rho_{\mathrm{S}}$ is the increase in roof, wall, or pavement albedo; and λ_{S} is the ratio of the modified surface area to the overall plan area.

A recent study modeling cool roofs and cool walls in the Los Angeles Basin reported a 0.72 K / 0.41 K reduction in summer-afternoon canyon air temperature at 14:00 local standard time (LST) upon increasing roof / wall albedo to 0.90 from 0.10 (Table 2 in Ref. [9]). Let "grid cell" (hereinafter, simply "cell") refer to the smallest horizontal region considered in an urban climate simulation, and let urban area refer to the part of the cell that is not rural. Treating roofs as horizontal, cell albedo rise = roof albedo rise × roof area

[6] We focus on afternoon (14:00 LST) reduction rather than daily mean reductions in canyon air temperature because our simplified approach can estimate the former for roofs, walls, and pavements, but estimate the latter for only roofs and walls.

fraction, where roof area fraction = roof area / cell area = (roof area / urban area) × urban area fraction. Rearranging, urban area fraction = (cell albedo rise / roof albedo rise) / (roof area / urban area).

The 2-D canyon geometries in Table S1 of Ref. [9] yield

- roof area / urban area = $R/(R+W)$ = 18.4%, 18.2%, and 18.6% for low-intensity residential, high-intensity residential, and commercial/industrial regions, respectively
- wall area / urban area = $2\,H/(R+W)$ = 35.6%, 35.7%, and 39.0% for low-intensity residential, high-intensity residential, and commercial/industrial regions, respectively

where R is roof width, W is ground width, and H is building height. Simple (unweighted) averages over the three urban area types yield

- roof area / urban area = 18.4%
- wall area / urban area = 36.8%

Reading the COOL_ROOF_HIGH (0.90) - CONTROL (0.10) cell albedo increase at 14:00 LST from Fig. 2a of Ref. [9] as 0.0655 yields

- urban area fraction = (cell albedo increase / roof albedo increase) / (roof area / urban area) = (0.0655 / 0.8) / (0.184) = 44.5%
- roof area fraction = roof area / cell area = (roof area / urban area) × urban area fraction = 18.4% × 44.5% = 8.2%
- wall area fraction = wall area / cell area = (wall area / urban area) × urban area fraction = 36.8% × 44.5% = 16.4%

Therefore,

- ACE_{roof} = cool-roof UHIE reduction / (roof albedo increase × roof area fraction) = 0.72 K / (0.80 × 8.2%) = 10.99 K
- ACE_{wall} = cool-wall UHIE reduction / (wall albedo increase × wall area fraction) = 0.41 K / (0.80 × 16.4%) = 3.13 K

$ACE_{roof} \approx 11$ K is mid-range for the Weather Research and Forecasting (WRF) episodic summer midday/afternoon/T_max results reported in Fig. 6a of Ref. [11], which shows median-ACE green triangles at about 3, 6, 11, and 18 K.

Another recent study modeling cool pavements in the Los Angeles Basin reported a 0.56 K reduction in canyon air temperature at 14:00 LST upon increasing pavement albedo to 0.50 from 0.10 (Table 2 in Ref.

[10]). Its first author has advised (personal communication, 2024-03-24) that in his simulation of the city of Los Angeles,

- pavement area / urban area = 50%
- urban area fraction = urban area / cell area = 59%

This yields

- pavement area fraction = pavement area / cell area = (pavement area / urban area) × urban area fraction = 29.5%
- $ACE_{pavement}$ = UHI reduction / (pavement albedo increase × pavement area fraction) = 0.56 K / (0.40 × 29.5%) = 4.75 K

These values of surface albedo increase, surface area fraction, neighborhood albedo increase, and ACE are summarized in Table A-1.

Table A-1. Calculation of albedo cooling effectiveness (ACE) values for LAC.

Surface	Canyon air temperature decrease at 14:00 LST, ΔT [K]	Increase in surface albedo, $\Delta\rho_S$ [-]	Modified surface area / neighborhood plan area, λ_S [-]	Increase in neighborhood albedo, $\Delta\rho_N = \Delta\rho_S\,\lambda_S$ [-]	Albedo cooling effectiveness, $-\Delta T/\Delta\rho_N$ [K]
Roof	0.72	0.80	8.2%	0.0656	10.99
Wall	0.41	0.80	16.4%	0.131	3.13
Pavement	0.56	0.40	29.5%	0.118	4.75

We used `CalculateField()` to add the following fields to the tract feature class:

- ACE_{roof} = value from Table A-1
- ACE_{wall} = value from Table A-1
- $ACE_{pavement}$ = value from Table A-1
- Tract_Area = Area_SQFT (field from original census table)
- Gross_Roof_Area_to_Tract_Area = Gross_Roof_Area / Tract_Area
- Gross_Wall_Area_to_Tract_Area = Gross_Wall_Area / Tract_Area
- Pavement_Area_to_Tract_Area = Pavement_Area / Tract_Area
- Roof_UHIE_Reduction_K = ACE_{roof} × Mean_Roof_Albedo_Increase × Gross_Roof_Area_to_Tract_Area
- Wall_UHIE_Reduction_K = ACE_{wall} × Wall_Albedo_Increase × Wall_Roof_Area_to_Tract_Area
- Pavement_UHIE_Reduction_K = $ACE_{pavement}$ × Mean_Pavement_Albedo_Increase × Pavement_Area_to_Tract_Area

- Roof+Wall+Pavement_UHIE_Reduction_K = Roof_UHIE_Reduction_K + Wall_UHIE_Reduction_K + Pavement_UHIE_Reduction_K

We note a few caveats.

1. We expect that UHIE reductions attained by increases in roof and wall albedo will be additive because little sunlight diffusely reflected from a roof will strike a wall, and vice-versa.

2. We expect that UHIE reductions attained by increases in roof and pavement albedo will be additive because little sunlight diffusely reflected from a roof will strike a pavement, and vice-versa

3. UHIE reductions attained from increases in wall and pavement albedo may combine in a complicated fashion because sunlight diffusely reflected from a pavement can strike a nearby wall, and vice-versa. Such analysis lies outside the scope of this study, but we note that the cool roof/cool wall study [9] and the cool pavement study [10] upon which we rely each consider wall-pavement reflections. Such reflections are further detailed in Ref. [12].

4. The extent to which we can raise gross roof albedo is reduced by the presence of heating, ventilation, and air conditioning (HVAC) equipment, solar equipment, walkways, and other features on the roof.

5. The extent to which we can raise gross wall albedo is reduced by openings in the wall (windows and doors).

6. Boosting pavement or wall albedo may increase the mean radiant temperature (MRT) and heat stress experienced by pedestrians [13]. (Net changes to MRT and heat stress depend on factors including clothing albedo and wind speed.)

3 UHIC recommendations, including links to the map layers (shapefiles or geodatabases) identifying buildings that would benefit from these measures

3.1 Overview

We present the results of the analysis described in Section 2 and share some guidance. All datasets generated in this Task have been shared with LAC ISD via ArcGIS geodatabases, and documented here.

Summary statistics for all Task 1 outputs are reported in Table A-2.

Table A-2. Tract-level summary statistics for all fields calculated in Task 1. Properties without listed units are dimensionless.

Property	Median	Mean	Min	Max	Standard Deviation	Fraction NoData
roof_FRACTION	0.27	0.25	0.00	0.60	0.10	0.1%
pavement_FRACTION	0.31	0.30	0.00	1.00	0.11	0.1%
road_paved_FRACTION	0.15	0.15	0.00	1.00	0.08	0.1%
sidewalk_FRACTION	0.03	0.03	0.00	0.16	0.02	0.1%
parking_lot_FRACTION	0.05	0.06	0.00	0.56	0.05	0.1%
driveway_FRACTION	0.05	0.05	0.00	0.47	0.03	0.1%
ground_natural_FRACTION	0.17	0.20	0.00	1.00	0.15	0.1%
road_unpaved_FRACTION	0.00	0.00	0.00	0.41	0.01	0.1%
other_human_made_FRACTION	0.07	0.07	0.00	0.83	0.05	0.1%
tree_FRACTION	0.13	0.15	0.00	0.93	0.10	0.1%
water_FRACTION	0.00	0.00	0.00	1.00	0.02	0.1%
tract_MEAN_ALBEDO	0.16	0.17	0.09	0.26	0.02	4.5%
roof_MEAN_ALBEDO	0.19	0.20	0.12	0.44	0.03	6.5%
Mean_Pavement_Albedo	0.15	0.15	0.12	0.24	0.01	6.6%
road_paved_MEAN_ALBEDO	0.14	0.14	0.10	0.24	0.02	6.2%
sidewalk_MEAN_ALBEDO	0.17	0.17	0.10	0.25	0.01	6.3%
parking_lot_MEAN_ALBEDO	0.14	0.14	0.10	0.25	0.02	6.4%
driveway_MEAN_ALBEDO	0.16	0.16	0.10	0.32	0.02	6.4%
ground_natural_MEAN_ALBEDO	0.16	0.17	0.12	0.27	0.01	6.2%
road_unpaved_MEAN_ALBEDO	0.17	0.17	0.09	0.32	0.04	33.6%
other_human_made_MEAN_ALBEDO	0.16	0.16	0.10	0.26	0.02	6.2%
tree_MEAN_ALBEDO	0.14	0.14	0.11	0.24	0.01	6.2%
water_MEAN_ALBEDO	0.12	0.14	0.08	0.58	0.04	46.9%
Mean_Tract_Albedo_Increase	0.17	0.16	0.00	0.35	0.05	7.0%
Mean_Roof_Albedo_Increase	0.33	0.33	0.01	0.51	0.04	6.9%
Mean_Pavement_Albedo_Increase	0.25	0.25	0.16	0.28	0.01	6.6%
Mean_Road_Paved_Albedo_Increase	0.26	0.26	0.16	0.30	0.02	6.2%
Mean_Sidewalk_Albedo_Increase	0.23	0.23	0.15	0.30	0.01	6.3%
Mean_Parking_Lot_Albedo_Increase	0.26	0.26	0.15	0.30	0.02	6.4%
Gross_Roof_Area_to_Tract_Area	0.25	0.24	0.00	0.58	0.09	2.6%
Gross_Wall_Area_to_Tract_Area	0.42	0.44	0.00	3.29	0.25	2.6%
Pavement_Area_to_Tract_Area	0.31	0.30	0.00	1.00	0.11	0.1%
Low_Slope_Fraction_of_Gross_Roof_Area	0.38	0.41	0.00	1.00	0.20	3.4%

Table A-2 (continued)

Property	Median	Mean	Min	Max	Standard Deviation	Fraction NoData
MEAN_TREE_PROXIMITY_GOOGLE	0.16	0.18	0.00	0.57	0.08	2.6%
MEAN_NATURAL_GROUND_PROXIMITY_GOOGLE	0.18	0.19	0.00	0.85	0.09	2.6%
MEAN_BUILDING_PROXIMITY_GOOGLE	0.30	0.29	0.00	0.81	0.07	2.6%
MEAN_BUILDING_PROXIMITY_LARIAC	0.23	0.23	0.00	0.54	0.07	2.6%
Mean_Cool_Roof_Albedo	0.51	0.52	0.40	0.70	0.06	3.4%
Mean_Driveway_Albedo_Increase	0.24	0.24	0.08	0.30	0.02	6.4%
UHII [°C·h]	4,953	7,168	9	33,153	6,735	26.6%
Roof_UHIE_Reduction_K [K]	0.75	0.76	0.00	2.44	0.30	6.9%
Wall_UHIE_Reduction_K [K]	0.72	0.75	0.00	5.62	0.42	2.6%
Pavement_UHIE_Reduction_K [K]	0.48	0.47	0.00	1.01	0.14	6.6%
Roof+Wall+Pavement_UHIE_Reduction_K [K]	1.11	1.15	0.00	5.24	0.53	7.0%

3.2 LCC fractions by tract

Figure A-11 - Figure A-14 show maps and histograms of roof, pavement, tree, and natural-ground LCC fractions, by tract. The median values of roof, pavement, tree, and natural ground fractions of individual tracts are 27%, 31%, 13%, and 17%, respectively (Table A-2), indicating that there are substantial roof and pavement areas available to modify, and substantial natural ground areas available to plant trees, where people live.

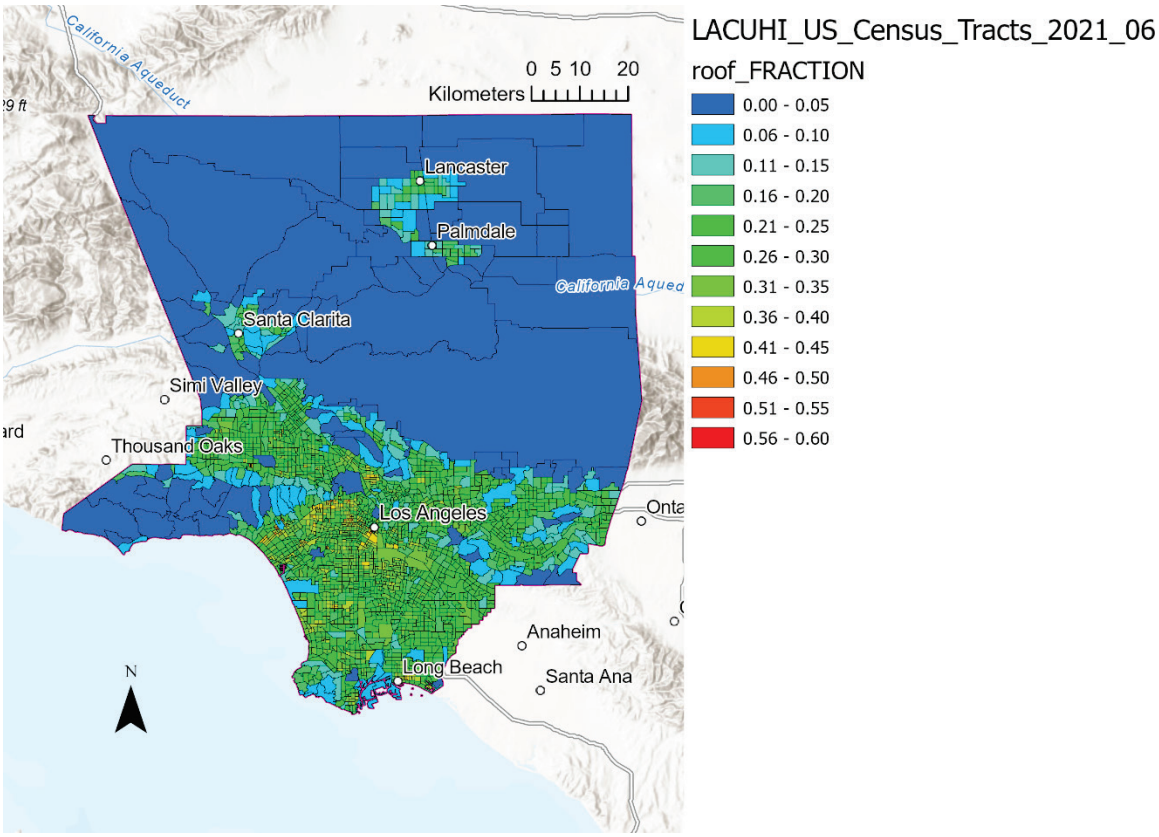

(a)

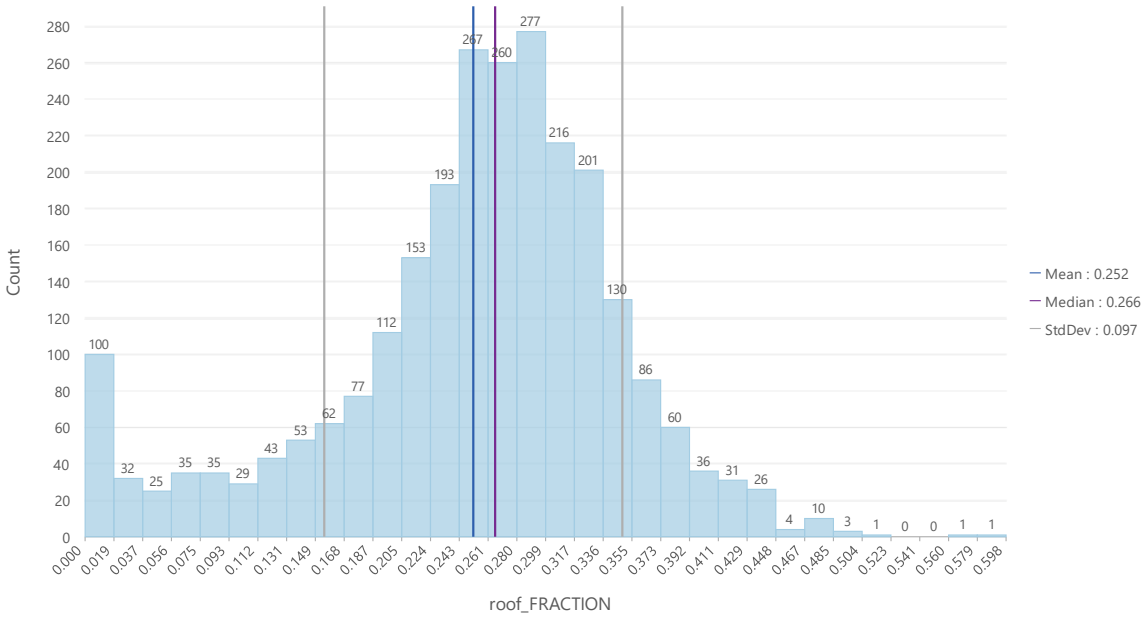

(b)

Figure A-11. Map (a) and histogram (b) of roof fraction by tract.

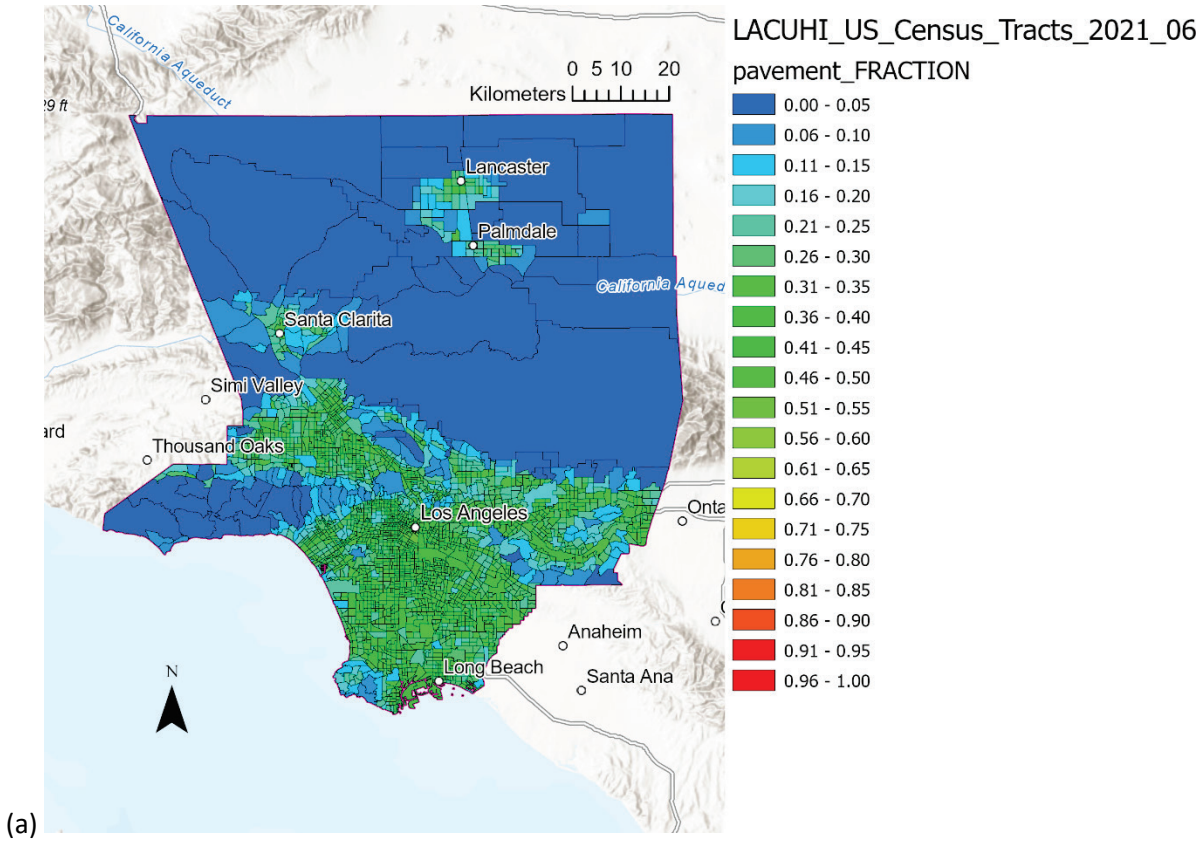

(a)

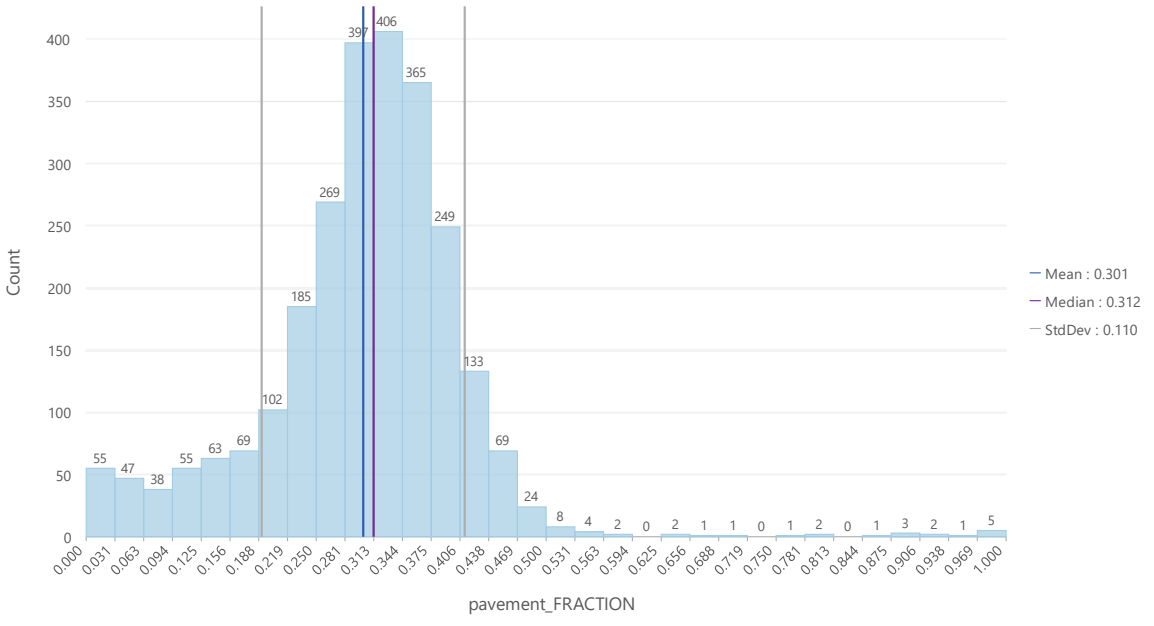

(b)

Figure A-12. Map (a) and histogram (b) of pavement fraction by tract.

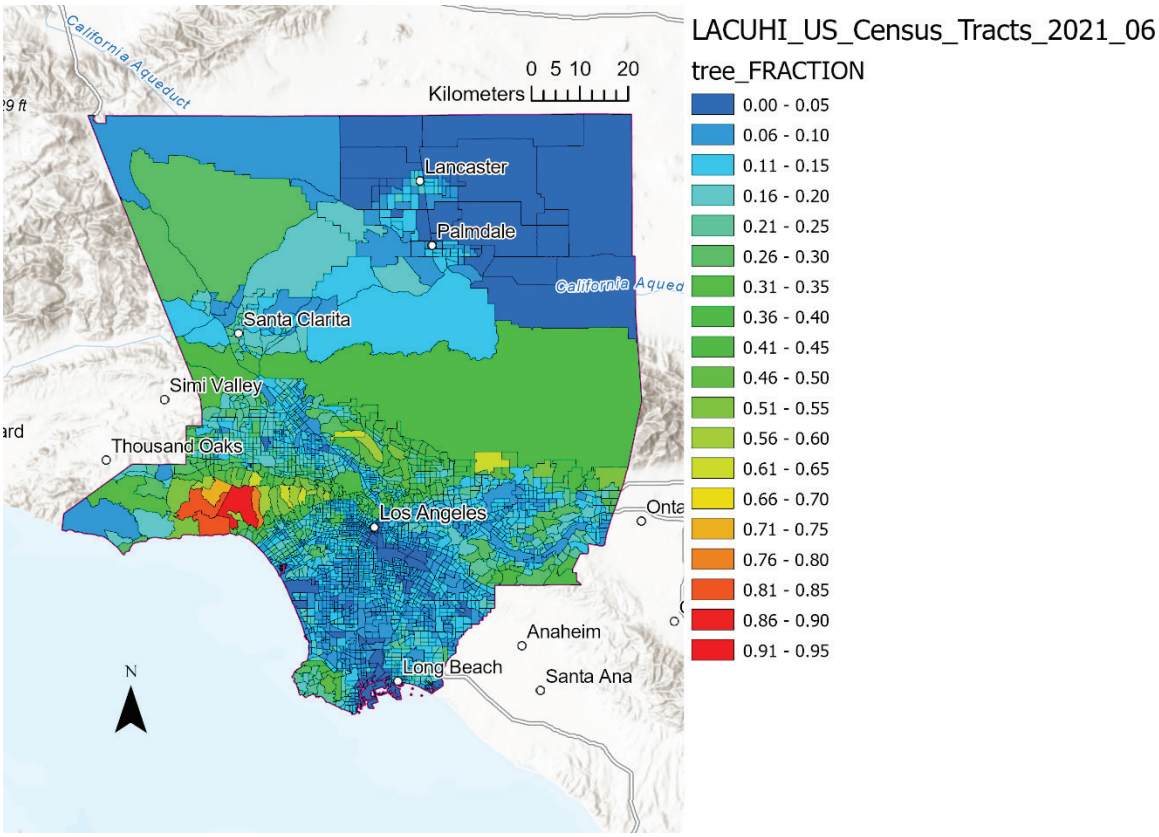

(a)

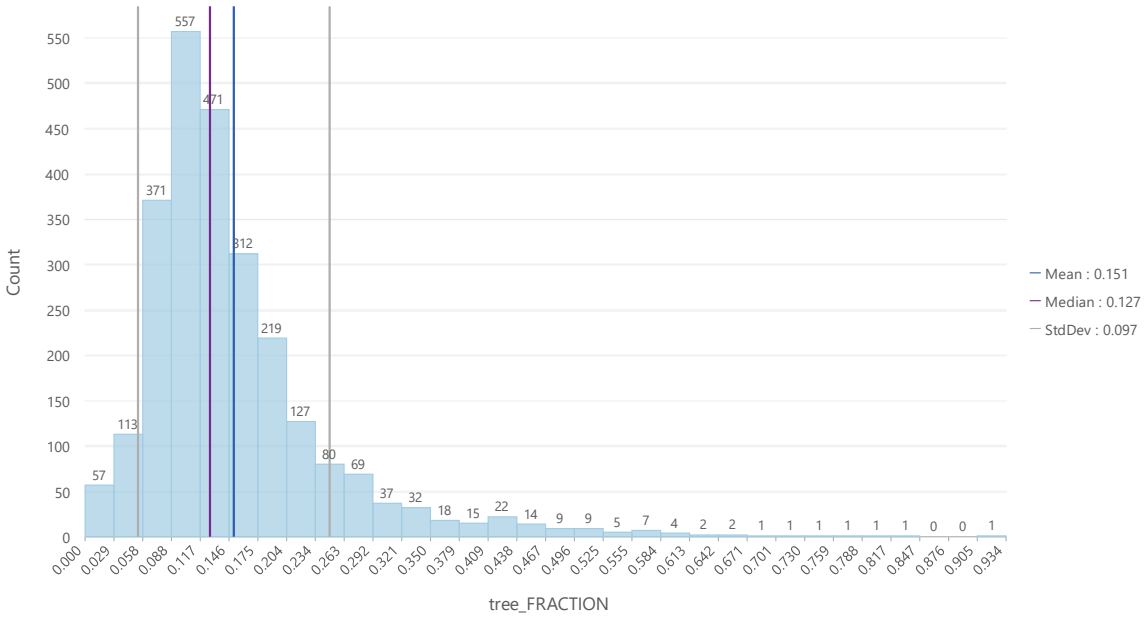

(b)

Figure A-13. Map (a) and histogram (b) of tree fraction by tract.

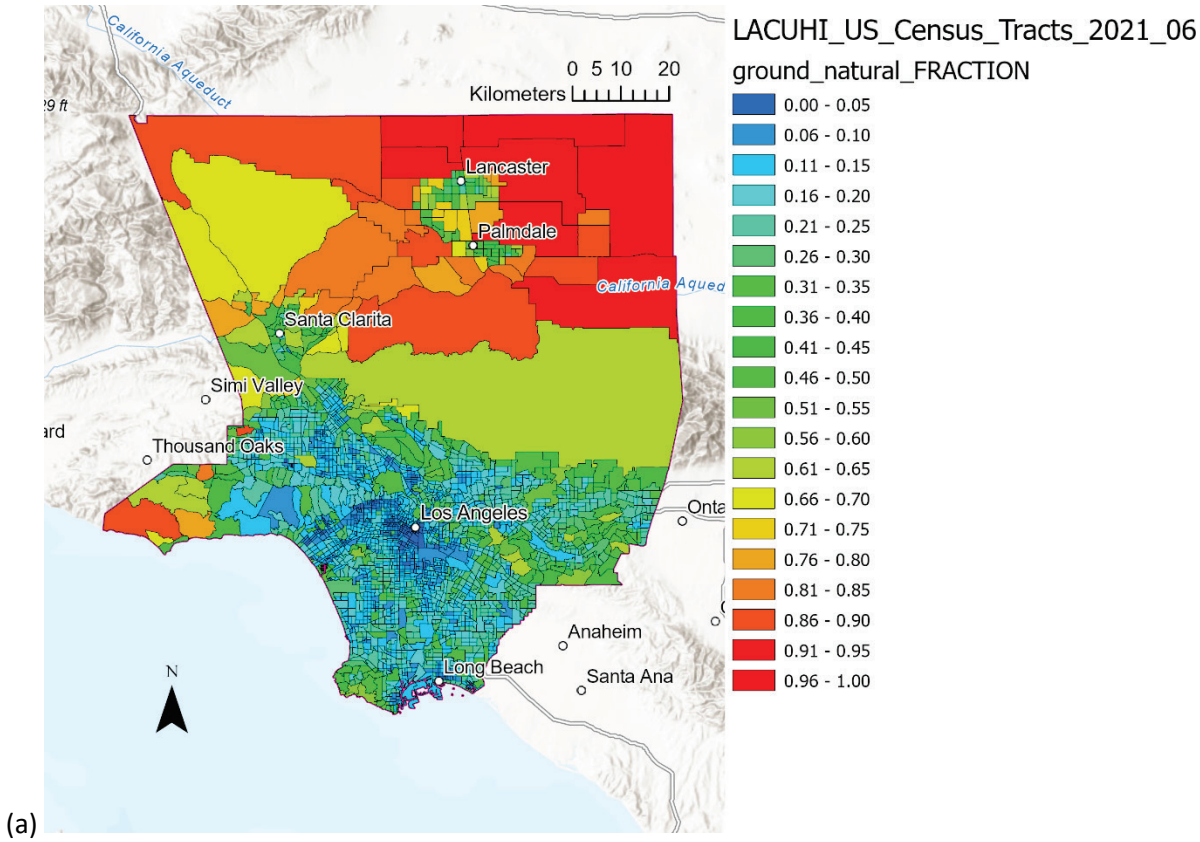

(a)

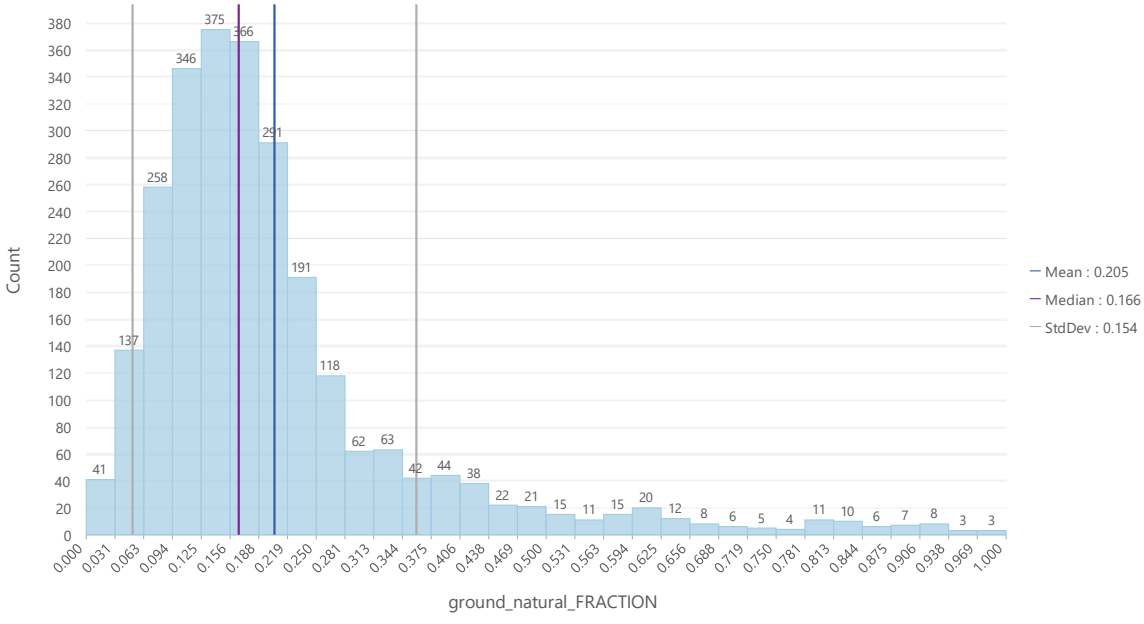

(b)

Figure A-14. Map (a) and histogram (b) of natural-ground fraction by tract.

3.3 Albedos and potential albedo increases by tract

Figure A-15 - Figure A-17 show maps and histograms of tract, roof, and pavement mean albedos, by tract. Median values of tract, roof, and pavement albedos are 0.16, 0.19, and 0.15, respectively (Table A-2), suggesting that on average they are currently quite dark.

Figure A-18 shows a map and histogram of the low-slope fraction of gross roof area by tract. The median value of 38% (Table A-2) indicates that in a typical tract, more than a third of the gross roof area could be surfaced with high-albedo (typically white) roofing products.

Figure A-19 - Figure A-21 show maps and histograms of potential increases to tract, roof, and pavement mean albedos by tract. Median values of potential increases to tract, roof, and pavement mean albedos are 0.17, 0.33, and 0.25, respectively (Table A-2), indicating substantial opportunities for brightening. (Potential increases to tract albedo will always be lower than potential increases to roof or pavement albedo because tracts contain other features, such as trees and natural ground, that will not be brightened.)

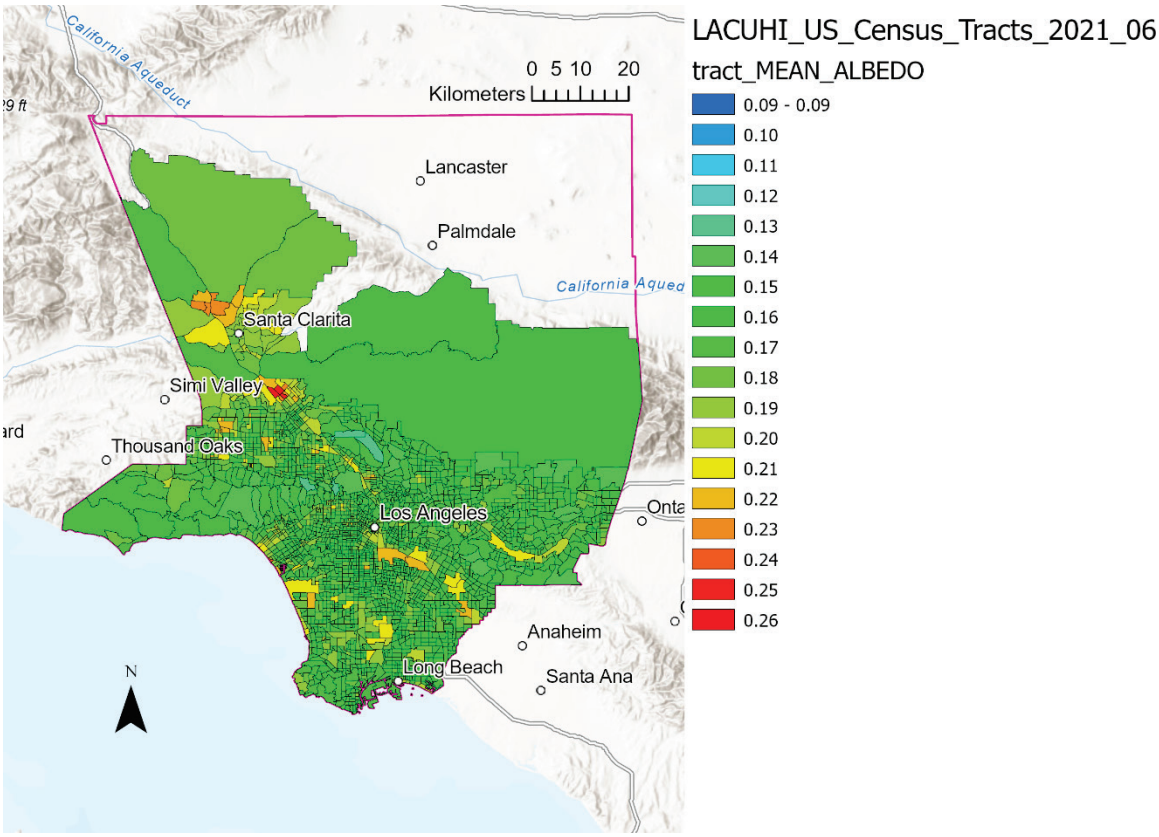

(a)

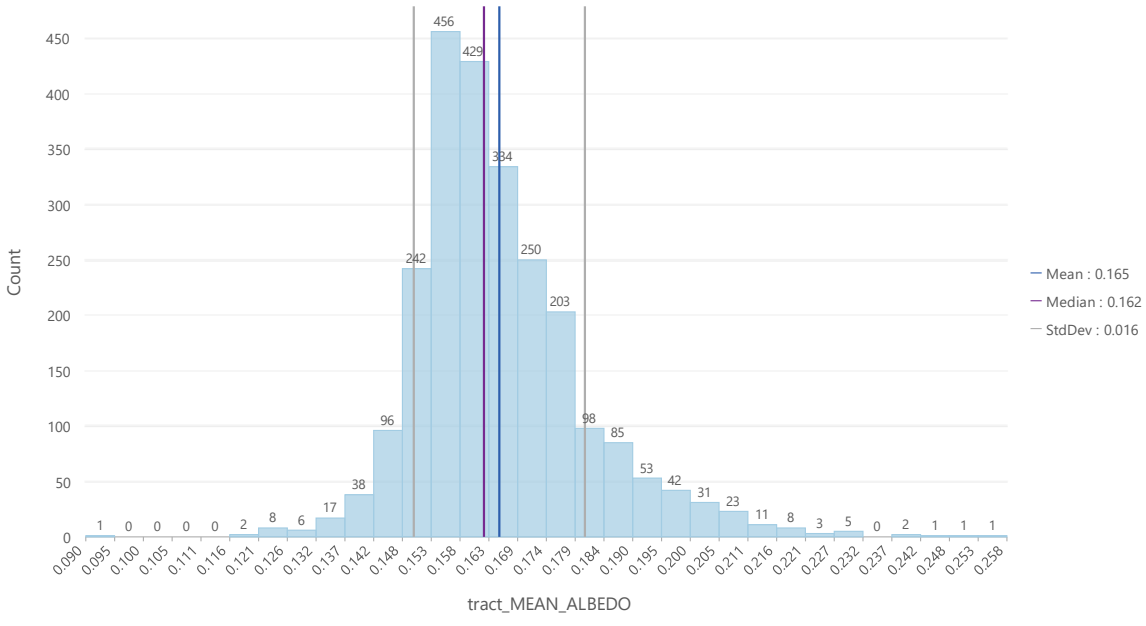

(b)

Figure A-15. Map (a) and histogram (b) of mean tract albedo by tract.

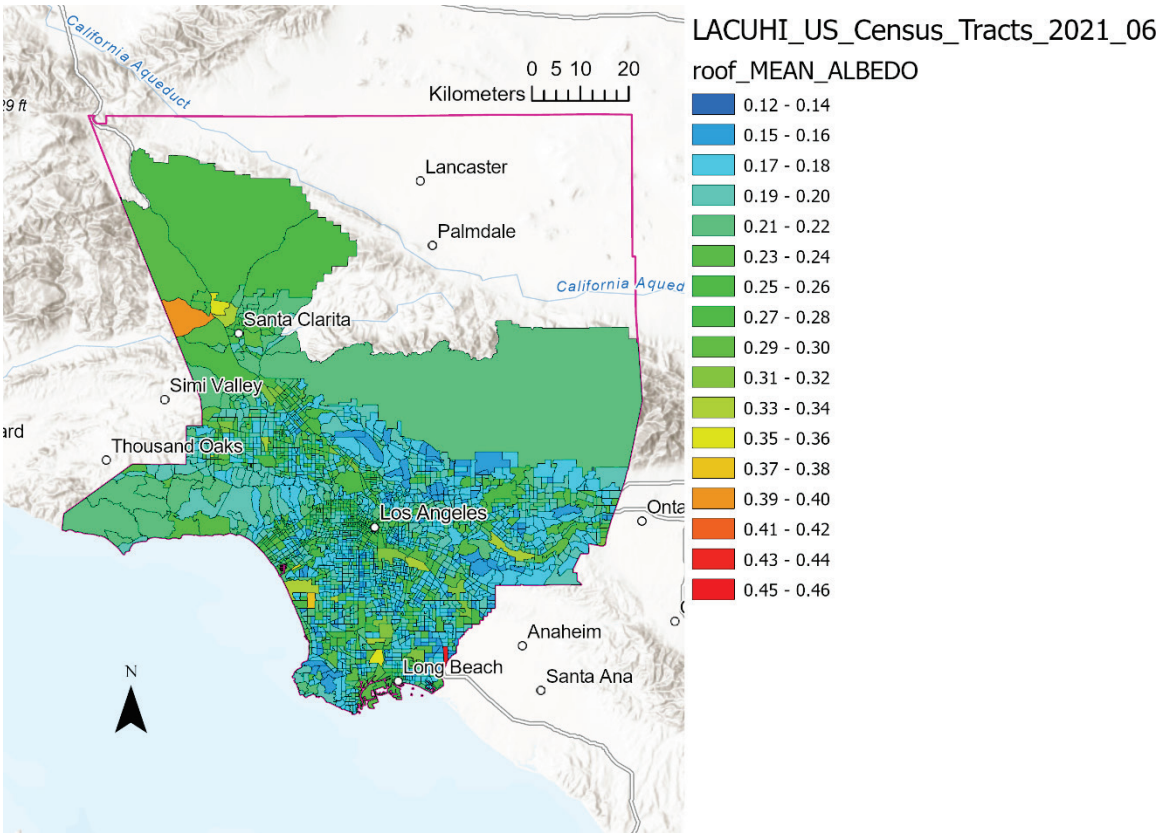

(a)

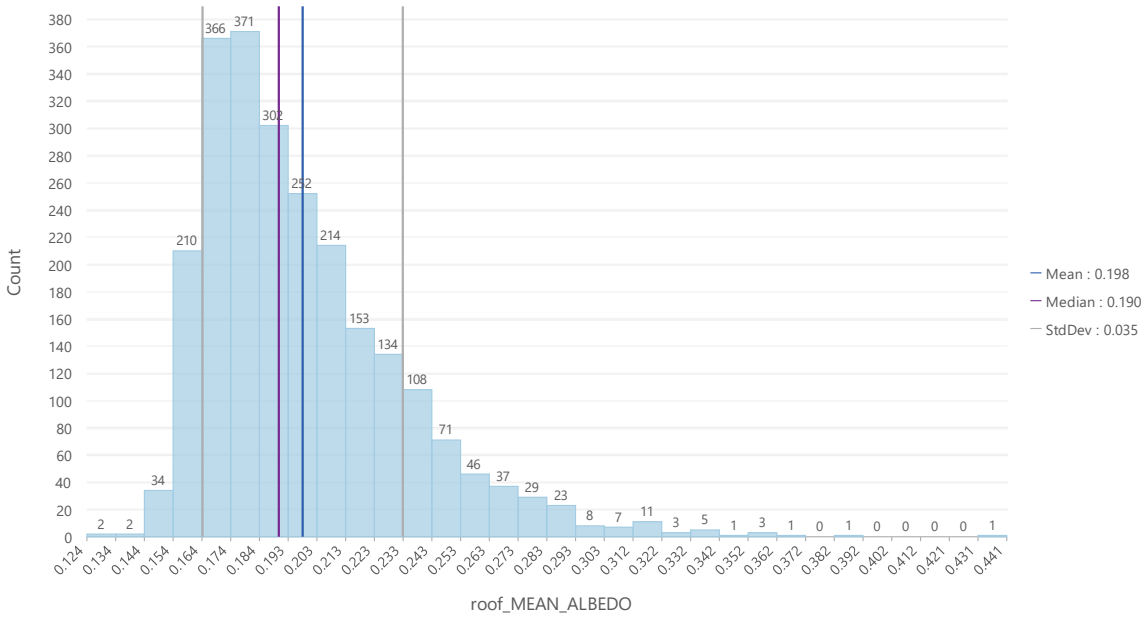

(b)

Figure A-16. Map (a) and histogram (b) of mean roof albedo by tract.

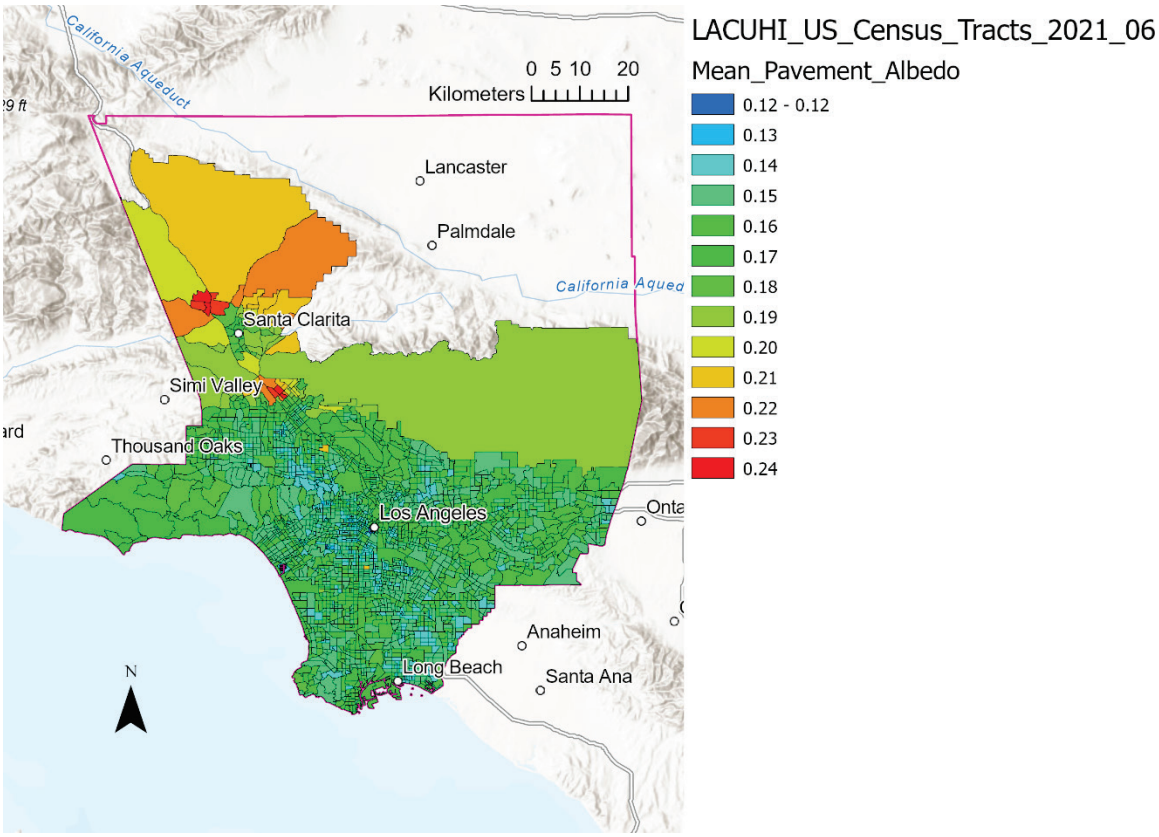

(a)

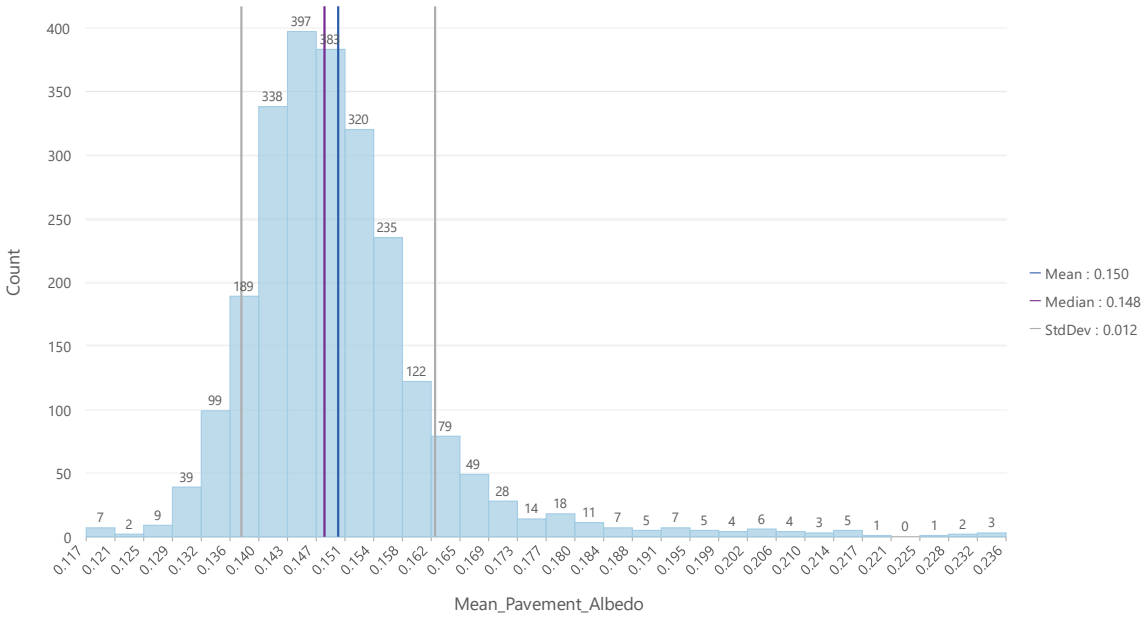

(b)

Figure A-17. Map (a) and histogram (b) of mean pavement albedo by tract.

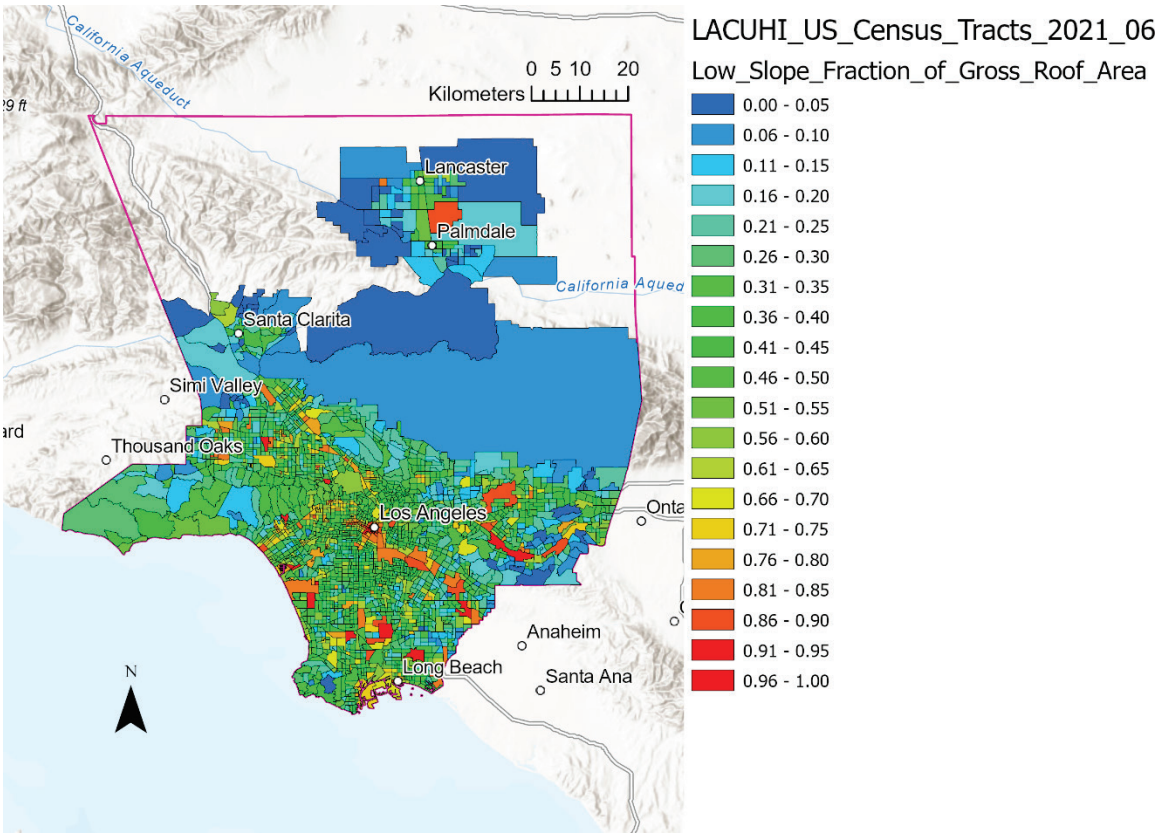

(a)

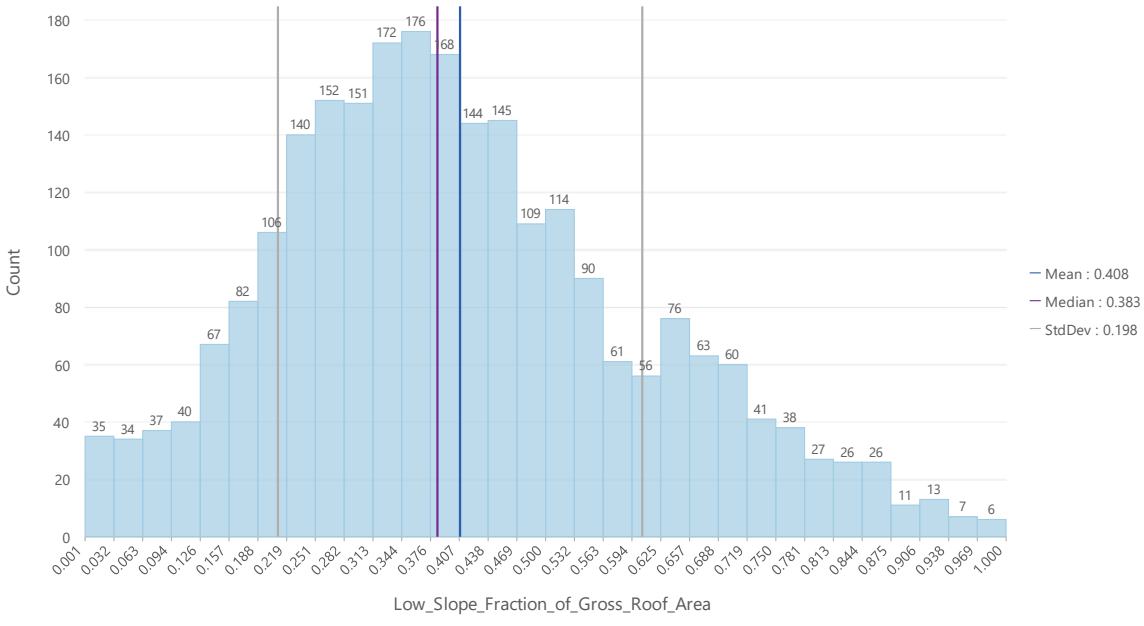

(b)

Figure A-18. Map (a) and histogram (b) of low-slope fraction of gross roof area by tract.

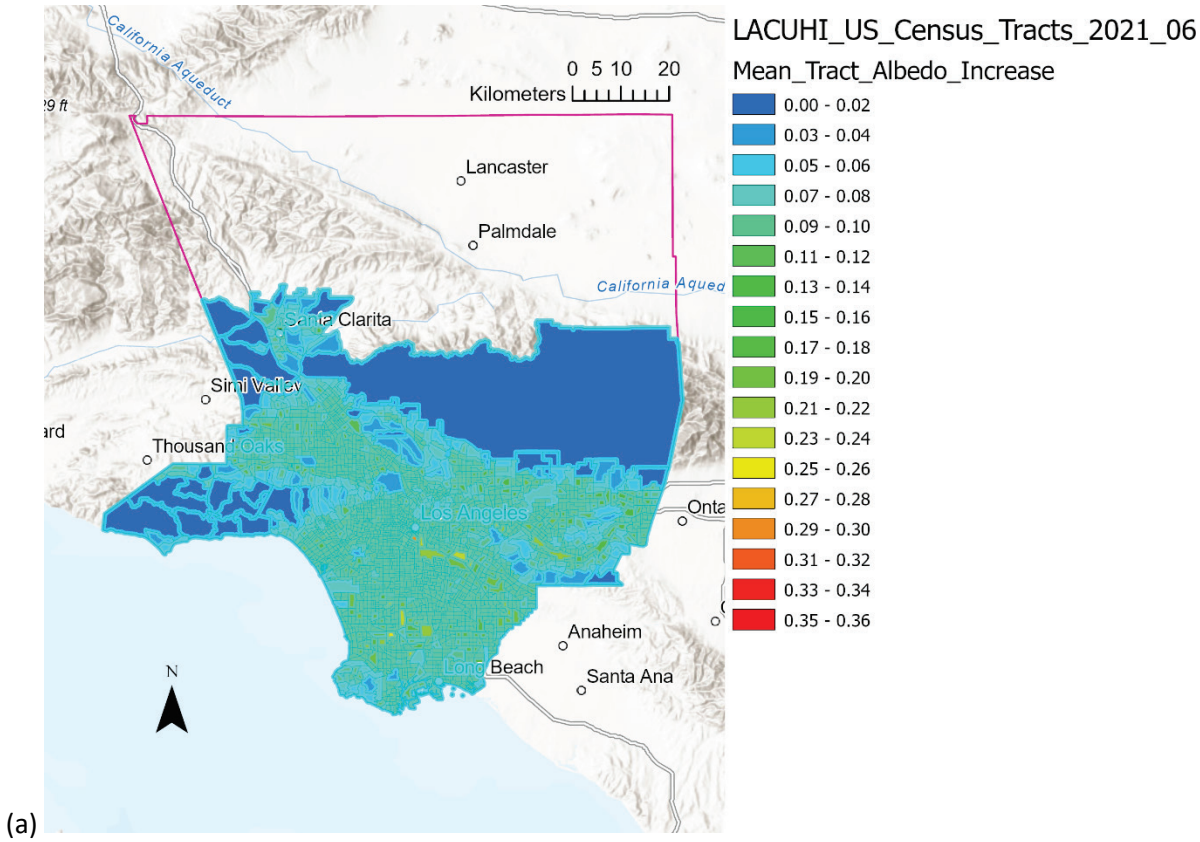

(a)

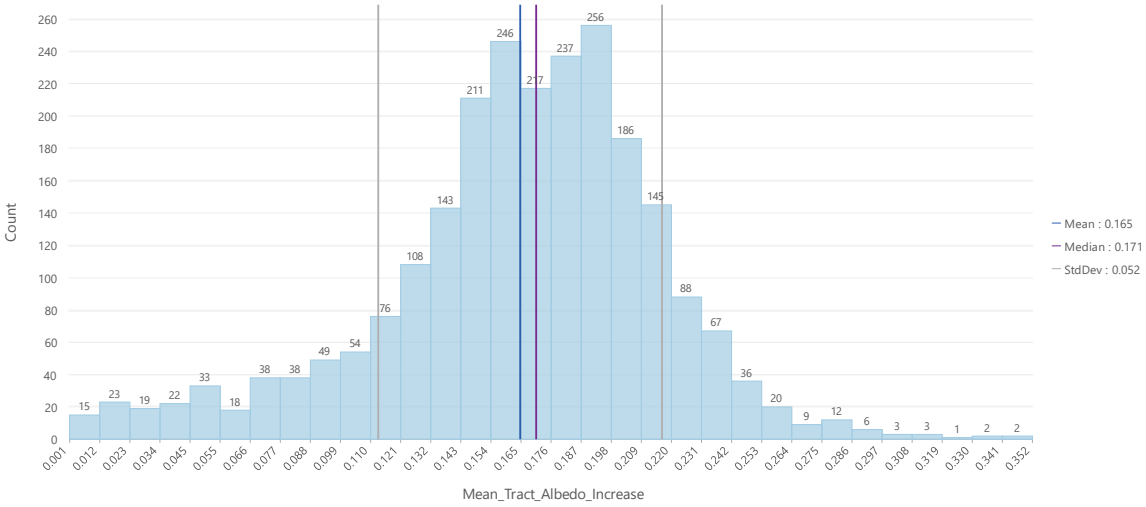

(b)

Figure A-19. Map (a) and histogram (b) of potential increase in mean tract albedo by tract.

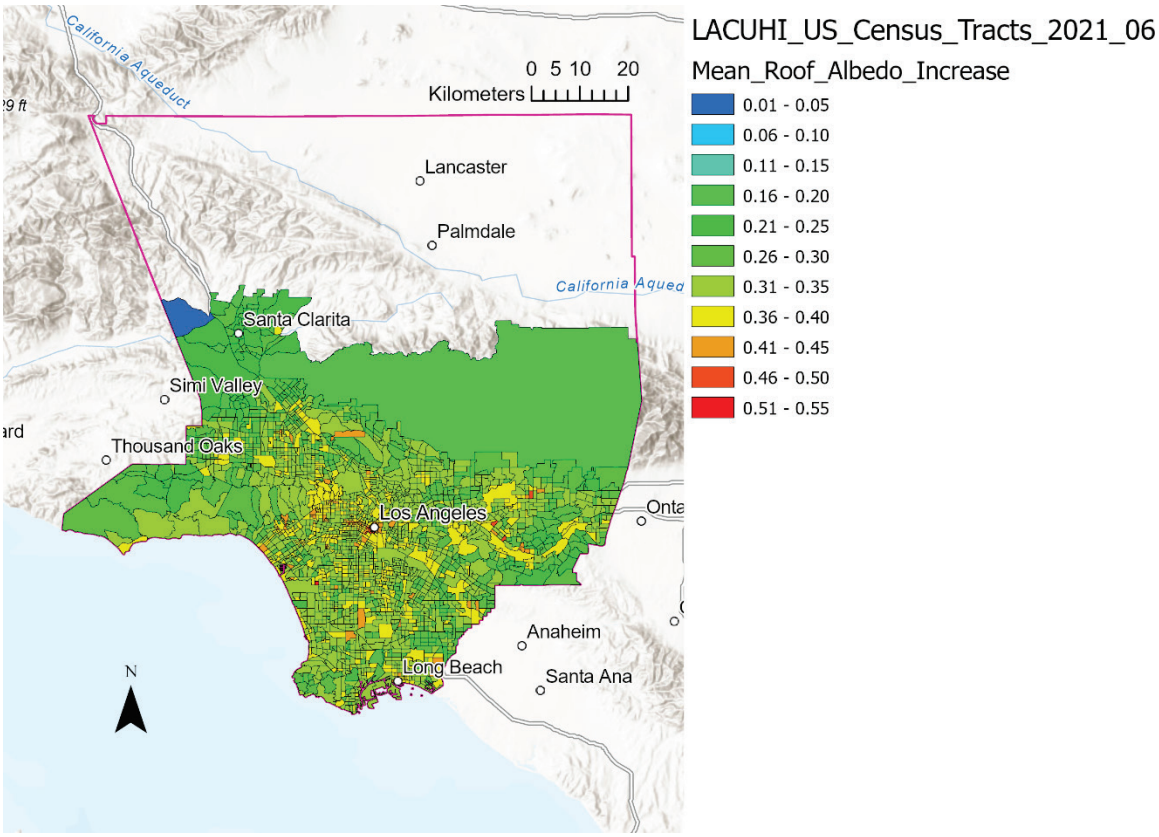

(a)

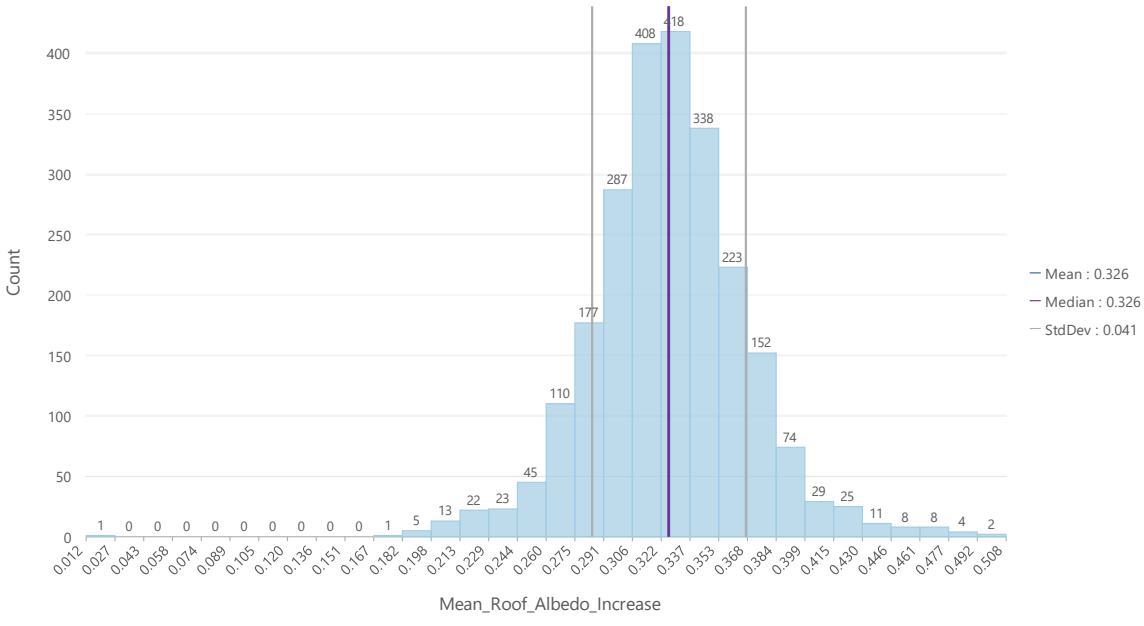

(b)

Figure A-20. Map (a) and histogram (b) of potential increase in mean roof albedo by tract.

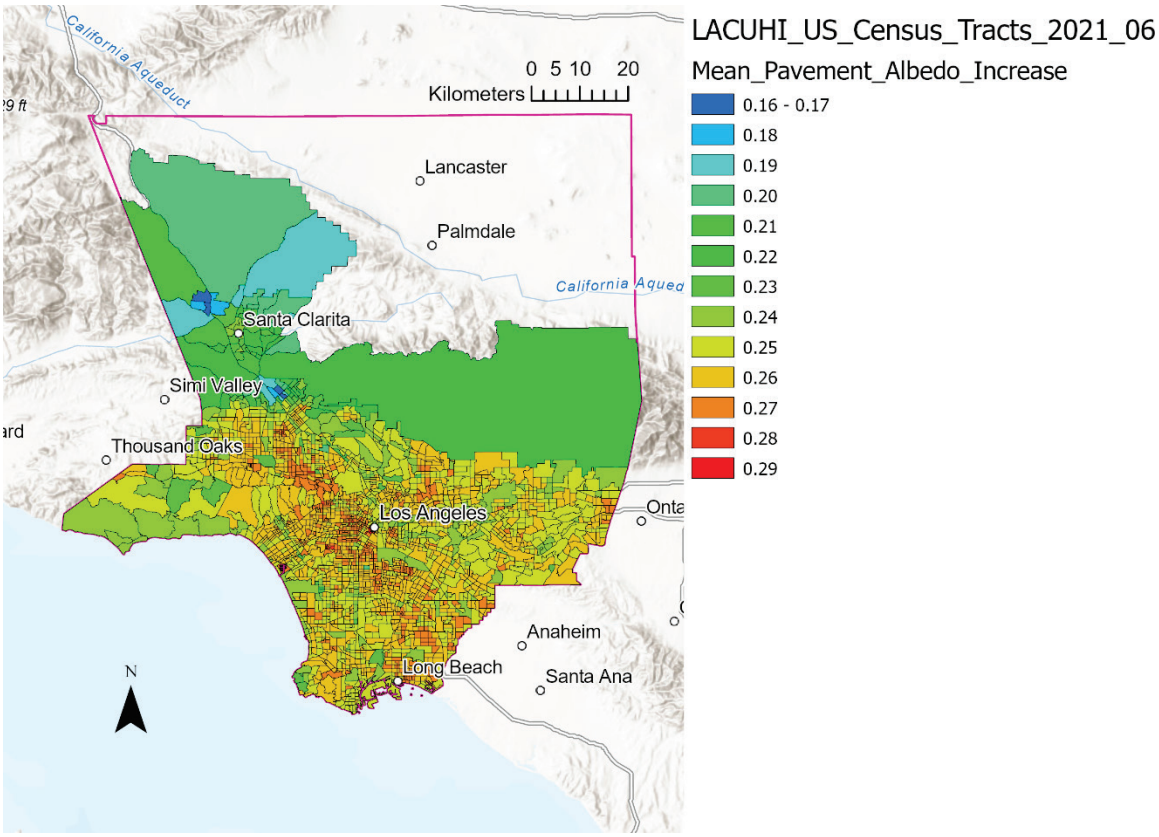

(a)

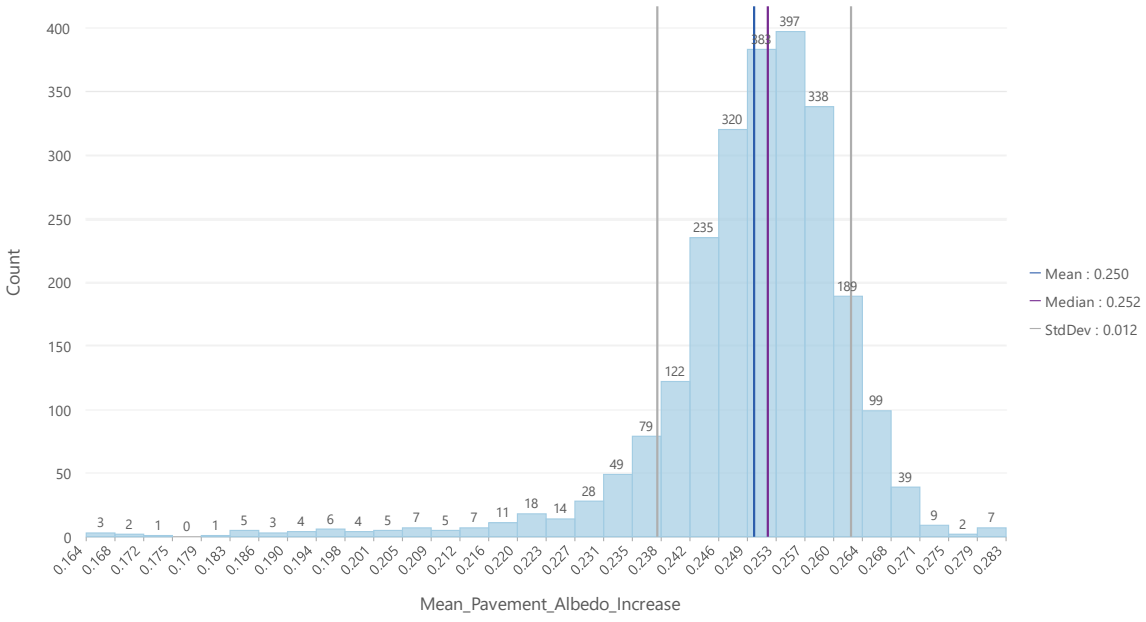

(b)

Figure A-21. Map (a) and histogram (b) of potential increase in mean pavement albedo by tract.

3.4 Tree, natural-ground, and building proximities by tract

Figure A-22 - Figure A-24 show maps and histograms of the proximities to LARIAC buildings of trees, natural ground, and other LARIAC buildings, by tract. Median values of tree, natural-ground, and LARIAC buildings proximities are 16%, 18%, and 23%, respectively (Table A-2), suggesting that (a) many buildings are not closely treed, (b) there is a modest amount of natural ground near buildings available to plant trees, and (c) the 10-m wide buffer around a building is more likely to contain neighboring buildings than trees or natural ground.

The shaded box in the scatterplot of natural ground proximity vs. tree proximity in Figure 25 contains tracts with below-median tree proximity (<16%) and above-median natural-ground proximity (>18%)—that is, tracts with high potential for planting shade trees.

The median value of wall density (ratio of gross wall area to tract area) is 42% (Table A-2). The scatterplot of building proximity vs. wall density in Figure A-26 shows that while building proximity rises with wall density—that is, tall buildings are clumped together, the shaded box contains tracts with above-median wall density (>42%) and below-median building proximity (<23%)—that is, tracts with high potential for cool walls. (Cool walls are also useful in tracts with lower wall density, so long as the building proximity is small.)

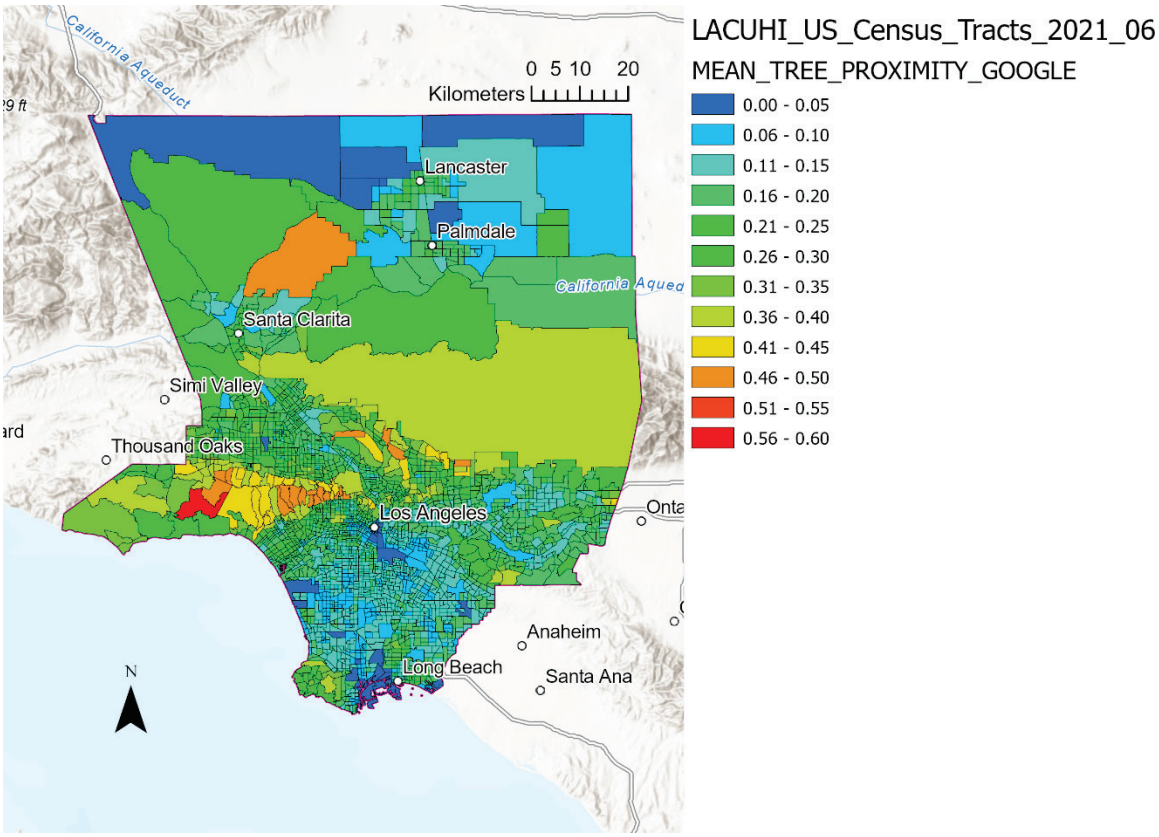

(a)

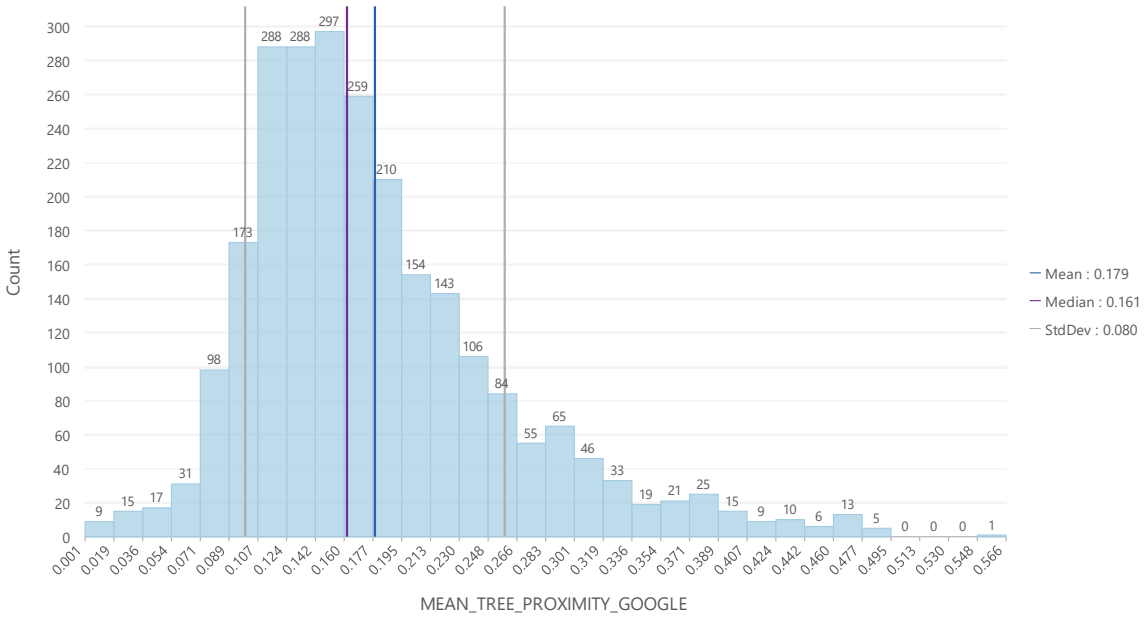

(b)

Figure A-22. Map (a) and histogram (b) of mean tree proximity by tract.

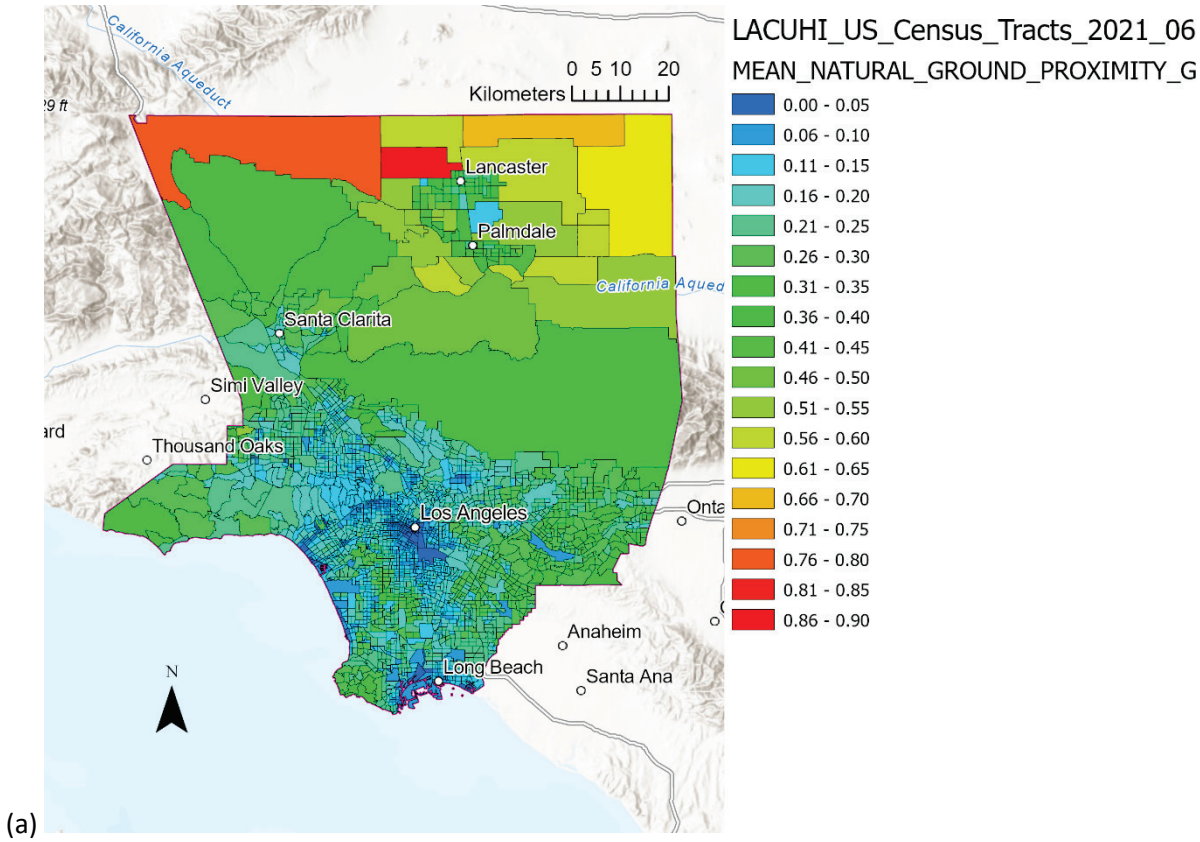

(a)

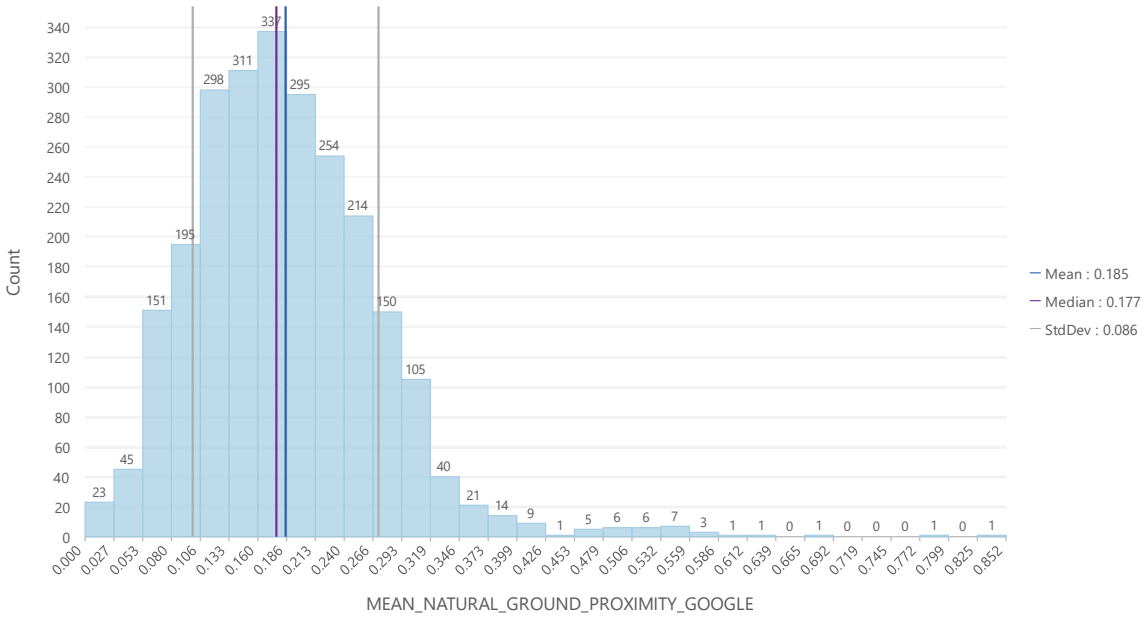

(b)

Figure A-23. Map (a) and histogram (b) of mean natural-ground proximity by tract.

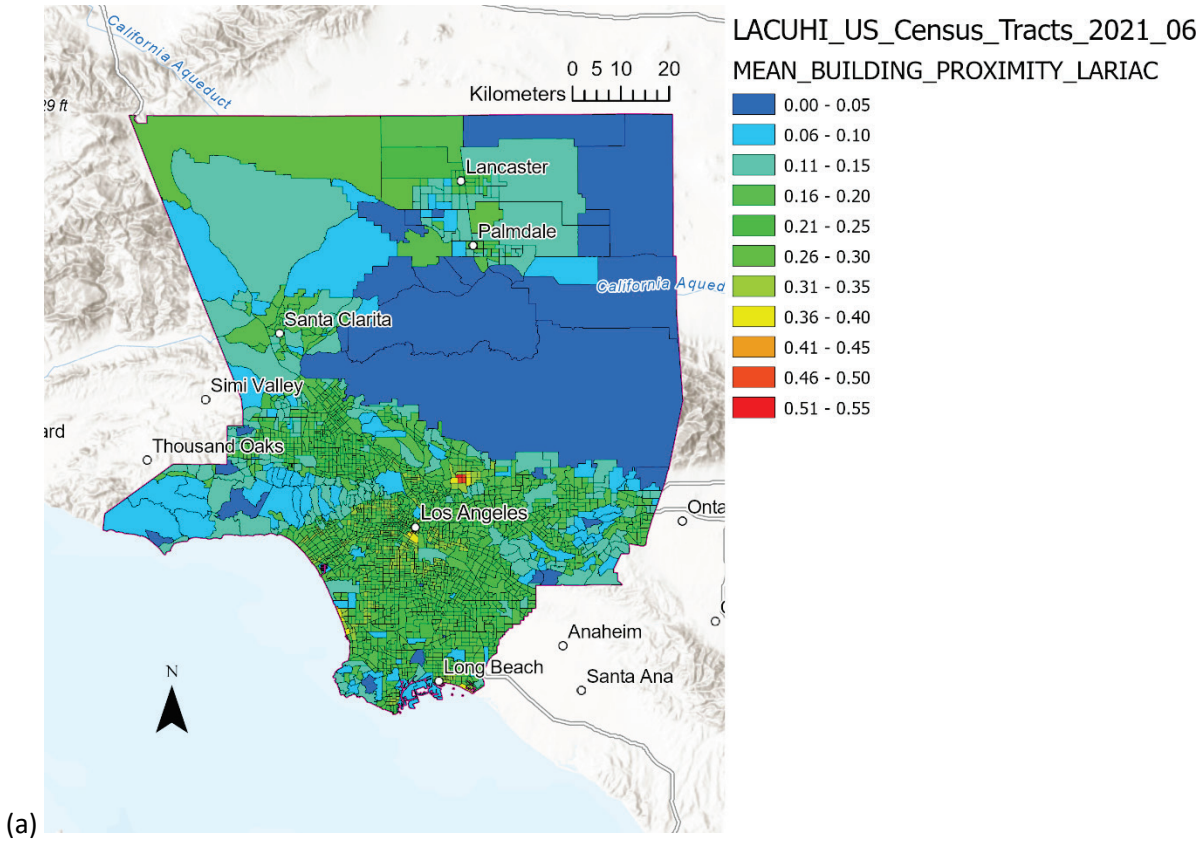

(a)

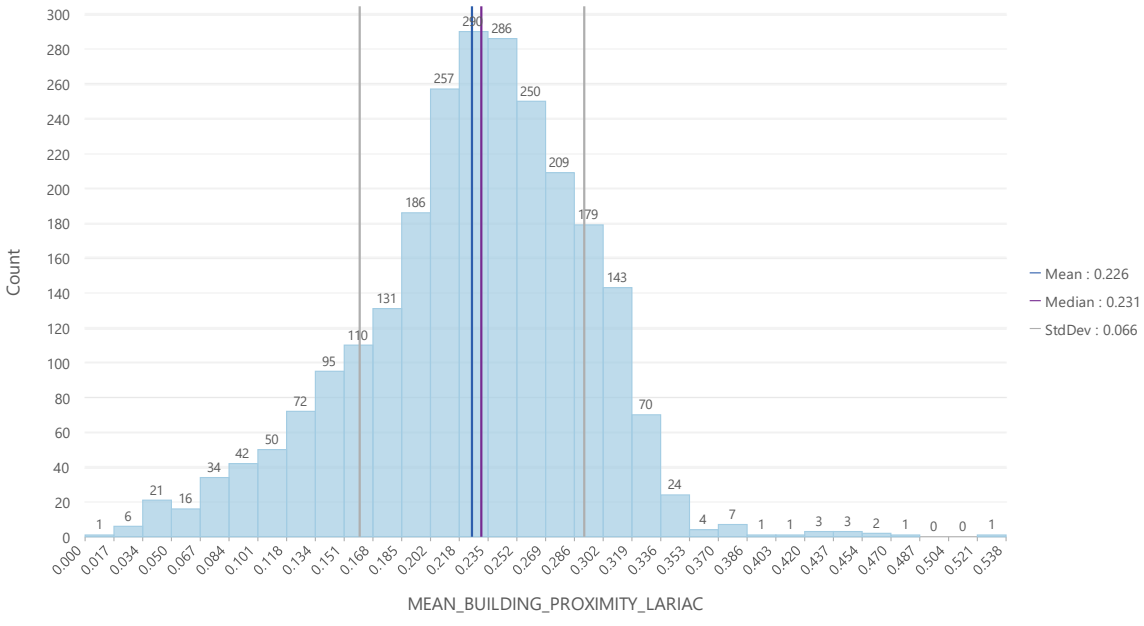

(b)

Figure A-24. Map (a) and histogram (b) of mean building proximity by tract.

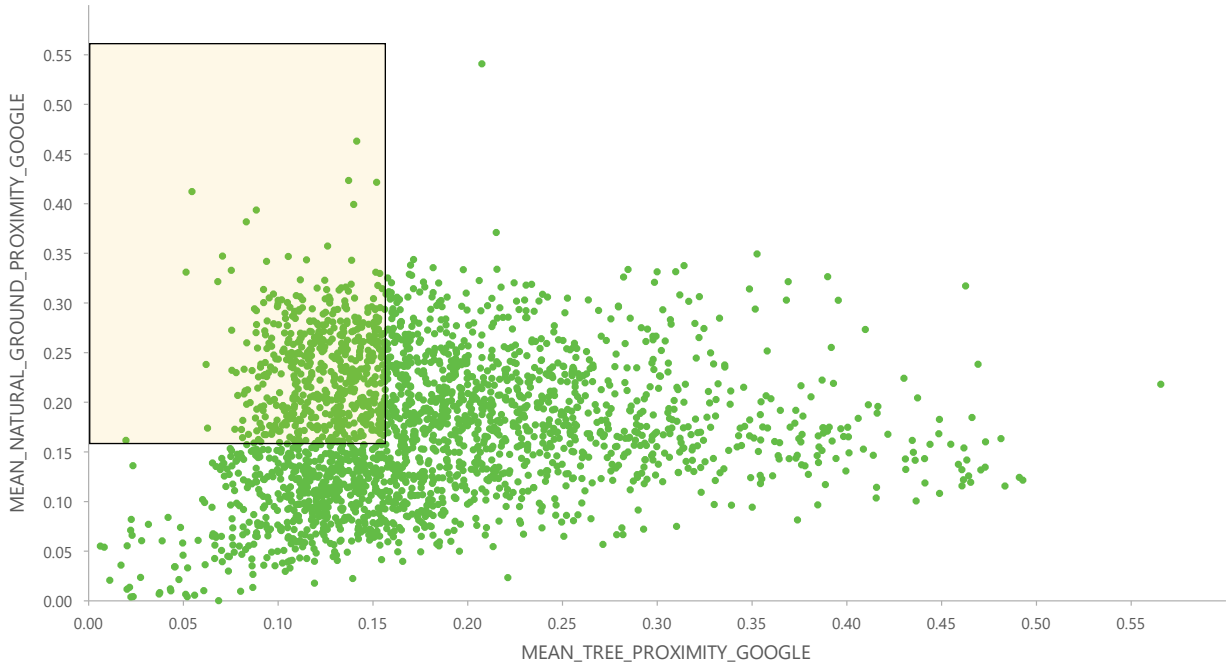

Figure 25. Scatterplot of mean natural-ground proximity vs. mean tree proximity, by tract. The shaded box contains tracts with below-median tree proximity (<16%) and above-median natural-ground proximity (>18%).

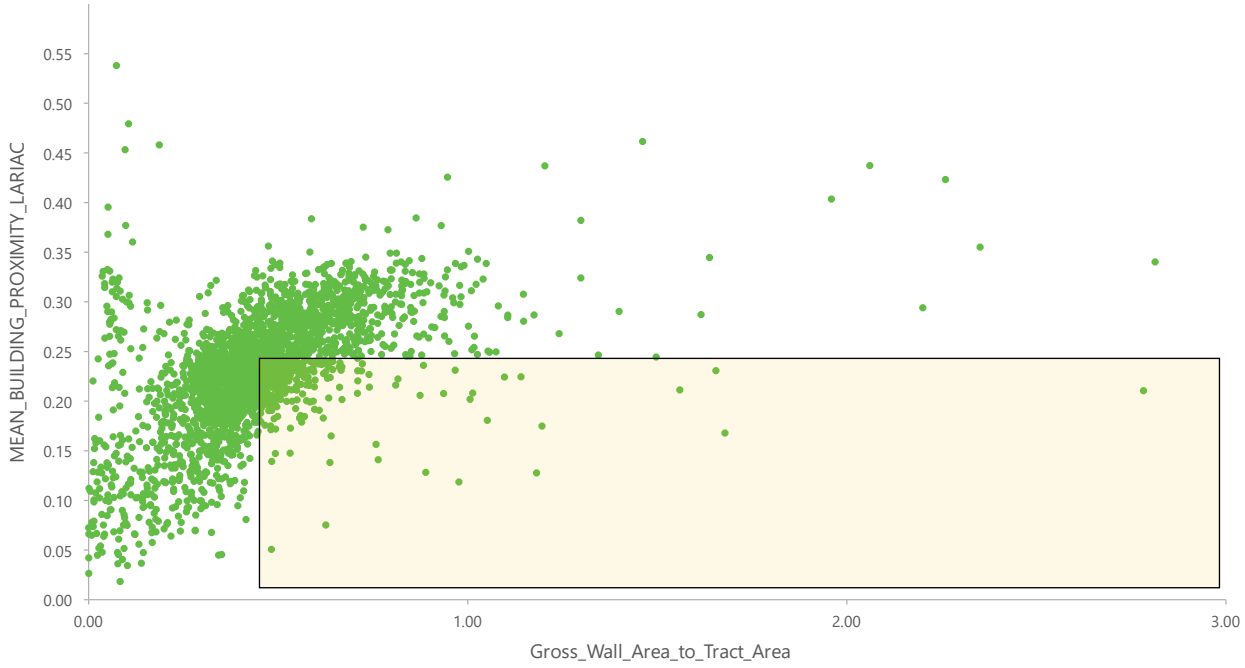

Figure A-26. Scatterplot of mean building proximity vs. wall density (ratio of gross wall area to tract area), by tract. The shaded box contains tracts with above-median wall density (>42%) and below-median building proximity (<23%).

3.5 Summer afternoon air temperature reduction

Figure A-27 - Figure A-29 show maps and histograms of roof, wall, and pavement density by tract. The median values of roof, wall, and pavement density are 25%, 42%, and 31%, respectively, indicating that a typical tract has substantially more gross wall area than gross roof area.[7] These spatial variations in surface density are responsible for the spatial variations in the following estimates of UHIE reduction.

Figure A-30- Figure A-33 show maps and histograms of potential cool-roof, cool-wall, cool-pavement, and cool roof + cool wall + cool pavement UHIE reduction (decrease in summer-afternoon canyon air temperature [K]) by tract. Median values of potential cool-roof, cool-wall, cool-pavement, and cool roof + cool wall + cool pavement UHIE reduction are 0.75, 0.72, 0.48, and 1.11 K, respectively. Walls yield smaller median UHIE reductions than roofs even though median wall density exceeds median roof density because the ACE for walls is only 28% of that for roofs (see Section 2.11). However, we can see that a cool-surface campaign targeting roofs, walls, and pavements could yield a median 1.1 K reduction in summer-afternoon air temperature.

Figure A-34 shows a map and histogram of UHII (summer-averaged reduction in UHIE) with median value 4,953 °C·h. which we relate to summer-afternoon cool roof + wall + pavement UHIE reduction in Figure A-35. The shaded box in Figure A-35 contains tracts with above-median UHII and above-median UHIE reduction—that is, hot places that could be cooled with these UHI countermeasures.

3.6 Opportunities for further analysis

The results presented in this section illustrate some of the potential for countermeasures to reduce unwanted solar heating of buildings and pavements in LAC and mitigate the UHIE. However, they are just a starting point. We recommend using GIS software to further analyze the geospatial data in the building, parcel, and tract feature classes and/or relate them to external data. Here are a few examples.

- **Using UHI countermeasures to reduce excess heat exposure.** What tracts in LAC have both high pollution burden per CalEnviroScreen [14] and high potential UHIE reduction?
- **Identifying cities or districts that could benefit from UHI countermeasures.** Which cities or districts contain the tracts with the top-decile or top-quartile values of roof/wall/pavement surface density, potential albedo increase, or potential UHIE reduction?
- **Identifying opportunities for accelerated replacement of roofs or pavements.** What is the roof/pavement age (years since last permitted installation or replacement) vs. potential increase in roof/pavement albedo, by parcel or tract?

[7] Of course, the ratio of *net* areas is likely to be lower than the ratio of *gross* areas because walls typically have more openings (windows and doors) than roofs (skylights).

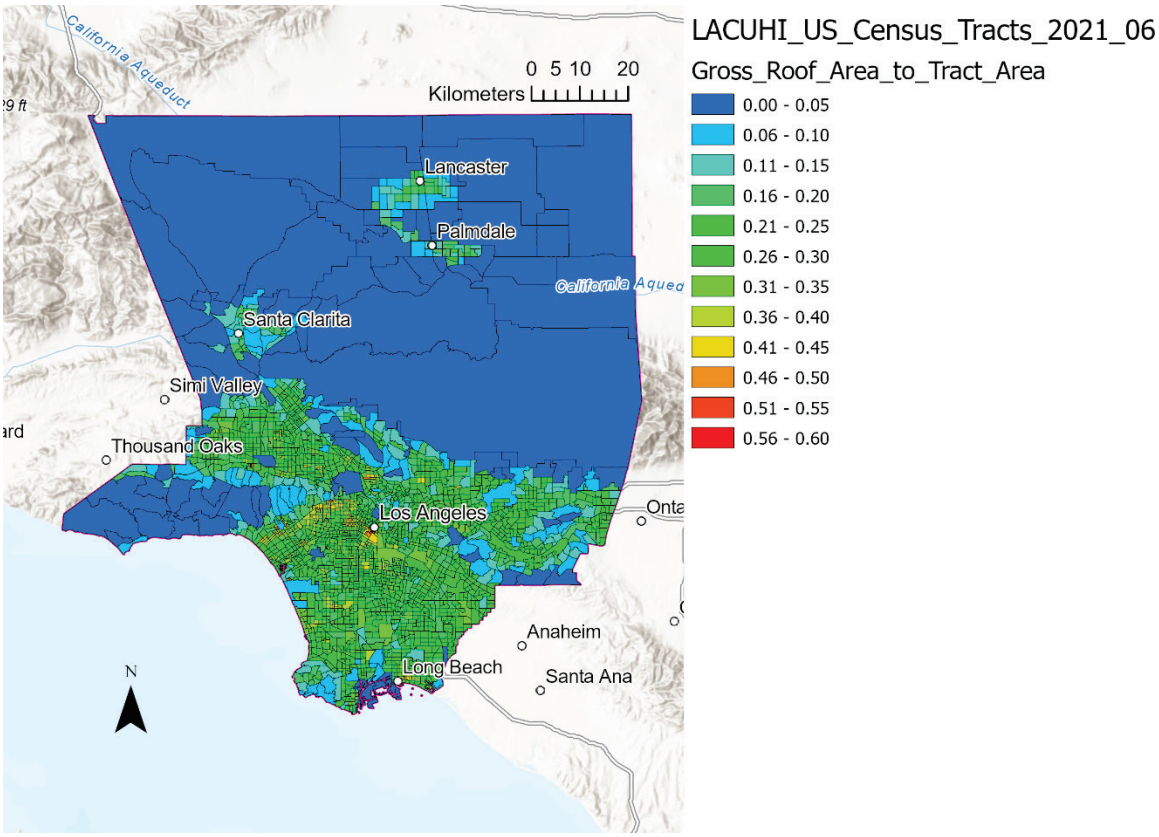

(a)

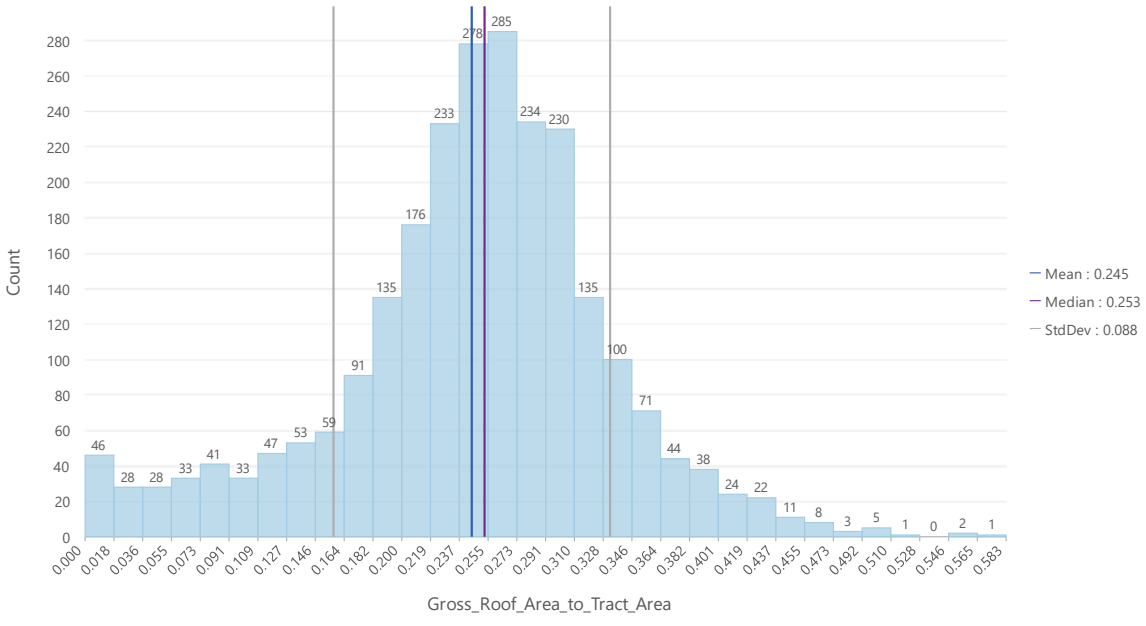

(b)

Figure A-27. Map (a) and histogram (b) of roof density (ratio of gross roof area to tract area) by tract.

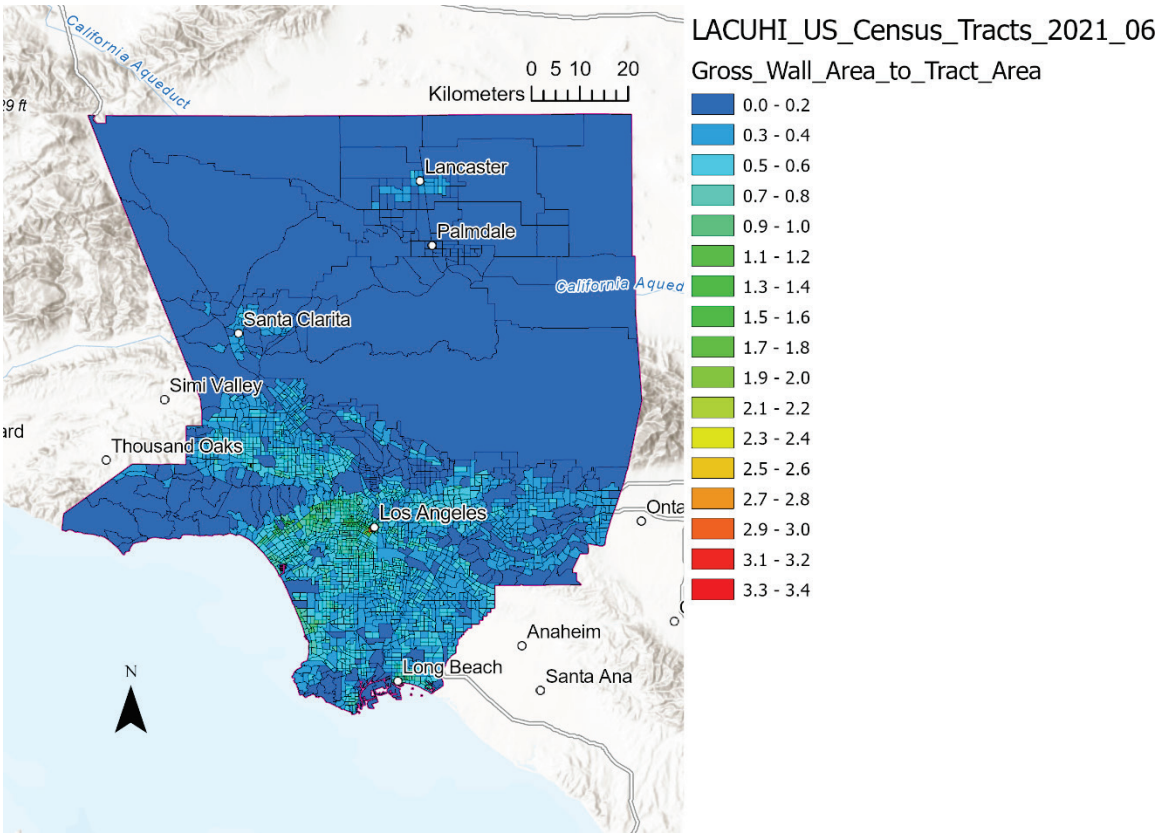

(a)

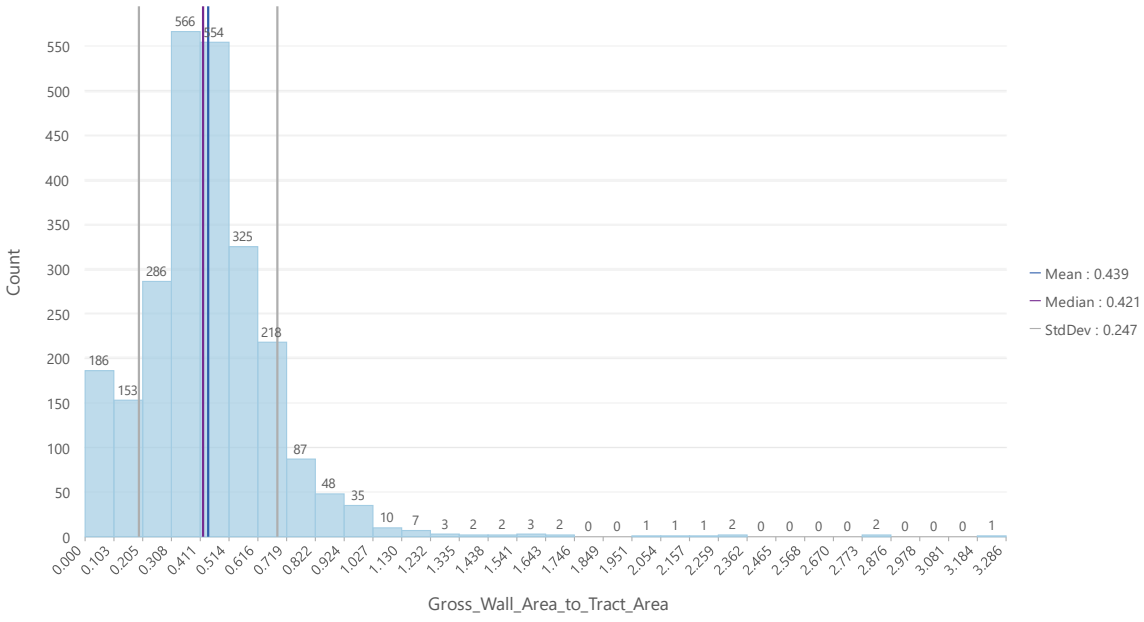

(b)

Figure A-28. Map (a) and histogram (b) of wall density (ratio of gross wall area to tract area) by tract.

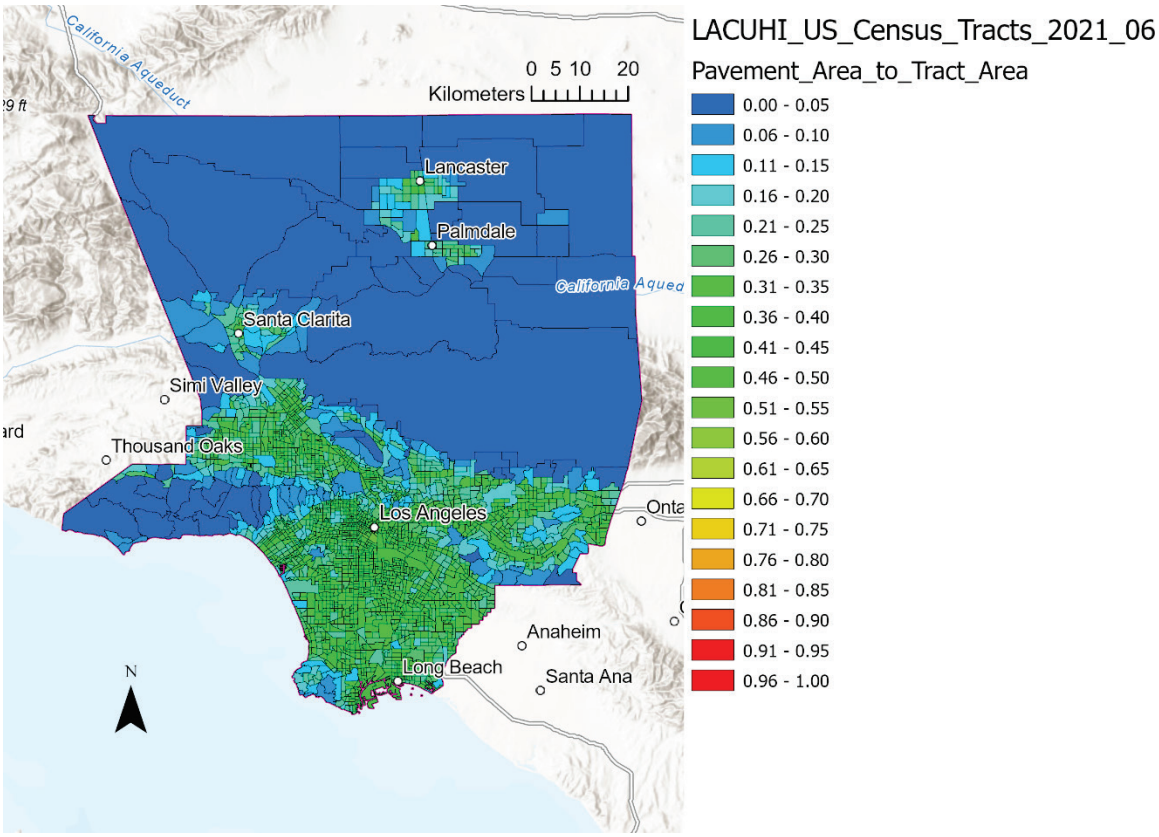

(a)

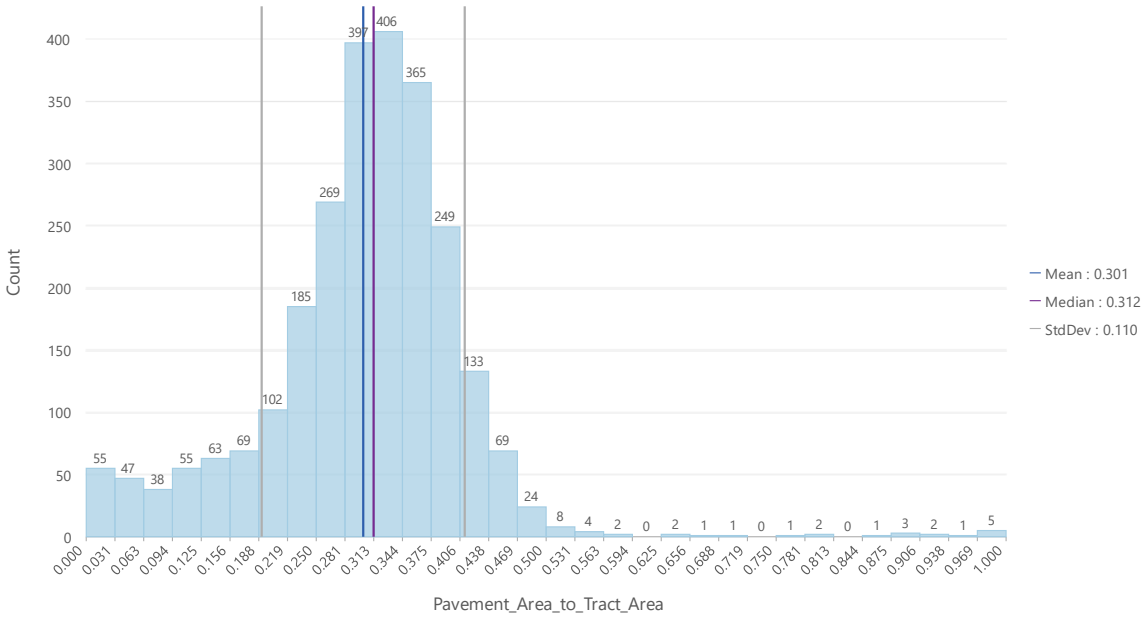

(b)

Figure A-29. Map (a) and histogram (b) of pavement density (ratio of pavement area to tract area) by tract.

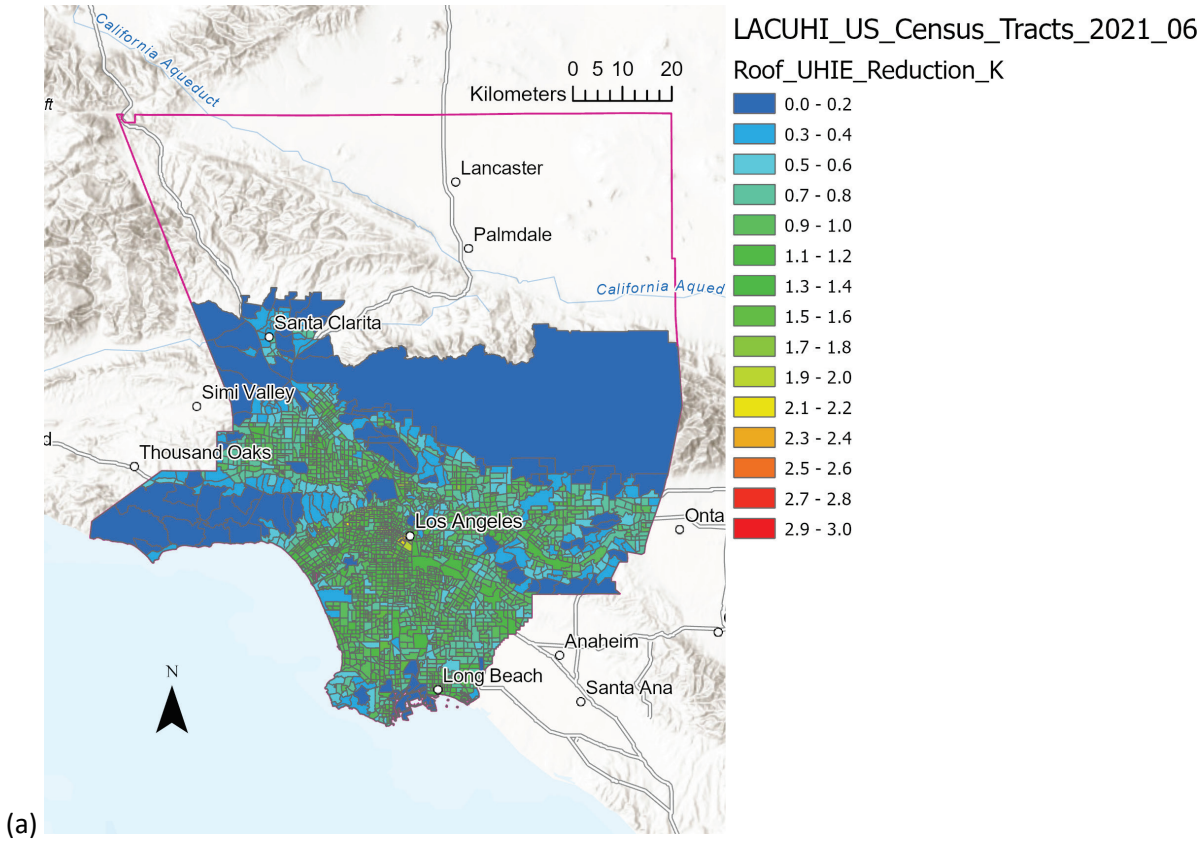

(a)

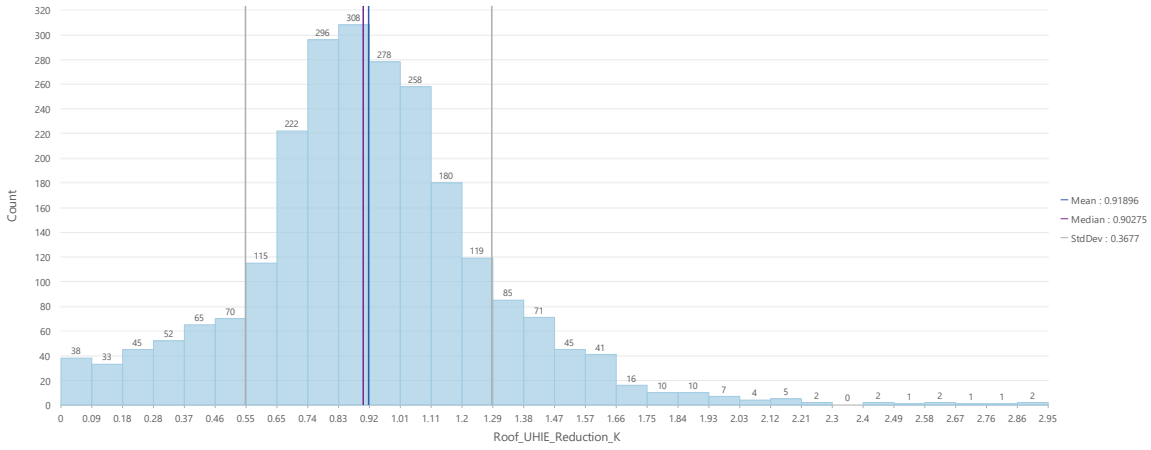

(b)

Figure A-30. Map (a) and histogram (b) of potential cool-roof UHIE reduction (decrease in summer-afternoon canyon air temperature [K]) by tract.

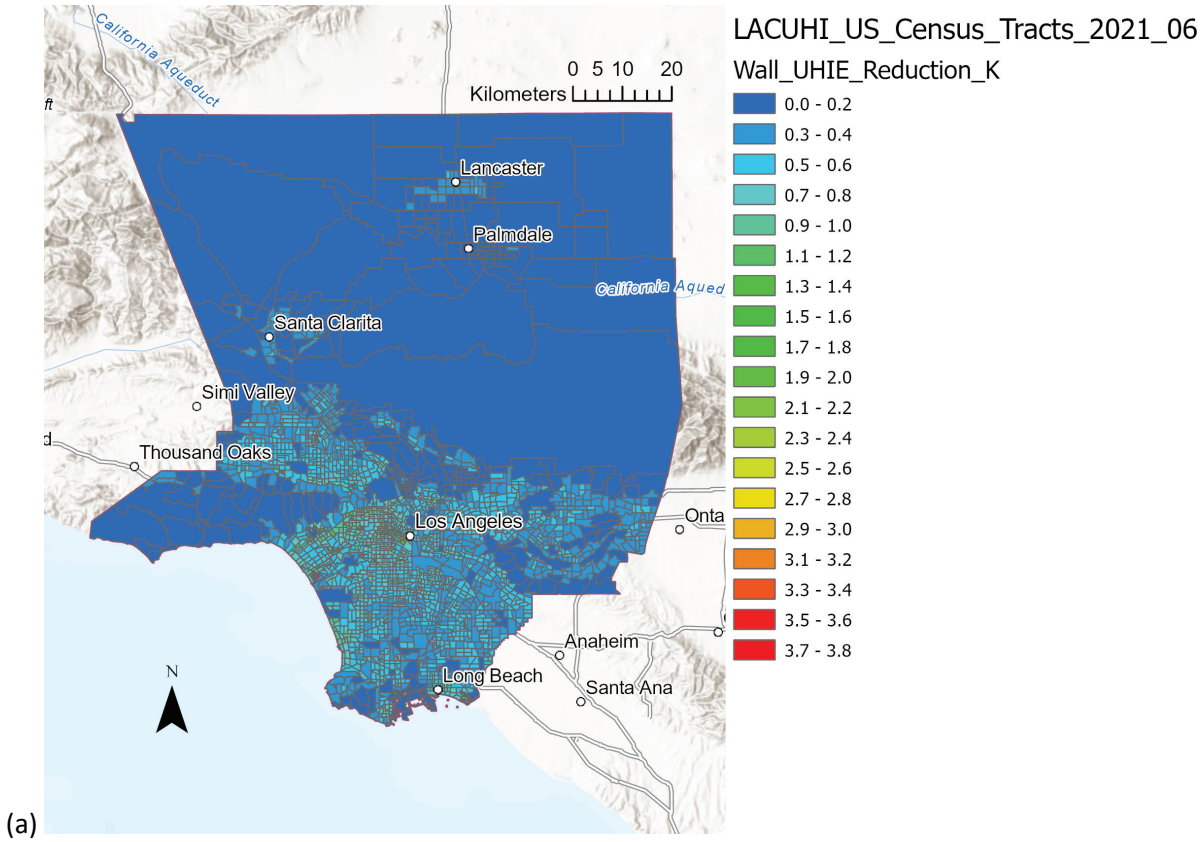

Figure A-31. Map (a) and histogram (b) of potential cool-wall UHIE reduction (decrease in summer-afternoon canyon air temperature [K]) by tract.

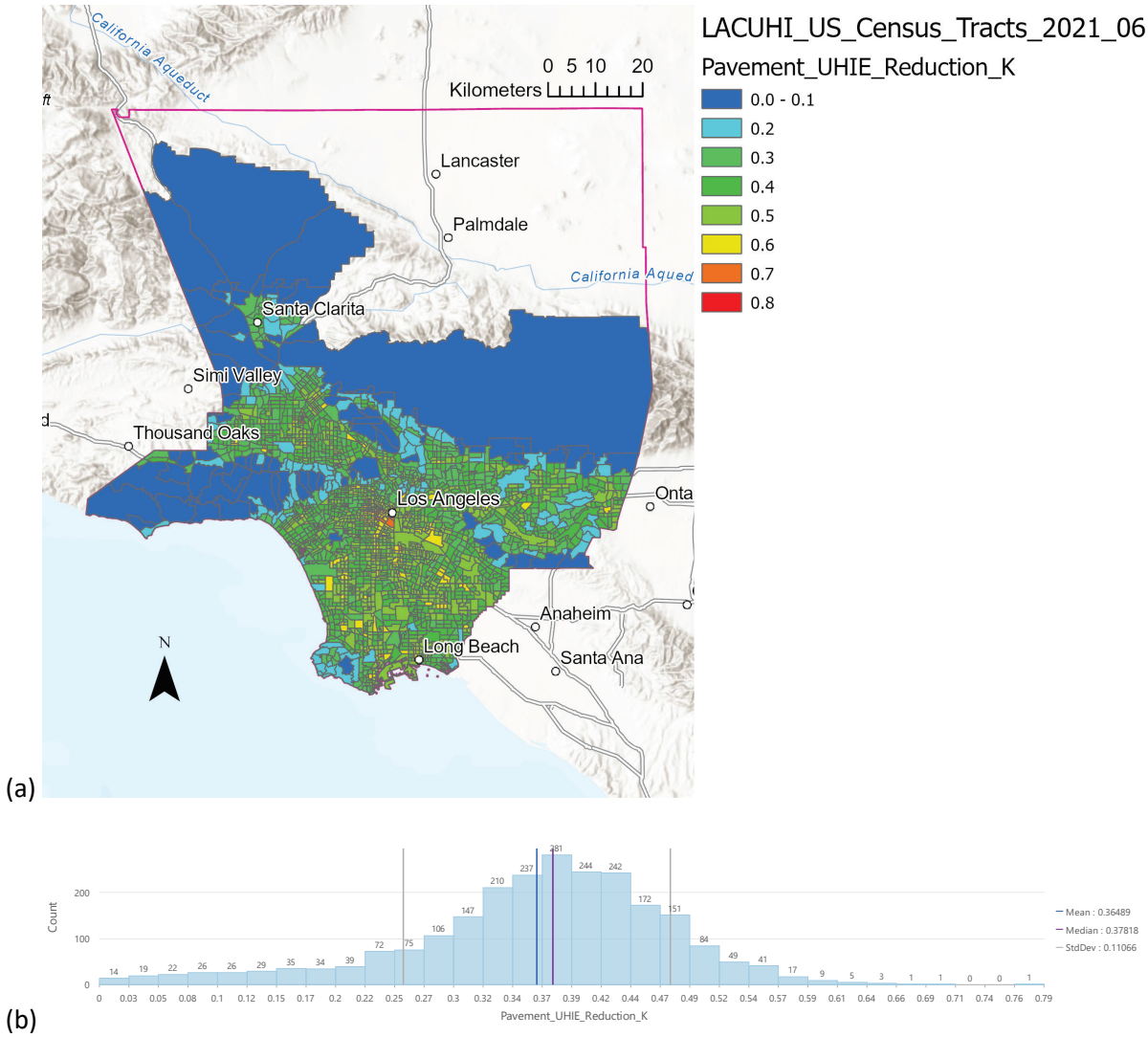

Figure A-32. Map (a) and histogram (b) of potential cool-pavement UHIE reduction (decrease in summer-afternoon canyon air temperature [K]) by tract

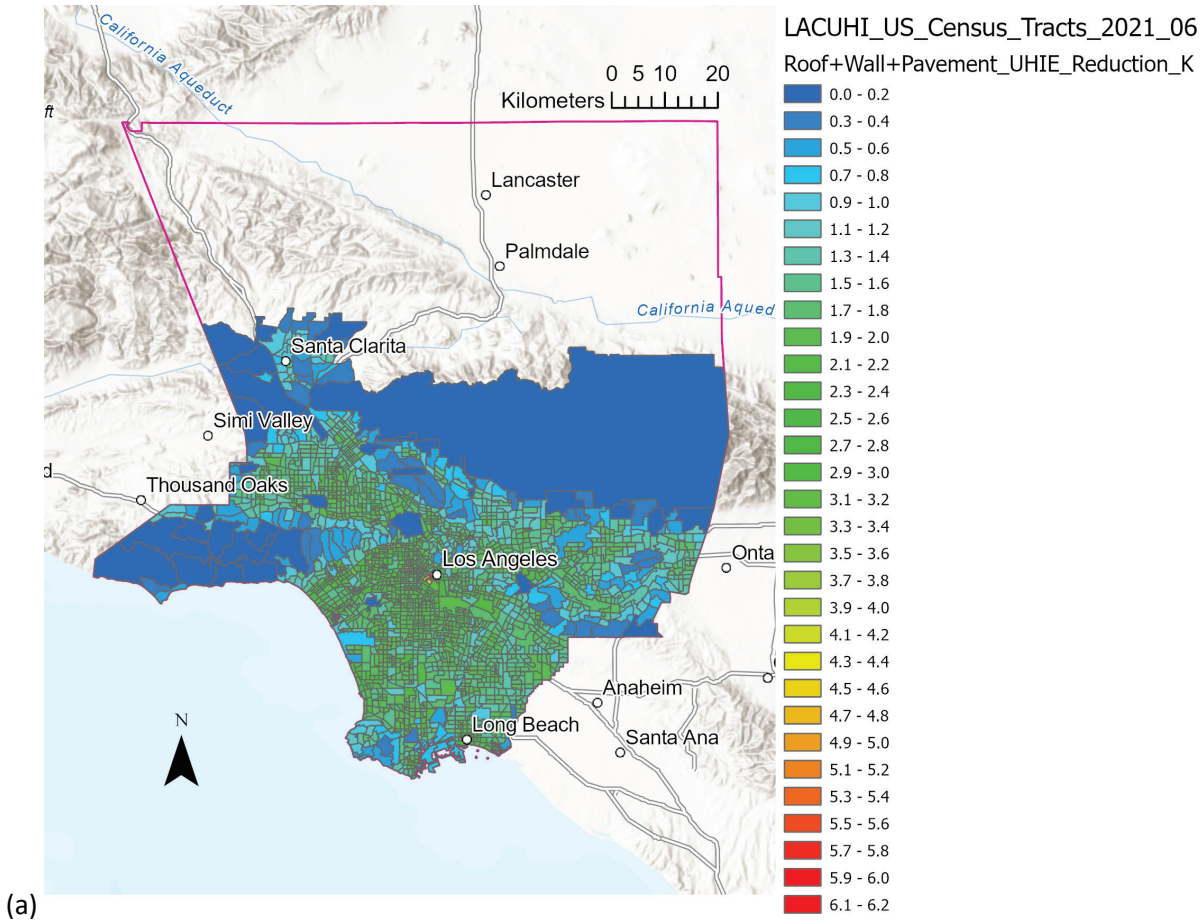

(a)

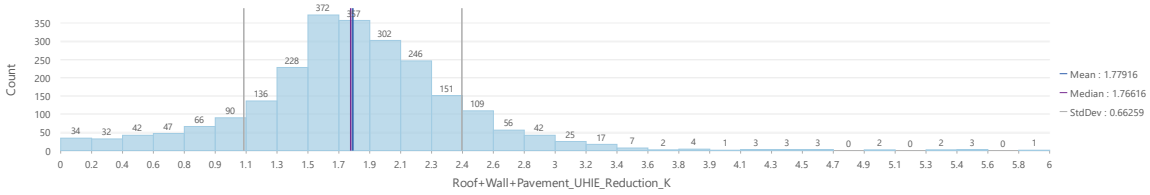

(b)

Figure A-33. Map (a) and histogram (b) of potential cool-roof + cool-wall + cool pavement UHIE reduction (decrease in summer-afternoon canyon air temperature [K]) by tract.

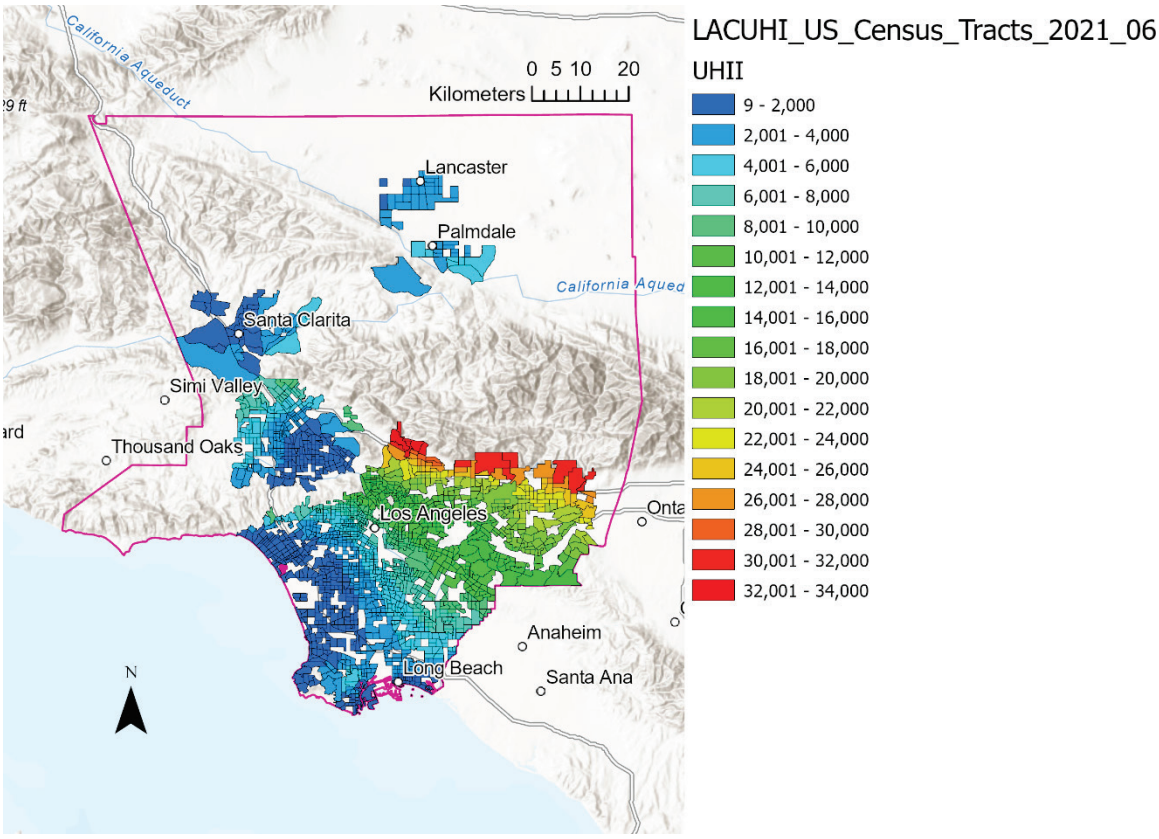

(a)

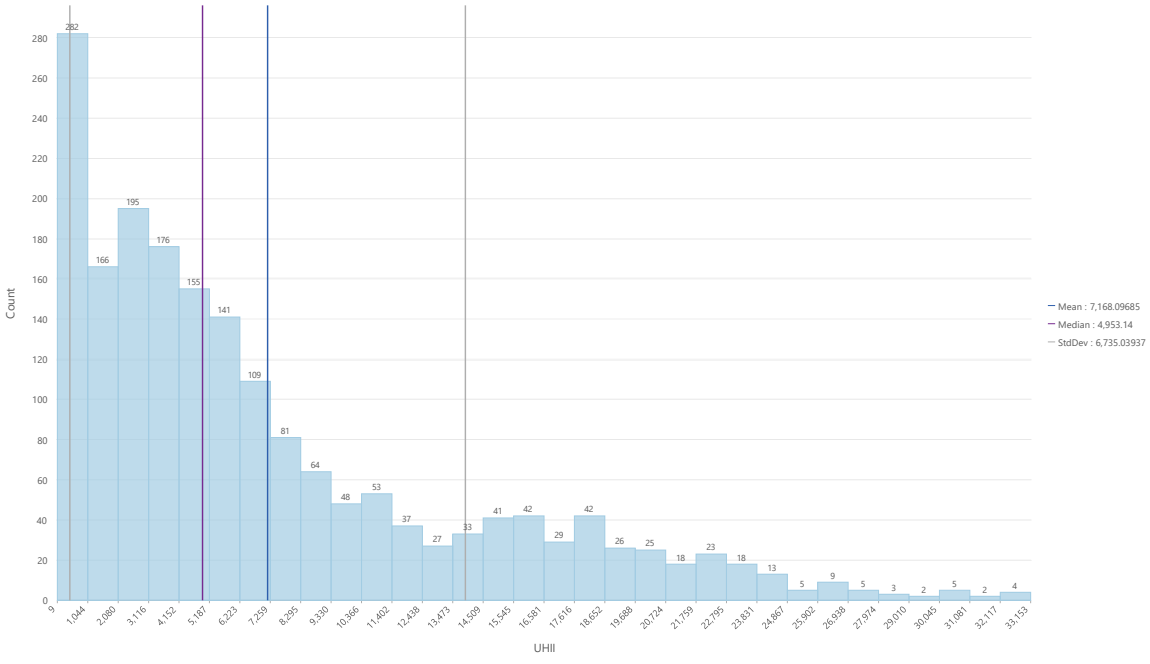

(b)

Figure A-34. Map (a) and histogram (b) of urban heat island index (UHII) [°C·hr] by tract.

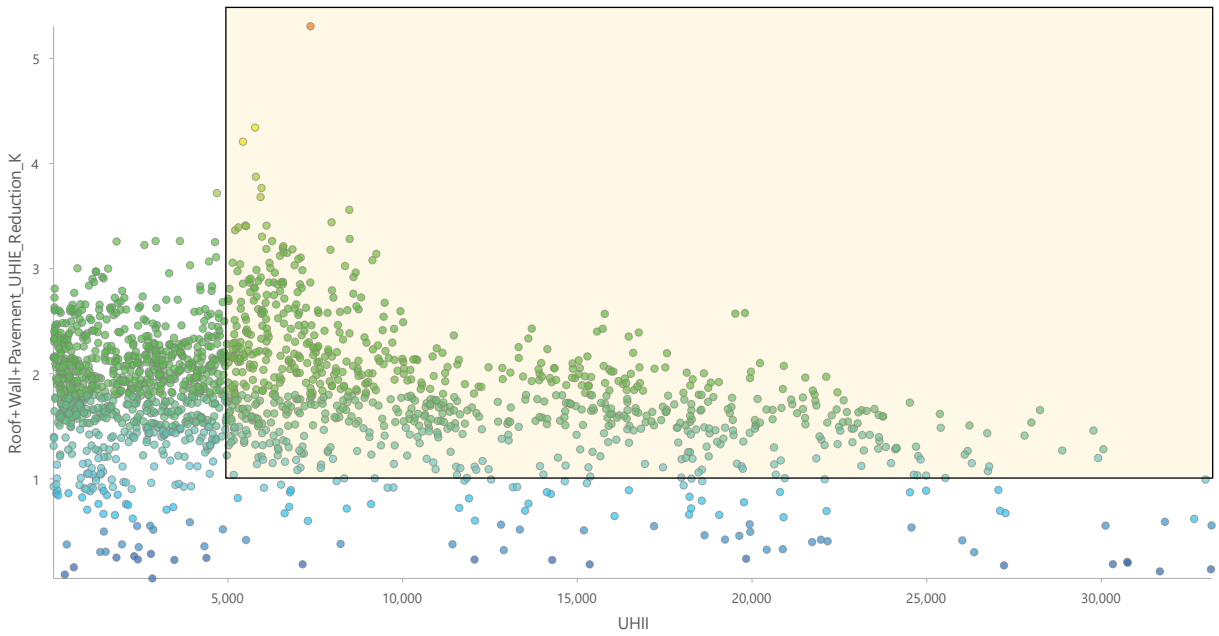

Figure A-35. Scatterplot of roof+wall+pavement UHIE reduction [K] vs. UHII [°C·hr]. The shaded box contains tracts with above-median UHII and above-median UHIE reduction.

References

[1] ESRI, Feature Class Definition | GIS Dictionary, (n.d.). https://support.esri.com/en-us/gis-dictionary/feature-class (accessed June 6, 2023).

[2] Steven Steinberg, An Dang, LARIAC: Los Angeles Region Imagery Acquisition Consortium, (n.d.). https://lariac-lacounty.hub.arcgis.com/ (accessed June 6, 2023).

[3] B. Dean, Urban Heat Island Index for California | CalEPA, (n.d.). https://calepa.ca.gov/climate/urban-heat-island-index-for-california/ (accessed June 6, 2023).

[4] H. Taha, Characterization of Urban Heat and Exacerbation: Development of a Heat Island Index for California, Climate 5 (2017) 59. https://doi.org/10.3390/cli5030059.

[5] ESRI, ArcGIS Pro, (n.d.). https://www.esri.com/en-us/arcgis/products/arcgis-pro/overview (accessed June 6, 2023).

[6] Cool Roof Rating Council, Low-Sloped Roofing Product Types, (n.d.). http://coolroofs.org/resources/low-sloped-roofing-product-types (accessed June 6, 2023).

[7] Cool Roof Rating Council, Steep-Sloped Roofing Products, (n.d.). http://coolroofs.org/resources/steep-sloped-roofing-products (accessed June 6, 2023).

[8] S. Thomas, Low-slope roofs and steep roofs, in: Building Code Basics: Building. Based on the 2009 International Building Code, Delmar Cengage Learning, Clifton Park, NY, 2010: pp. 130–134. http://media.iccsafe.org/news/eNews/2013v10n1/2009_ibc_bcbseries_pages130-132.pdf.

[9] J. Zhang, A. Mohegh, Y. Li, R. Levinson, G. Ban-Weiss, Systematic Comparison of the Influence of Cool Wall versus Cool Roof Adoption on Urban Climate in the Los Angeles Basin, Environ. Sci. Technol. 52 (2018) 11188–11197. https://doi.org/10.1021/acs.est.8b00732.

[10] A. Mohegh, P. Rosado, L. Jin, D. Millstein, R. Levinson, G. Ban-Weiss, Modeling the climate impacts of deploying solar reflective cool pavements in California cities, Journal of Geophysical Research 122 (2017) 6798–6817. https://doi.org/10.1002/2017JD026845.

[11] E.S. Krayenhoff, A.M. Broadbent, L. Zhao, M. Georgescu, A. Middel, J.A. Voogt, A. Martilli, D.J. Sailor, E. Erell, Cooling hot cities: a systematic and critical review of the numerical modelling literature, Environ. Res. Lett. 16 (2021) 053007. https://doi.org/10.1088/1748-9326/abdcf1.

[12] P.J. Rosado, G. Ban-Weiss, A. Mohegh, R.M. Levinson, Influence of street setbacks on solar reflection and air cooling by reflective streets in urban canyons, Solar Energy 144 (2017) 144–157. https://doi.org/10.1016/j.solener.2016.12.026.

[13] E. Erell, D. Pearlmutter, D. Boneh, P.B. Kutiel, Effect of high-albedo materials on pedestrian heat stress in urban street canyons, Urban Climate 10 (2014) 367–386. https://doi.org/10.1016/j.uclim.2013.10.005.

[14] J. Witteborg, About CalEnviroScreen, OEHHA (2019). https://oehha.ca.gov/calenviroscreen/about-calenviroscreen (accessed June 7, 2023).